

PASCAL



Dep	Mod	Ran	Sect	Shelf	Tray	Item
P	1	04	38	07	08	001

Engine  
T  
1966  
H 972

[Redacted]

Gemmill Engineering Library  
  
U18300 3113195  
U18300 3113195



ANALYSIS OF CATALYTIC  
ORTHO-PARAHYDROGEN REACTION MECHANISMS

by

Harold Lee Hutchinson

B.S., University of Utah, 1962

M.S., University of Colorado, 1964

A thesis submitted to the Faculty of the Graduate  
School of the University of Colorado in partial  
fulfillment of the requirements for the degree of

Doctor of Philosophy

Department of Chemical Engineering

1966

This Thesis for the Doctor of Philosophy degree by

Harold Lee Hutchinson

has been approved for the

Department of

Chemical Engineering

by

  
\_\_\_\_\_

Paul L. Barrick

  
\_\_\_\_\_

Lee F. Brown

Date October 14, 1965

## ACKNOWLEDGMENTS

The author wishes to acknowledge the financial support of the Aeronautical Systems Division, Air Force Systems Command, under whose Contract AF 33(616)-7654 this work was begun. He also wishes to express his appreciation to the University of Colorado and to Continental Oil Company, who provided fellowships to the author during the period in which this work was in progress.

Thanks are due to Dr. Paul L. Barrick, who directed the work, and to Dr. Lee F. Brown, who gave timely suggestions throughout the course of the work. Mr. Donald L. Page was invaluable in rendering assistance with the construction of the experimental apparatus.

To the author's wife, Joann, must go his thanks for her patience and understanding, which made this work possible. She helped in many tangible and many more intangible ways with the completion of this project and to her it is gratefully dedicated.

Hutchinson, Harold Lee (Ph.D., Chemical Engineering)

Analysis of Catalytic Ortho-parahydrogen Reaction  
Mechanisms

Thesis directed by Professor Paul L. Barrick

The low temperature ortho-parahydrogen shift reaction has long been considered to be an ideal one for the study of catalytic reaction mechanisms. This is due to its being a simple reaction in which the reactant is easily purified, side reactions are non-existent, and heat effects are quite small. For these reasons a large number of studies have been conducted on this reaction. Most investigators have concluded that their kinetic data at temperatures below  $100^{\circ}\text{K}$  were explained by a first-order reaction rate law. However, there have been a few investigators who did not agree that the reaction is a simple first-order reaction and theoretical investigation showed that, except under certain conditions, the reaction should not be of first-order type.

An apparatus was therefore devised which could be used to collect kinetic data at  $76^{\circ}\text{K}$  for the reaction. A hydrous ferric oxide gel catalyst was used to promote the reaction and a pressure range of 30 to 1010 psia in geometric intervals was covered. Since the ortho-parahydrogen reaction is reversible at  $76^{\circ}\text{K}$ , a study of the reaction in both directions is quite useful in determining a reaction mechanism--according to the principal of microscopic reversibility, the mechanism must be the same in both directions. No single investigation on the reaction in both directions using the same catalyst and covering identical pressures and temperatures has previously been

reported.

Rate expressions based on different sets of theoretical assumptions are derived and tested against the data. Models which assume a three-step mechanism consisting of adsorption, surface reaction, and desorption are postulated and an expression is derived when each of the three in turn controls the rate of reaction. Four different types of adsorption laws are used in developing mechanisms. The names of Langmuir, Temkin, Elovich, and Freundlich are associated with these adsorption laws. In addition, for the Langmuir case, an expression is derived which postulates that none of the three steps controls the rate.

The results show that a good correlation of the data is obtained from both the Langmuir and Elovich models. However, there is a deviation with pressure which is not predicted by the theory in the rate constants of the Elovich expressions, and there is a difference in value between the rate constants of the Langmuir expression for the forward and reverse directions. It is shown that if some of the basic assumptions of the Langmuir model are modified, e.g., if adsorbent surface heterogeneity or interactions between adsorbate molecules are assumed, both of which result in a non-uniform heat of adsorption, then the experimental variation in the Langmuir rate constants can be predicted. It is concluded that a model in which the reactant adsorbs onto the surface with a non-uniform heat of adsorption, reacts, and then the product desorbs from the surface, with the surface reaction being the rate-controlling step, is the best explanation of the ortho-para-hydrogen shift reaction.

This abstract is approved as to form and content. I recommend its publication.

Signed Paul L. Barrick  
Faculty member in charge of dissertation

## TABLE OF CONTENTS

CHAPTER		PAGE
I	Introduction - - - - -	1
II	Previous Work - - - - -	7
III	Theory	
	A. General - - - - -	13
	B. Surface Mechanisms - - - - -	14
	C. Langmuir Kinetics - - - - -	17
	D. Simultaneous Steps Controlling - - -	19
	1. Two Steps Controlling - - - - -	20
	2. No Steps Controlling - - - - -	21
	E. A Variation of Temkin Kinetics - - -	22
	F. Elovich Kinetics - - - - -	25
	G. Freundlich Kinetics - - - - -	27
	H. The Integrated Rate Equations	
	1. The General Rate Equation - - - -	29
	2. Importance of the Reversible Reaction - - - - -	30
	3. Integration of the Langmuir Rate Equation - - - - -	32
	4. Integration of the Modified Temkin, Elovich, and Freundlich Rate Equations - - - - -	39
IV	Apparatus and Procedure - - - - -	43
V	Results - - - - -	47
VI	Discussion of Results	
	A. Freundlich Kinetics - - - - -	51
	B. Modified Temkin Kinetics - - - - -	57
	C. Elovich Kinetics - - - - -	60
	D. Langmuir Kinetics - - - - -	72
	E. First-Order Kinetics - - - - -	87

CHAPTER	PAGE
VII	Conclusions
	A. Comparison of Models - - - - - 94
	B. Significance of Project - - - - - 96
VIII	Recommendations of Further Work - - - - - 98
IX	Notation - - - - - 102
X	Bibliography - - - - - 104
XI	Appendices
	A. Adsorption Phenomena
	1. Adsorption - - - - - 109
	2. Desorption - - - - - 113
	3. Adsorption Isotherms - - - - - 114
	4. Adsorption of Mixtures - - - - - 125
	B. The Separation Factor - - - - - 131
	C. Diffusion
	1. Bulk Diffusion - - - - - 141
	2. Pore Diffusion - - - - - 144
	D. Space Velocity Curves from Langmuir Rate Equations - - - - - 153
	E. Space Velocity Curves from Elovich Rate Equation - - - - - 160
	F. Langmuir Rate Plots - - - - - 168
	G. Elovich Rate Plots - - - - - 184
	H. Data - - - - - 197

## LIST OF FIGURES

FIGURE		PAGE
1	Schematic of Apparatus - - - - -	44
2	Space Velocities from Langmuir Rate Equation for Runs 68 and 69 - - - - -	48
3	Freundlich Plot for Run 68 - - - - -	52
4	Freundlich Plot for Run 69 - - - - -	53
5	Space Velocities from Freundlich Rate Equation for Runs 68 and 69 - - - - -	54
6	Modified Temkin Plot for Run 68 - - - - -	58
7	Modified Temkin Plot for Run 69 - - - - -	59
8	Elovich-Adsorption Controlling - Plot for Run 68 - - - - -	62
9	Elovich-Desorption Controlling - Plot for Run 68 - - - - -	63
10	Elovich-Desorption Controlling - Plot for Run 69 - - - - -	64
11	Elovich Plot for Run 68 - - - - -	66
12	Elovich Plot for Run 69 - - - - -	67
13	Elovich Rate Constant as a Function of Pressure - - - - -	71
14	Langmuir Plot for Run 68 - - - - -	73
15	Langmuir Plot for Run 69 - - - - -	74
16	Rate Constant $k$ as a Function of Pressure - - - - -	88
17	Rate Constant $k'$ as a Function of Pressure - - - - -	89
18	First-Order Plot for Run 68 - - - - -	91
19	First-Order Plot for Run 69 - - - - -	92
20	First-Order Space Velocity Curves for Runs 68 and 69 - - - - -	93
21	Langmuir Adsorption Plot - - - - -	120
22	Temkin Adsorption Plot - - - - -	121
23	Freundlich Adsorption Plots - - - - -	122

LIST OF FIGURES (Continued)

FIGURE	PAGE
24	Space Velocities from Langmuir Rate Equation for Runs 60 and 61 - - - - - 154
25	Space Velocities from Langmuir Rate Equation for Runs 65 and 66 - - - - - 155
26	Space Velocities from Langmuir Rate Equation for Runs 70 and 71 - - - - - 156
27	Space Velocities from Langmuir Rate Equation for Runs 72 and 73 - - - - - 157
28	Space Velocities from Langmuir Rate Equation for Runs 76 and 77 - - - - - 158
29	Space Velocities from Langmuir Rate Equation for Runs 80 and 81 - - - - - 159
30	Space Velocities from Elovich Rate Equation for Runs 60 and 61 - - - - - 161
31	Space Velocities from Elovich Rate Equation for Runs 65 and 66 - - - - - 162
32	Space Velocities from Elovich Rate Equation for Runs 68 and 69 - - - - - 163
33	Space Velocities from Elovich Rate Equation for Runs 70 and 71 - - - - - 164
34	Space Velocities from Elovich Rate Equation for Runs 72 and 73 - - - - - 165
35	Space Velocities from Elovich Rate Equation for Runs 76 and 77 - - - - - 166
36	Space Velocities from Elovich Rate Equation for Runs 80 and 81 - - - - - 167
37	Langmuir Plot for Run 60 - - - - - 169
38	Langmuir Plot for Run 61 - - - - - 170
39	Langmuir Plot for Run 65 - - - - - 171
40	Langmuir Plot for Run 66 - - - - - 172
41	Langmuir Plot for Run 70 - - - - - 173
42	Langmuir Plot for Run 71 - - - - - 174
43	Langmuir Plot for Run 72 - - - - - 175

LIST OF FIGURES (Continued)

FIGURE		PAGE
44	Langmuir Plot for Run 73 - - - - -	176
45	Langmuir Plot for Run 76 - - - - -	177
46	Langmuir Plot for Run 77 - - - - -	178
47	Langmuir Plot for Run 80 - - - - -	179
48	Langmuir Plot for Run 81 - - - - -	180
49	Langmuir Plot for Run 82 - - - - -	181
50	Langmuir Plot for Run 83 - - - - -	182
51	Langmuir Plot for Run 85 - - - - -	183
52	Elovich Plot for Run 60 - - - - -	185
53	Elovich Plot for Run 61 - - - - -	186
54	Elovich Plot for Run 65 - - - - -	187
55	Elovich Plot for Run 66 - - - - -	188
56	Elovich Plot for Run 70 - - - - -	189
57	Elovich Plot for Run 71 - - - - -	190
58	Elovich Plot for Run 72 - - - - -	191
59	Elovich Plot for Run 73 - - - - -	192
60	Elovich Plot for Run 76 - - - - -	193
61	Elovich Plot for Run 77 - - - - -	194
62	Elovich Plot for Run 80 - - - - -	195
63	Elovich Plot for Run 81 - - - - -	196

LIST OF TABLES

TABLE		PAGE
I	Summary of Langmuir Rate Expressions - - -	33
II	Freundlich Rate Constants as a Function of n - - - - -	55
III	Elovich Rate Constants - - - - -	68
IV	Constants for Langmuir Rate Expression - -	76
V	Properties of Constants k and k' - - - - -	81
VI	Behavior of k*, A, B, and D with changes in $\int \theta_H$ - - - - -	83
VII	Separation Factors - - - - -	136

## I. INTRODUCTION

This paper presents the results of an experimental study into the catalytic rate of conversion between ortho-hydrogen and parahydrogen. The purpose of the investigation was to compare various reaction-rate mechanisms and determine which gives the best representation of what is happening on the catalytic surface. In order to better achieve this goal, the reaction was run in both directions.

The existence of two different forms of molecular hydrogen can be predicted by consideration of the nuclear rotational partition functions for molecular hydrogen. This fact was first noticed in 1927 by Dennison [19], Heisenberg [33], and Hund [35], who predicted the existence of the para form (in which the nuclear spins are pictured as being anti-parallel) and the ortho form (in which the nuclear spins are parallel). These workers showed that the ratio of ortho- to parahydrogen in an equilibrium mixture is a function of temperature and that the equilibrium composition-temperature relationship could be predicted purely from statistical mechanical considerations. In 1929 Bonhoeffer and Harteck [5] and McLennan and McLeod [45] experimentally verified Dennison's findings and also showed that the exchange between the two forms could be catalytically promoted.

Since that time considerable effort has been expended in studying the ortho-para-hydrogen transition. There have been two principal reasons for doing so. The first has been that since the reaction itself is simple, it is an ideal one for studying catalytic mechanisms and reaction routes. There are only two molecules involved in the conversion, hence, no side reactions are possible, and there

is no volume change upon reaction. Heat effects are relatively small (the heat of reaction is  $338 \text{ cal g-mole}^{-1}$  at  $77^\circ\text{K}$ ) and thus, isothermality of reaction conditions should be relatively easy to maintain. It is relatively easy to obtain a pure stream and a difference in thermal conductivity between the ortho- and para- forms makes the analysis of the sample relatively easy.

The second reason for studying the ortho-parahydrogen reaction concerns the expanding need for liquid hydrogen in recent years. This has resulted in two general directions of effort. The first is the search for catalysts which will promote the reaction more effectively. The second is the acquisition of design data for hydrogen liquifiers. This situation comes about because of the energy difference between the ortho and para states and because of the composition-temperature relationship. The ortho state is the high energy state and is the dominating state at high temperatures ( $> 150^\circ\text{K}$ ). At liquid hydrogen temperatures ( $20^\circ\text{K}$ ) the equilibrium is shifted to the para state. The reaction



is exothermic, but is quite slow if allowed to proceed in a homogeneous phase. If the conversion is not catalytically promoted at the time of liquefaction, the homogeneous liquid-phase transition will gradually occur and since the heat of reaction is greater than the heat of vaporization the liquid will boil off as the reaction progresses. Thus, studies of the rate of conversion of ortho- to parahydrogen are necessary.

Among the workers who have investigated the mechanism of the reaction, there appears to be some disagreement on the mechanism. Most early investigators found that their data could be represented by a first-order rate law. Some of the more recent workers have shown that a first-order rate law did not adequately describe their data.

One of the objectives of the present paper is to examine the assumptions that lead to first-order kinetics and determine whether or not these assumptions remain valid for the present catalyst. As the reaction is reversible, it is very useful to study the kinetics in both directions for several reasons. First, much of the difficulty in obtaining a mechanism for the reaction has been that no single investigator has studied the forward and reverse reactions at the same time using the same catalyst under identical conditions of pressure and temperature. The result has been that a first-order mechanism has been used more often to represent the forward reaction, i.e., ortho to para conversion, and the reverse reaction or "back conversion," i.e., para to ortho, has not been correlated as well by first-order kinetics (Cf. Keeler, et. al. [40]). Secondly, studies of both forward and reverse reactions can be used to corroborate one another. According to the principle of microscopic reversibility, the reaction must proceed via the same mechanism in both directions. Thus the same mechanism should be obtained for forward and reverse reactions.

There are several phenomena that are associated with a catalytic reaction mechanism. Each of these affects the rate of reaction to a greater or lesser extent, depending upon the particular reaction which is under study. The

effects of each of these separate phenomena on the rate must be examined and fully understood by the experimentalist in order that he may present the complete picture of the kinetics. Principally, there are four effects that must be considered: interparticle (bulk) diffusion, intraparticle (pore) diffusion, adsorption and desorption, and surface reaction. The latter two fall into the broader category of what will be referred to in the present work as "surface kinetics." The present investigation is concentrated upon the topic of surface kinetics, as the operating conditions for the present series of experiments were chosen so as to be outside the realm of diffusion effects. (The methods of attack that have been used on these problems are outlined in Appendix C.)

Adsorption and desorption represent the forward and reverse processes of the same phenomenon. Since there is no per se chemical reaction involved in these processes, it is possible to study them outside the realm of the chemical reaction. However, such studies constitute a separate task in themselves and are outside the scope of the present work. They are included here in only as they contribute to the overall reaction rate model. An abbreviated discussion of some of the more well-known theories of adsorption and desorption is contained in Appendix A.

In particular, there are three commonly accepted models of adsorption and desorption. The difference in these three lies in the manner in which the molecules are assumed to adsorb onto the surface and the way in which the molecules thereby affect the heat of reaction. One of these models pictures a uniform surface with no molecular interactions on the surface. The other two assume

different types of non-uniform surfaces. Rate equations will be derived based upon each of these three models of adsorption and the data will be correlated against these equations in order to explain which of the three is the most likely one to be encountered in the reaction.

The surface reaction itself represents, at one extreme, a chance for the researcher to delve into the finer points of quantum and perhaps statistical mechanics in order to determine how the actual conversion of an ortho- to a parahydrogen molecule occurs. However, the concern in the present work is not the actual molecular interactions that occur on the surface, but rather how these interactions affect the overall kinetic mechanism.

This investigation examines the factors that contribute to the rate law--namely adsorption of the reactant, surface reaction, and desorption of the product--how the various possible combinations of these factors affect the resulting rate equation and how well the rate equations obtained predict the experimental behavior of the ortho-parahydrogen shift reaction.

In kinetics work, the most frequent approach has been to postulate that these three steps, i.e., adsorption, surface reaction, and desorption, occur in sequence, and that one of them controls the rate of reaction. The form of the rate law corresponding to this assumption is then examined and compared with the experimental results. In many studies, adsorption onto a uniform surface has been used as a basis for development and the rate expressions are derived from the point. In the present work, the effects of both uniform and a non-uniform surface upon the rate laws are examined. This is considered to be necessary

because most adsorption data are shown to be better correlated by laws which assume a non-uniform type of surface coverage than by those in which a uniform surface is assumed [44], including the hydrogen-ferric oxide gel system studied in the present investigation [15]. The data for the hydrogen-ferric oxide gel system are discussed in Appendix A. The chief reason for the assumption of a uniform surface in kinetics work has been that the resulting rate expressions have been much more amenable as a means of correlating data and developing design equations than have expressions which are developed from the assumption of a non-uniform surface.

It is also possible that the hypothesis of there being a rate-controlling step does not necessarily hold. This premise will be examined for the case of a uniform surface in order to determine how such an assumption may affect the rate law.

The purpose of this investigation is thus to study the most frequently used kinetic models for developing rate equations, apply them to one of the simplest known reactions, and compare the results of these models with experimental data. In this way, insight into the validity of these models may be gained, and the reaction mechanism of the catalytically promoted ortho-parahydrogen shift reaction may be elucidated.

## II. PREVIOUS WORK

Ever since the discovery of two forms of molecular hydrogen [19, 33, 35], much work has been performed in studying the rate of conversion between them. There are several reviews available which present this work. Barrick and Brown [1] have compiled a literature survey of the subject and Trapnell [55] and Schmauch and Singleton [51] have reviewed in detail the work that has been performed to date on the kinetics of the reaction.

Most investigators have reported that their data can be represented by a first-order rate expression as shown by Eq. (1).

$$r = k_r (c_o - c_{oe}) = k_r (c_{pe} - c_p) \quad (1)$$

where

$r$  = reaction rate, g-mole  $\text{min}^{-1} \text{cm}^{-3}$  catalyst.

$c_o, c_p$  = ambient ortho and parahydrogen concentrations, respectively, g-moles  $\text{cm}^{-3}$ .

$c_{oe}, c_{pe}$  = equilibrium ortho and parahydrogen concentrations, respectively, g-moles  $\text{cm}^{-3}$ .

$k_r$  = reaction rate constant,  $\text{min}^{-1}$ .

Among the later investigators who have reported that their rate data could be correlated by a first-order rate law are Harrison and McDowell [27, 28], who studied the reverse reaction (para- to orthohydrogen) over  $\alpha\alpha$ -diphenyl- $\beta$ -picryl hydrazyl, zinc oxide, and mixtures of the two at pressures from 25 torr to 56 torr and at temperatures from 90°K to 290°K. Chapin and Johnston [13] also reported first-order kinetics for the forward reaction over a chromia-alumina catalyst at temperatures from 55 to 195°K

at a pressure of 28 atm., and over the pressure range 5-100 atm. at 77°K. Buyanov [10, 11, 12] reported first-order rate constants for the forward conversion over ten different catalysts at temperatures of 64°K and 78°K and at pressures from 60 torr to 150 atm. Weitzel, Blake, and Konecnik [57] reported that at a temperature of 76°K and a pressure of 22.2 psia, the forward reaction over a hydrous ferric oxide gel catalyst appeared to follow first-order kinetics. Similar results were obtained by Wakao, Selwood, and Smith [56], who studied the forward reaction over a nickel on aluminum oxide catalyst at 77°K and over the pressure range 55 to 415 psia. The first two of the studies above were carried out in static systems, while the latter three were conducted with flow systems.

Among the later investigators, however, there is not universal agreement that the reaction is actually a simple first-order reaction at cryogenic temperatures. When Weitzel, et. al. [57] studied the reverse reaction, they found a deviation from first-order kinetics, which they had not noticed in their forward conversion data. According to the principle of microscopic reversibility, if an overall first-order rate law specifies the mechanism of the reaction, it should be obeyed in both directions. In a later paper, Keeler, Weitzel, Blake, and Konecnik [40] reported deviations from first-order kinetics in their data for the forward conversion over ferric oxide gel catalyst at 76°K and pressures in the range 17 to 312 psia.

Cunningham and Johnston [16] in their study of the forward (ortho- to para) reaction in the liquid phase at 20°K over alumina-supported ferric oxide and chromic oxide catalysts, derived an equation which can be expressed in

the form

$$r = \frac{k(c_{pe} - c_p)}{1 + k'c_p} \quad (2)$$

The results of Cunningham and Johnston were well-correlated by the integrated form of Equation (2) and were not particularly well explained by the integrated form of the first-order rate expression Eq. (1). Hutchinson [36] also found that his data for the gas phase reverse reaction over a ferric oxide gel catalyst in the temperature range 40 to 80°K and in the pressure range 42 to 1012 psia were better represented by Eq. (2) than Eq. (1). It is reported by Clark, Kucirka, Jambhekar, and Schmauch [14] that there is some deviation from first order in their data for the forward conversion over three very active catalysts at temperatures from 74 to 91°K. They ascribe this deviation to diffusion effects. It appears upon examination of the literature that most of the workers who have observed deviations in the reaction from first-order kinetics have been working with very active catalysts and, in the case of Cunningham and Johnston [16], at high hydrogen concentrations. The significance of this fact is that there is probably a higher degree of surface coverage by the hydrogen than was observed by the earlier workers. It will be shown in Section III that under conditions of low surface coverage, it is indeed possible to observe a first-order reaction, and that at higher surface coverages, a first-order rate law should not result.

There are three steps involved in the surface mechanism--adsorption, surface reaction, and desorption.

As far as the surface reaction step is concerned, two fundamental methods of producing an ortho-parahydrogen

transition have been proposed. The first method consists of dissociating the hydrogen molecules and allowing them to recombine [48]. The second involves the interaction between an inhomogeneous magnetic field and the magnetic field that is associated with the nuclear spin of the hydrogen molecule [6]. Although the former has been observed at temperatures as low as liquid air ( $90^{\circ}\text{K}$ ) [26], the dissociation mechanism is generally regarded as being unimportant at temperatures below  $150^{\circ}\text{K}$  [55]. Interaction between the hydrogen molecule and an inhomogeneous magnetic field (such as that found in the region of a paramagnetic molecule), is generally believed to be the mechanism of the surface reaction at cryogenic temperatures [55].

Adsorption and desorption play a major role in the development of a catalytic reaction rate mechanism. Generally, it has been found that the kinetic law will acquire the form of the adsorption law [34,53]. There has been some controversy, however, over the validity of postulating one mechanism as superior to another [7,58]. Weller [58] has pointed out that the classical Langmuir-Hinshelwood approach (which is developed in Section III.C) is based upon the physically unrealistic assumption of an ideal surface. He argues that attempts to explain data on the basis of a Langmuir-Hinshelwood expression are merely empirical curve-fitting rather than corroboration of a theory. He further maintains that one might just as well use an empirical power law rate expression of the Freundlich type in dealing with rate data, as this type of expression (for an irreversible reaction, at least) is much easier to integrate. He also cites three examples of reactions for which the data are correlated as well by a Freundlich-type

expression as by a Langmuir type.

In reply to Weller's arguments, Boudart [7] points out that, while indeed most rate data can be fitted by either type of rate law, there are some advantages to be gained by using the mechanism approach. He argues that better development and control of catalyst and reactor conditions can be obtained if something is known about surface conditions. Both he and Weller cite the case of the ammonia synthesis reaction in developing their arguments. A look at this reaction is instructive.

The synthesis of ammonia from nitrogen and hydrogen over an iron catalyst has been one of the most widely studied of catalyzed reactions. Two reviews that cover the subject (there are others) are those of Frankenburg [23] and Bokhoven, et.al. [4]. Most investigators who have studied the ammonia synthesis agree that the rate can be expressed by Eq. (A).

$$r = k_f p_N \left( \frac{p_H}{p_A} \right)^3 - k_b \left( \frac{p_A}{p_H} \right)^2 \quad (A)$$

where

- $r$  = rate of formation of ammonia
- $k_f, k_b$  = forward and reverse reaction rate constants.
- $p_N$  = partial pressure of nitrogen.
- $p_H$  = partial pressure of hydrogen.
- $p_A$  = partial pressure of ammonia.
- $m, n$  = constants.

Eq. (A) was first derived by Temkin and Pyzhev [54], who assumed that adsorption of nitrogen was the rate-controlling step. However, instead of assuming a Langmuir-type of adsorption, they assumed that the adsorption was of the type

that is explained by a Temkin adsorption isotherm [31]. This isotherm assumes a type of surface on which the heat of adsorption varies linearly with the amount of surface that is covered.

Boudart [7] makes the statement that, under certain conditions, a rate expression which is derived from the Langmuir approach assuming nitrogen adsorption is the rate-controlling step will reduce to the Temkin-Pyzhev expression, Eq. (A). In a later work, Ozaki, Taylor, and Boudart [46] verified this conclusion.

A similar approach will be presented in the present work. Rate equations will be derived which are based upon the Langmuir, Temkin, and Freundlich theories of adsorption. No matter which approach is advocated, the importance of adsorption in formulating rate expressions for catalyzed reactions is agreed upon. Unfortunately, a method for obtaining adsorption data for orthohydrogen and parahydrogen separately has not yet been found. Clark, et.al. [15] have obtained total hydrogen adsorption isotherms for two different catalysts over the temperature range 63 to 194°K. Correlations based upon the three general adsorption isotherms are presented for these data in Appendix A of the present work.

### III. THEORY

#### A. General

Catalytic reactions in which the reactants constitute a separate phase from the catalyst are ordinarily postulated as occurring via a series of individual and separate reaction steps. For a gaseous reaction which is catalyzed by a porous solid, such as the ortho-parahydrogen reaction on ferric oxide gel, these individual reactions take place in the following sequence: (1) The reactants diffuse from the bulk gas phase to the pore mouths and then (2) diffuse into the interior of the solid. (3) The reactants are adsorbed onto the surface, and (4) they react on the surface to form products. The products then follow the reverse order, i.e., they (5) desorb from the surface, (6) diffuse to the exterior surface of the solid, and (7) diffuse from the pore mouths into the bulk gas phase.

The development of a rate equation which included all the above seven steps would be an immense task due to the intractable mathematics involved and the results would probably be unusable in a number of cases, such as reactor design. Hence, there has not been a great deal of effort expended in this direction.

Generally, the procedure has been to perform kinetic experiments outside the realm where diffusion effects are expected [60] and to treat only the surface steps. Appendix C outlines some of the work that has been done on diffusion (both interparticle and intraparticle) in the ortho-parahydrogen shift reaction. The present work was performed in pressure and flow regimes where diffusion effects were not encountered and consequently these effects

will not be considered in the following development. For the three surface reactions, it is usually postulated that one of them is slower than the other two. This step is known as the rate-controlling step. The other two reactions (for a reversible reaction) are said to be in "equilibrium." What is meant is that the reverse reactions proceed at a rate almost equal to their corresponding forward reactions --the only difference between the two being the net forward rate of reaction. The assumption of a rate-controlling step is quite effective in that the mathematical expressions which result are not cumbersome and that useful results can sometimes be predicted. This is the procedure that will be followed subsequently in developing a reaction rate model.

#### B. Surface Mechanisms

The present work was undertaken to study the surface mechanism, or "surface kinetics," which consists of the adsorption, reaction, and desorption steps. The primary concern is with the rates of each of these steps. In general, the rates of adsorption and desorption will depend upon which particular model (Langmuir, Temkin, or Freundlich) is used to describe the manner in which the adsorbate is adsorbed onto the surface of the adsorbent. Appendix A treats in detail the theory of adsorption and desorption and the development of adsorption isotherms. The rate laws for the different adsorption models are also presented in Appendix A and these will be used presently in the development of the reaction rate laws for the ortho-parahydrogen conversion. However, before this can be accomplished, something must be said concerning the

actual surface reaction itself.

It has been stated [cf., 5,6,20,21,22,48] that there are only two types of actual surface mechanisms which will cause the ortho-para transition in hydrogen. These are either dissociation and recombination of the hydrogen molecules, or interaction of the undissociated hydrogen molecule with an inhomogeneous magnetic field. Since the experimental reaction temperatures were quite low (less than 100°K) and the dissociation energy of the hydrogen molecule is relatively high (about 100 kcal [4]), it is considered quite unlikely that dissociation is an important factor in the present series of experiments. Moreover, Wigner [59] and Kalckar and Teller [39] have shown that molecular interaction of hydrogen with an inhomogeneous magnetic field such as one encountered in the region of a paramagnetic molecule or ion will indeed promote the ortho-para transition. In addition, early work on the hydrogen-deuterium exchange [26] showed that -183°C or 90°K is about the lowest temperature at which the exchange took place. Thus, it is quite likely that the surface reaction itself will be a unimolecular surface reaction, with the rate law given by Eq. (3).

$$r_s = k_o \theta_o - k_p \theta_p \quad (3)$$

where

$\theta_o$  = fraction of available surface covered by orthohydrogen molecules.

$\theta_p$  = fraction of available surface covered by parahydrogen molecules.

$k_o, k_p$  = surface rate constants, g-moles min<sup>-1</sup>.

$r_s$  = rate of reaction, g-moles min<sup>-1</sup>.

In all of the subsequent development, it will be assumed that Eq. (3) describes the surface reaction itself.

As it now stands, Eq. (3) is of little direct value in that  $\theta_o$  and  $\theta_p$  cannot be measured directly. Therefore, steps must be taken in order to obtain the rate law in terms of variables which can be measured, i.e.,  $c_o$  and  $c_p$ , the ortho- and parahydrogen gas-phase concentrations respectively.

The only manner in which this can be accomplished is to take into account the adsorption and desorption rates, since the laws which describe these rates provide the relationships between the gas phase and the surface phase concentrations of reactants and products. This is the reason that the adsorption and desorption steps must be included in the category of surface kinetics.

Attention is now focused upon the development of the overall kinetic laws, one of which will be used to describe the rate of the ortho-parahydrogen reaction. Rate laws will be derived based upon each of four well-known adsorption-desorption models--those of Langmuir, Temkin, Elovich, and Freundlich. These models encompass the following three types of surface coverage:

1. Uniform surface with no molecular interactions and constant heat of adsorption.
2. Molecular interactions or non-uniform surface effects such that the heat of adsorption varies linearly with surface coverage.
3. Surface heterogeneity or molecular interactions such that the heat of

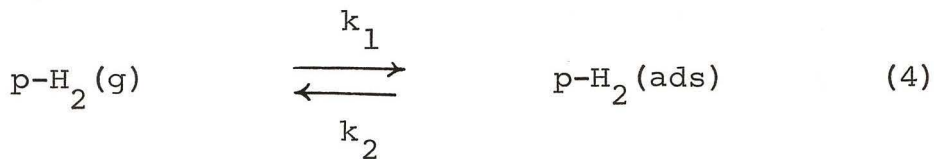
adsorption varies exponentially with surface coverage.

### C. Langmuir Kinetics

The simplest case to treat is that of a uniform surface--the Langmuir-Hinshelwood model. This case for the reverse (para-to-ortho) reaction has been treated in detail in previous works by Barrick, et.al. [2] and Hutchinson [36] but the highlights of the development will be presented here.

If one step is assumed to be rate-controlling, there are three cases to be considered. These are (1) adsorption controlling, (2) surface reaction controlling, and (3) desorption controlling. The method of attack is similar in all cases; the difference lies in the mathematical details. Consequently, the procedure will be illustrated only by a derivation of the case of Langmuir adsorption with the adsorption of parahydrogen step controlling. For the other situations, the final results of the derivations will be presented.

The overall reaction is the conversion of para- to orthohydrogen. The steps are written as follows (At this point these steps as shown imply no particular type of adsorption):





where

$$k_1, k_2, k_3, k_4, k_5, k_6 = \text{rate constants.}$$

For Langmuir kinetics the rate equations which correspond to the reactions given by Eqs. (4), (5), and (6) are

$$r_{\text{ad}} = k_1 c_p (1 - \theta_o - \theta_p) - k_2 \theta_p \quad (7)$$

$$r_s = k_3 \theta_p - k_4 \theta_o \quad (3a)$$

$$r_{\text{des}} = k_5 \theta_o - k_6 c_o (1 - \theta_o - \theta_p) \quad (8)$$

At this point the assumption of a rate-controlling step is brought into use. In the present illustration adsorption of parahydrogen is considered to be the rate-controlling step. Thus, Eqs. (3a) and (8) become

$$k_3 \theta_p = k_4 \theta_o \quad (3b)$$

$$k_5 \theta_o = k_6 c_o (1 - \theta_o - \theta_p) \quad (8a)$$

$\theta_o$  and  $\theta_p$  are eliminated between Eqs. (3b) and (8a) and the results are substituted into Eq. (7). The resulting equation is the rate law for the case of adsorption controlling, which is Eq. (9).

$$r = \frac{k_1 k_3 k_5 c_p - k_2 k_4 k_6 c_o}{k_3 k_5 + (k_3 k_6 + k_4 k_6) c_o} \quad (9)$$

Similar treatments can be worked for the cases of surface reaction controlling and desorption controlling. For the case in which surface reaction controls, Eqs. (7) and (8) are equated to zero. Elimination of  $\theta_o$  and  $\theta_p$  as variables from the resulting equations yields the rate law, Eq. (10), for the case when surface reaction controls.

$$r = \frac{k_1 k_3 k_5 c_p - k_2 k_4 k_6 c_o}{k_2 k_5 + k_1 k_5 c_p + k_2 k_6 c_o} \quad (10)$$

Similarly, the rate law for desorption of orthohydrogen controlling is given by Eq. (11).

$$r = \frac{k_1 k_3 k_5 c_p - k_2 k_4 k_6 c_o}{k_2 k_4 + (k_1 k_3 + k_1 k_4) c_p} \quad (11)$$

#### D. Simultaneous Steps Controlling

The development of rate expressions for the situation in which more than one step is postulated to be rate-controlling has rarely been attempted. The reason for this has already been stated: the mathematics are extremely involved and the resulting expressions are, in general, too cumbersome to handle for normal usage. However, in the case of the ortho-parahydrogen reaction, there is some hope that additional information may be gained if the assumptions of multistep-controlling reactions are put to use. Consequently, the development in the following two sections is presented. It is assumed that Eqs. (7), (3a), and (8) still represent the rates corresponding to the individual steps.

## 1. Two-Steps Controlling

The two-step case results when only one of the three reaction steps (i.e., adsorption, surface reaction or desorption) is assumed to be in equilibrium. Again there are three instances which must be considered, namely those when each of the three steps in its turn is in equilibrium. As in Section III.C, the treatment will be outlined for one case and the results only will be presented for the other two.

The first case that will be considered is if the adsorption step is in equilibrium. Then Eqs. (7), (3a), and (8) become

$$k_1 c_p (1 - \theta_o - \theta_p) = k_2 \theta_p \quad (7a)$$

$$r = k_3 \theta_p - k_4 \theta_o \quad (3a)$$

$$= k_5 \theta_o - k_6 c_o (1 - \theta_o - \theta_p) \quad (8)$$

If  $\theta_p$  and  $\theta_o$  are eliminated between Eqs. (7a) and (8) and the results are substituted into Eq. (3a), the reaction rate is given by Eq. (12)

$$r = \frac{k_1 k_3 k_5 c_p - k_2 k_4 k_6 c_o}{(k_2 k_4 + k_2 k_5) + (k_1 k_3 + k_1 k_4 + k_1 k_5) c_p + k_2 k_6 c_o} \quad (12)$$

The procedure is tedious but not particularly difficult. For the case when surface reaction is in equilibrium, elimination of  $\theta_o$  and  $\theta_p$  between Eqs. (7) and (3b) and substitution of the results into Eq. (8) yields Eq. (13), the desired rate law.

$$r = \frac{k_1 k_3 k_5 c_p - k_2 k_4 k_6 c_o}{(k_2 k_4 + k_3 k_5) + (k_1 k_3 + k_1 k_4) c_p + (k_3 k_6 + k_4 k_6) c_o} \quad (13)$$

A similar treatment can be carried out when the desorption step is in equilibrium. Eq. (14) presents the rate law for this case.

$$r = \frac{k_1 k_3 k_5 c_p + k_2 k_4 k_6 c_o}{(k_2 k_5 + k_3 k_5) + k_1 k_5 c_p + (k_2 k_6 + k_3 k_6 + k_4 k_6) c_o} \quad (14)$$

## 2. No Steps Controlling

The last and most difficult case to be considered results when none of the reactions is assumed to be in equilibrium. Again, Eqs. (7), (3a), and (8) provide the starting point.

$$r = k_1 c_p (1 - \theta_o - \theta_p) - k_2 \theta_p \quad (7)$$

$$= k_3 \theta_p - k_4 \theta_o \quad (3a)$$

$$= k_5 \theta_o - k_6 c_o (1 - \theta_o - \theta_p) \quad (8)$$

If  $\theta_o$  and  $\theta_p$  are eliminated between Eqs. (7) and (8), the results are given by Eqs. (15) and (16).

$$\theta_o = \frac{k_2 k_6 c_o + r(k_2 + k_1 c_p + k_6 c_o)}{k_2 k_5 + k_1 k_5 c_p + k_2 k_6 c_o} \quad (15)$$

$$\theta_p = \frac{k_1 k_5 c_p - r(k_5 + k_1 c_p + k_6 c_o)}{k_2 k_5 + k_1 k_5 c_p + k_2 k_6 c_o} \quad (16)$$

Substitution of Eqs. (15) and (16) into Eq. (3a) yields the result

$$r = \frac{k_1 k_3 k_5 c_p - k_2 k_4 k_6 c_o}{(k_2 k_4 + k_2 k_5 + k_3 k_5) + (k_1 k_3 + k_1 k_4 + k_1 k_5) c_p + (k_2 k_6 + k_3 k_6 + k_4 k_6) c_o} \quad (17)$$

Thus, in the case of the ortho-parahydrogen reaction at least, the equations for the multistep-controlling reactions can be derived. The significance of these results will be discussed later.

#### E. A Variation of Temkin Kinetics

A second case which may be considered in developing a reaction model is suggested by the adsorption rate equations presented in Appendix A.4. These equations attempt to account for not only variation in heat of adsorption with surface coverage, but also effects of interaction between the two species which are being adsorbed. The equations which are involved are transcendental functions, so that the quantities  $\theta_o$  and  $\theta_p$ , which could be found explicitly in terms of  $x$  and  $(1-x)$  in the preceding development, can no longer be solved for directly. The following treatment outlines a method for developing a rate expression using the present type of adsorption for the case when surface reaction controls the overall reaction rate. In this situation, the rate laws are given by Eqs. (18), (3a), and (19).

$$r_{ad} = k_1 c_p (1 - \theta_o - \theta_p) e^{-a_1 \theta_p - a_2 \theta_o} - k_2 \theta_p e^{b_1 \theta_p + b_2 \theta_o} \quad (18)$$

$$r = k_3 \theta_p - k_4 \theta_o \quad (3a)$$

$$r_{des} = k_5 \theta_o e^{b_5 \theta_o + b_6 \theta_p} - k_6 c_o (1 - \theta_o - \theta_p) e^{-a_5 \theta_o - a_6 \theta_p} \quad (19)$$

where

$$a = \alpha / RT \quad (\text{See Appendix A}).$$

$$b = \beta / RT.$$

If surface reaction controls, Eqs. (18) and (19) are set equal to zero and the results are substituted into Eq. (3a). The result is shown in Eq. (20).

$$r = \ln \left[ \frac{\left( \frac{k_1}{k_2} c_p \frac{(1 - \theta_o - \theta_p)}{\theta_p} \right)^{n_1}}{\left( \frac{k_6}{k_5} c_o \frac{(1 - \theta_o - \theta_p)}{\theta_o} \right)^{n_2}} \right] \quad (20)$$

where

$$n_1 = [k_3 (b_2 + a_2) + k_4 (b_1 + a_1)] / [(b_5 + a_5) (b_1 + a_1) - (b_6 + a_6) (b_2 + a_2)].$$

$$n_2 = [k_3 (b_5 + a_5) + k_4 (b_6 + a_6)] / [(b_5 + a_5) (b_1 + a_1) - (b_6 + a_6) (b_2 + a_2)].$$

At equilibrium,  $r = 0$ , and  $x = x_e$ ,  $\theta_p = \theta_{pe}$ , and  $\theta_o = \theta_{oe}$ . Thence, Eq. (20) takes the form of Eq. (20a).

$$\left[ \frac{k_1 c_{pe} (1 - \theta_{oe} - \theta_{pe})}{k_2 \theta_{pe}} \right]^{n_1} = \left[ \frac{k_6 c_{oe} (1 - \theta_{oe} - \theta_{pe})}{k_5 \theta_{oe}} \right]^{n_2} \quad (20a)$$

Substitution of Eq. (20a) into Eq. (20) yields the rate law, Eq. (21).

$$r = k \ln \left\{ \left[ \frac{x(1-\theta_o - \theta_p)\theta_{pe}}{x_e(1-\theta_{oe} - \theta_p)\theta_p} \right]^n \left[ \frac{(1-x_e)(1-\theta_{oe} - \theta_{pe})\theta_o}{(1-x)(1-\theta_o - \theta_p)\theta_{oe}} \right] \right\} \quad (21)$$

where

$$k = n_2.$$

$$n = n_1/n_2.$$

The separation factor  $s$  is defined as (See Appendix B)

$$s = \frac{\frac{\theta_o}{\theta_p}}{\frac{c_o}{c_p}} = \frac{\frac{\theta_{oe}}{\theta_{pe}}}{\frac{c_{oe}}{c_{pe}}} \quad (22)$$

Eq. (22) may be used to eliminate  $\theta_o$ ,  $\theta_p$ ,  $\theta_{oe}$ , and  $\theta_{pe}$  from Eq. (21). It is also assumed that  $(1-\theta_o - \theta_p)$  equals  $(1-\theta_{oe} - \theta_{pe})$ . The result is given by Eq. (23).

$$r = k \ln \left\{ \left[ \frac{s(1-x) + x}{s(1-x_e) + x_e} \right]^n \left[ \frac{s(1-x_e) + x_e}{s(1-x) + x} \right] \right\}$$

$$= k(n-1) \ln \left[ \frac{s(1-x) + x}{s(1-x_e) + x_e} \right] \quad (23)$$

Eq. (23) will be known in this work as the modified Temkin rate expression, although there is no record of his having developed such an expression. The adsorption process which was used herein is similar (for the separate species) to that which is used in developing the Temkin adsorption isotherm [31].

## F. Elovich Kinetics

The next case to which the technique of combining the adsorption and reaction models will be applied is that where the rate of adsorption is described by the Elovich equation. As Low [44] points out, there is not a unique derivation of the Elovich equation, so that a rigorous theoretical interpretation may not be ascribed to those systems which obey it, but it has been found to describe adsorption rate data for a large number of systems and hence will be presented herein. The equations which are subsequently derived cannot be taken as rigorous, as no account is taken of the effect of the presence of one specie on the rate of adsorption of the second specie. However, the results may serve to suggest a relation which may serve as a good empirical representation of the data.

The reactions themselves may, as before, be represented by Eqs. (4), (5), and (6). Likewise, the surface reaction itself is still assumed to be first-order, as represented by Eq. (3a). The rates of adsorption and desorption are now governed by an equation of the Elovich type [29,44] (Appendix A). The rate laws are given by Eqs. (24), (3a), and (25).

$$r_{ad} = k_1 c_p e^{-\alpha_1 \theta_p / RT} - k_2 e^{\beta_1 \theta_p / RT} \quad (24)$$

$$r_s = k_3 \theta_p - k_4 \theta_o \quad (3a)$$

$$r_{des} = k_5 e^{\beta_2 \theta_o / RT} - k_6 c_o e^{-\alpha_2 \theta_o / RT} \quad (25)$$

where

$\alpha, \beta$  = constants as defined in Appendix A.

$R$  = gas constant =  $1.998 \text{ cal g-mole}^{-1} \text{ } ^\circ\text{K}^{-1}$ .

$T$  = temperature,  $^\circ\text{K}$ .

The subsequent treatment of Eqs. (24), (3a), and (25) is identical to the treatment of Eqs. (7), (3a), and (8) above in that one step is assumed to be rate-controlling, the remaining two are assumed to be in equilibrium.

The results of the algebraic manipulations of Eqs. (24), (3a), and (25) are given by Eqs. (26), (27), and (28), which show the rate equations when adsorption, surface reaction, and desorption, respectively, control the rate of reaction.

$$r = k_d \left[ \frac{x}{x_e} \left( \frac{1-x}{1-x_e} \right)^{-a_1} - \left( \frac{1-x}{1-x_e} \right)^{b_1} \right] \quad (26)$$

$$r = \ln \left[ \left( \frac{x}{x_e} \right)^{\frac{k_3}{b_1 + a_1}} \left( \frac{1-x}{1-x_e} \right)^{\frac{k_4}{b_2 + a_2}} \right] \quad (27)$$

$$r = k_f \left[ \left( \frac{x}{x_e} \right)^{b_2} - \left( \frac{1-x}{1-x_e} \right) \left( \frac{x}{x_e} \right)^{-a_2} \right] \quad (28)$$

where

$$a_1 = \alpha_1 / RT.$$

$$a_2 = \alpha_2 / RT.$$

$$b_1 = \beta_1 / RT.$$

$$b_2 = \beta_2 / RT.$$

$k_d, k_f$  = reaction rate constants,  $\text{g-mole cm}^{-3} \text{ min}^{-1}$ .

$k_d$ , and  $k_f$  are proportional to the total hydrogen concentration,  $c_H$ , raised to some power  $n$ , where  $n$  is a function of the rate constants of Eqs. (24), (3a), and (25).

The case of Elovich kinetics cannot, unfortunately, be further enlarged by attempts to develop a rate expression when more than one step controls the reaction rate, as was done in the case of Langmuir-Hinshelwood kinetics. The reason for this is that transcendental functions are involved and the algebra shows no promise of being able to produce an explicit expression for  $r$  in terms of  $c_p$ , etc. Therefore, attention is turned to the final case that will be considered in the present work.

#### G. Freundlich Kinetics

The development in Appendix A is an attempt to provide a theoretical justification for the empirical Freundlich isotherm. Although the development makes use of some rather broad (and perhaps questionable) assumptions, the Freundlich isotherm (and rate equation) have often proved useful as a means of correlating data. This is particularly true for irreversible reactions. However, the development will be carried out for the reversible reaction, since the hydrogen adsorption data of Clark, et.al. [15] were found to be more nearly correlated by a Freundlich isotherm than by the Langmuir or Temkin isotherms (Appendix A). Again, as with the Elovich case, the results should not be given a strict theoretical interpretation, but should be taken as a possible good empirical correlation.

The procedure is analogous to that which was used in deriving the Langmuir and Elovich rate laws. The reactions

are again given by Eqs. (4) through (6). The adsorption rates are now based upon the Freundlich adsorption isotherm. The rate equations are given by Eqs. (29), (3a), and (30).

$$r_{ad} = k_1 c_p^{1/n} - k_2 \theta_p \quad (29)$$

$$r_s = k_3 \theta_p - k_4 \theta_o \quad (3a)$$

$$r_{des} = k_5 \theta_o - k_6 c_o^{1/m} \quad (30)$$

where

$m, n =$  constants as defined in Appendix A.

However, in the case of the Freundlich isotherm, the same form of rate law is obtained no matter which step is assumed to be rate-controlling. This is true because there is no experimental way to distinguish between the constants  $k_1$  through  $k_6$ . The rate law is given by Eq. (31).

$$r = k c_H^{1/n} \left[ x^{1/n} - x_e^{1/n} \left( \frac{1-x}{1-x_e} \right)^{1/m} \right] \quad (31)$$

Again, as in the case of Elovich kinetics, the case when more than one reaction controls is extremely difficult to treat analytically and is not considered.

The problem now arises of experimental determination of which of the above rate laws best describes the surface kinetics of the ortho-parahydrogen reaction. The development below outlines the method of attack which was used on this problem.

## H. The Integrated Rate Equations

### 1. The General Rate Equation

The previous sections have shown how the various possible rate laws can be predicted. The question remains of determining which of these rate laws best explains the experimental data.

In the present series of experiments, an isothermal, plug-flow, integral reactor was used to collect the data. The rate expression for a differential plug-flow reactor has been presented in several places (e.g., 42, 52, 60). It is given by Eq. (32).

$$-r \, dV_r = F \, c_H \, dx \quad (32)$$

where

$-r$  = rate of disappearance of parahydrogen,  
g-moles<sup>-1</sup> min<sup>-1</sup> (cm catalyst)<sup>-3</sup>.

$V_r$  = volume of catalyst, cm<sup>3</sup>.

$F$  = total feed rate, cm<sup>3</sup> hydrogen min<sup>-1</sup>.

$c_H$  = total hydrogen concentration, g-moles cm<sup>-3</sup>.

$x$  = mole fraction parahydrogen.

The task is the integration of Eq. (31). In order to accomplish this, Eq. (32) is rearranged slightly as follows:

$$\begin{aligned} -r &= F c_H \frac{dx}{dV_r} \\ &= c_H \frac{dx}{d(V_r/F)} \\ &= c_H \frac{dx}{d\tau} \end{aligned} \quad (32a)$$

The variable  $\tau$  is known as the "space time" [41] and is the

reciprocal of the space velocity,  $(F/V_r)$ .

The expressions that have been derived previously for  $r$  are substituted, one at a time, into Eq. (32a) and the resulting equations are integrated. The integration limits are  $x = x_1$  at  $\tau = 0$  (mole fraction parahydrogen at the reactor entrance) and  $x = x_2$  at  $\tau = \tau$  (mole fraction parahydrogen at the reactor exit).  $x_2$  and  $\tau$  are the experimentally measured variables, so that the integrated form of Eq. (32a) provides a relationship between  $x_2$  and  $\tau$  against which the experimental data may be checked to see if a correlation exists. The details of this process are made clear below. Before these details are presented, it is necessary that one understands the significance of the reversible reaction.

## 2. Importance of the Reversible Reaction

A great many reactions may be considered as being irreversible, both in the kinetic and thermodynamic sense. This is so because the thermodynamic equilibrium of these reactions is so far displaced in one direction that the equilibrium concentrations of reactant molecules are insignificant compared to the product concentrations. When these cases are encountered, the rate laws can take on relatively simple forms and the integration of Eq. (31a) sometimes presents little difficulty.

However, such is not the case with the ortho-parahydrogen reaction. Only for the case of low temperatures ( $< 30^\circ\text{K}$ ) and the reaction



is the equilibrium concentration of reactant negligible in

comparison to the equilibrium concentration of product. The present series of experiments were conducted at approximately 75°K and at this temperature, the equilibrium mixture consists of an approximately 51:49 ratio of para- to orthohydrogen. This fact provides both an advantage and a disadvantage to studying the reaction rate. The disadvantage is that the reaction can in no way be considered irreversible, and while not a serious drawback, this does complicate the integration of Eq. (32a) due to the nature of the rate laws. The advantage is that the reaction may be carried out in both directions merely by providing either an orthohydrogen-rich or parahydrogen-rich feed stream.

Considerable advantage may be had by running both reactions: the main reason is that it may be used in order to verify the reaction mechanism. According to the principle of microscopic reversibility, if the reaction proceeds via a certain mechanism in one direction, then it must proceed via exactly the same mechanism in the opposite direction. For example, if adsorption of orthohydrogen is the slow step in the ortho-to-para conversion, then desorption of orthohydrogen must be the slow step in the para-to-ortho conversion. The implication of this fact is that the rate laws which were derived above for the para-to-ortho conversion must be identical for the ortho-to-para conversion. Thus, no matter which direction the reaction is run, for a given pressure and temperature, the same constants should be obtained from the data. If they are not, then the assumed mechanism is not correct.

At this point it is well to note that it is possible, based on the above development, that an incorrect conclusion could be drawn from the data if the reaction were to

be run in one direction only. For example, one might achieve a correlation by using the Elovich rate law for adsorption of parahydrogen controlling (Eq. 26). He would obtain three constants from his data and go on to say that this was the mechanism. He might also notice that another rate law, such as one based on a Langmuir-Hinshelwood development, appeared to correlate his data. However, without prior information, he concluded that the Elovich approach gave better results. However, if now someone came along with data for the reverse reaction and showed that the three constants that he obtained using the same rate law were entirely different from those of the first investigator, whereas his constants based upon the Langmuir equation appeared to be essentially in agreement with those obtained by the first investigator, the conclusion would be that the Langmuir correlation was the correct one and not the Elovich.

The above development has shown that there is a definite advantage to running the reaction in both directions and what that advantage is. Attention is returned to the task of integrating the rate equations.

### 3. Integration of the Langmuir Rate Equation

Table I lists all the Langmuir rate expressions that have been previously derived. Upon examination of these expressions, it is obvious that they are all of the form

$$r = \frac{k_1 k_3 k_5 c_p - k_2 k_4 k_6 c_o}{A + Bc_p + Dc_o} \quad (33)$$

where

A, B, and D are different combinations of the rate constants  $k_1$  through  $k_6$ , depending upon which rate

Table I. Summary of Langmuir Rate Expressions

## A. Basic equations.

$$r_a = k_1 c_p (1 - \theta_o - \theta_p) - k_2 \theta_p$$

$$r_s = k_3 \theta_p - k_4 \theta_o$$

$$r_d = k_5 \theta_o - k_6 c_o (1 - \theta_o - \theta_p)$$

## B. Rate equations.

1. Adsorption controls.  $r_s = r_d = 0$ ;  $r_a = r$ .

$$r = \frac{k_1 k_3 k_5 c_p - k_2 k_4 k_6 c_o}{k_3 k_5 + (k_3 k_3 + k_4 k_6) c_o}$$

2. Surface reactions controls.  $r_a = r_d = 0$ ;  $r_s = r$ .

$$r = \frac{k_1 k_3 k_5 c_p - k_2 k_4 k_6 c_o}{k_2 k_5 + k_1 k_5 c_p + k_2 k_6 c_o}$$

3. Desorption controls.  $r_a = r_s = 0$ ;  $r_d = r$ .

$$r = \frac{k_1 k_3 k_5 c_p - k_2 k_4 k_6 c_o}{k_2 k_4 + (k_1 k_3 + k_1 k_4) c_p}$$

4. Adsorption in equilibrium.  $r_a = 0$ ;  $r_s = r_d = r$ .

$$r = \frac{k_1 k_3 k_5 c_p - k_2 k_4 k_6 c_o}{(k_2 k_4 + k_2 k_5) + (k_1 k_3 + k_1 k_4 + k_1 k_5) c_p + k_2 k_6 c_o}$$

5. Surface reaction in equilibrium.  $r_s = 0$ ;  $r_a = r_d = r$ .

$$r = \frac{k_1 k_3 k_5 c_p - k_2 k_4 k_6 c_o}{(k_2 k_4 + k_2 k_5) + (k_1 k_3 + k_1 k_4) c_p + (k_3 k_6 + k_4 k_6) c_o}$$

Table I. Continued

6. Desorption in equilibrium.  $r_d = 0$ ;  $r_a = r_s = r$ .

$$r = \frac{k_1 k_3 k_5 c_p - k_2 k_4 k_6 c_o}{(k_2 k_5 + k_3 k_5) + k_1 k_5 c_p + (k_2 k_6 + k_3 k_6 + k_4 k_6) c_o}$$

7. No step controls.  $r_a = r_s = r_d = r$ .

$$r = \frac{k_1 k_3 k_5 c_p - k_2 k_4 k_6 c_o}{(k_2 k_4 + k_2 k_5 + k_3 k_5) + (k_1 k_3 + k_1 k_4 + k_1 k_5) c_p + (k_2 k_6 + k_3 k_6 + k_4 k_6) c_o}$$

expression is under consideration. Eq. (32) may be rearranged slightly to the form

$$r = \frac{\frac{k_1 k_3 k_5 c_H}{c_{oe}} (c_p - c_{pe})}{A + Bc_p + Dc_o}$$

$$= \frac{k^* (c_p - c_{pe})}{A + Bc_p + Dc_o} \quad (32a)$$

where

$$k^* = k_1 k_3 k_5 c_H / c_{oe}.$$

$$c_H = \text{total hydrogen concentration, g-mole cm}^{-3}.$$

$$c_{pe} = \text{equilibrium parahydrogen concentration, g-mole cm}^{-3}.$$

$$c_{oe} = \text{equilibrium orthohydrogen concentration, g-mole cm}^{-3}.$$

Since  $c_p + c_o = c_H$ , Eq. (32a) may be further rearranged to

$$r = \frac{k(c_p - c_{pe})}{1 + k' c_p} \quad (33b)$$

where

$$k = k^* / (A + Dc_H).$$

$$k' = (B-D) / (A + Dc_H).$$

Finally, Eq. (33b) may be put in terms of  $x$ , the mole fraction parahydrogen, in the following manner:

$$r = \frac{kc_H(x - x_e)}{1 + k'c_Hx} \quad (33c)$$

It should be noted at this point that the constant  $k'$  can be either positive or negative, depending upon whether  $B$  is greater than  $D$  or vice versa. For the present it will be treated as a positive constant.

If now Eq. (33c) is substituted into Eq. (32a) and the integration is performed, the result is given by Eq. (34).

$$-k\tau = k'c_H(x_2 - x_1) + (1 + k'c_Hx_e) \ln \left( \frac{x_2 - x_e}{x_1 - x_e} \right) \quad (34)$$

In order that the rate equation may be checked and that the constants  $k$  and  $k'$  may be determined, Eq. (34) is rearranged into the slope-intercept form of a straight line. Eq. (35) shows this form.

$$\frac{\ln \left( \frac{x_2 - x_e}{x_1 - x_e} \right)}{x_2 - x_1} = \frac{-k}{1 + k'c_Hx_e} \frac{\tau}{x_2 - x_1} - \frac{k'c_H}{1 + k'c_Hx_e} \quad (35)$$

In order to check if the Langmuir-Hinshelwood model is correct, a plot of  $\ln[(x_2 - x_e)/(x_1 - x_e)]/(x_2 - x_1)$  vs.  $\tau/(x_2 - x_1)$  is made with the experimental data. If the model is correct, a straight line will pass through the experimental points. The slope and intercept of this line may be used for the determination of  $k$  and  $k'$ . The relationships are given by Eqs. (36) and (37).

$$k = \frac{-S}{(1 + x_e I)} \quad (36)$$

$$k' = \frac{-I}{c_H(1 + x_e I)} \quad (37)$$

where

$S$  = slope.

$I$  = intercept.

If the Langmuir-Hinshelwood mechanism, in the form of Eq. (33), is found to correlate the data, the question then arises; what is happening on the surface? The answer to this must be provided by an examination of the constant  $k'$ . Comparison of Table I with Eq. (33a) reveals the following facts:

- 1) If adsorption of parahydrogen controls,  $B = 0$ , and  $k'$  is negative and inversely dependent upon  $c_H$ .
- 2) If surface reaction controls,  $k'$  is either positive or negative, depending on whether  $B$  is greater than  $D$  or vice versa;  $k'$  is also inversely dependent upon  $c_H$ .
- 3) If desorption of orthohydrogen controls,  $D = 0$  and  $k'$  is a positive constant.
- 4) If adsorption of parahydrogen is in equilibrium, it is most likely that  $B$  is greater than  $D$ . Thus  $k'$  will be positive and inversely dependent upon  $c_H$ .
- 5) If surface reaction is in equilibrium, the case is the same as case 2.
- 6) If desorption of orthohydrogen is in equilibrium, it is quite likely that  $D$  is greater than  $B$  and thus  $k'$  will be negative and inversely dependent upon  $c_H$ .

- 7) For the case when no step controls, the situation is the same as in cases 2 and 5.

From these statements, it is apparent that, with the single exception of case 3, determination of what is actually occurring on the surface cannot be made. However, in view of the fact that an exact rate expression has been derived with no assumption of a rate-controlling step, it is perhaps not necessary in the present case to be concerned with the postulation that one or more steps control the reaction rate. The matter becomes one of merely determining whether or not the Langmuir rate expression correlates the data--if so, then one has justification for using it. If not, then it must be assumed that one of the assumptions that led to the development of the Langmuir rate expression is incorrect--most probably, the assumption of a uniform surface.

An interesting sidelight to be noted here is that if B and D are equal,  $k'$  becomes equal to zero and consequently the rate law becomes a simple first order rate law. However, due to the existence of a factor which is known as the "separation factor" (See Appendix B), B and D are probably not equal.

Appendix B shows that the separation factor,  $s$ , is the ratio of the adsorption equilibrium constants,  $k_1/k_2$  and  $k_6/k_5$ , for ortho- and parahydrogen. Thus,  $s$  can be obtained from the data if the kinetics are described by a Langmuir-Hinshelwood mechanism, surface rate controlling (Eq. (1)). As is shown in Appendix B,  $s$  is temperature dependent and is not equal to unity. Thus, the reaction cannot be a simple first-order reaction except under the following circumstances.

- 1) Diffusion controlling. If the reaction is much faster than the interparticle mass transfer rate, no matter what the actual surface kinetics (including pore diffusion) are, a first-order rate law will be observed. This is due to the form of the diffusion equation, (Appendix C), which describes a simple first-order process.
- 2) Low surface coverage. If the surface coverage is sparse enough so that the terms  $(1 - \theta_p - \theta_o)$ ,  $\exp(-\alpha \theta)$ , and  $\exp(\beta \theta)$  in Eqs. (7) and (8) are constant, the adsorption step will be independent of the surface coverage and a first-order rate law will be observed, no matter which of the three steps is rate-controlling.

#### 4. Integration of the Modified Temkin, Elovich, and Freundlich Rate Equations

Although the rate equations which are based upon Temkin and Freundlich adsorption are different, the procedure for integrating them is the same. Hence they are grouped together for treatment.

The rate equations are given by Eqs. (23), (26), (27), (28), and (31). Eqs. (26) and (31) may be considered as being two-parameter expressions; the others are three-parameter expressions. (The Langmuir expression is also a two-parameter expression). It is felt that in the present case, using anything other than a two (or one) parameter expression is highly questionable in that, for one thing, there is no assurance that the values of the three parameters will be unique. Further, it will be seen that numerical integration involving trial parameters is

necessary in order to perform the integration. One constant in each rate expression is not involved in the trial parameter integration; the rest are. Thus, if it is necessary to substitute more than one trial parameter at a time, unless some device such as a power series representation is used, the trials might not converge. Hence, only two parameter expressions will be considered.

The justification for eliminating one of the parameters from the Elovich rate expression is as follows: if non-activated adsorption of both ortho- and parahydrogen is assumed, then the constants  $a_1$  and  $a_2$  will be equal to zero. Under these conditions, Eqs. (26) and (28) may be reduced to

$$r = k \left[ \frac{x}{x_e} - \left( \frac{1-x}{1-x_e} \right)^{b_1} \right] \quad (26a)$$

$$r = k \left[ \left( \frac{x}{x_e} \right)^{b_2} - \frac{1-x}{1-x_e} \right] \quad (28a)$$

Eq. (27) may be rearranged to

$$r = k \ln \left[ \left( \frac{x}{x_e} \right)^n \frac{1-x_e}{1-x} \right] \quad (27a)$$

where

$$k = k_4 / (b_2 + a_2).$$

$$n = [k_3 / (b_1 + a_1)] / [k_4 / (b_2 + a_2)].$$

The Freundlich equation, Eq. (31) may be reduced to a two-parameter equation if  $m = n$ . Under this condition,

$$r = k_{c_H}^{1/n} \left[ x^{1/n} - \frac{1}{K_{eq}} \left( \frac{1}{K_{eq}} \right)^{1/n} (1-x)^{1/n} \right] \quad (31a)$$

where

$$K_{\text{eq}} = (1-x_e)/x_e.$$

The justification for this reduction to two parameters is that the separation factor should be independent of total pressure (See Appendix B). However, it should be remembered that the assumptions on which the statistical mechanical derivation of the separation factor is based include the assumption of a uniform surface. The Freundlich equation assumes a non-uniform surface so that unless the surface coverage is in a region where non-uniform effects are not serious the reduction to two parameters is not rigorous.

None of the above expressions are analytically integratable. When they are substituted into Eq. (32a) the results can be expressed in the form

$$\frac{-k\tau}{c_H} = \int_{x_1}^{x_2} \frac{dx}{r} \quad (32b)$$

where  $r$  is one of the above rate expressions. The procedure will be to substitute  $r$  into Eq. (32b) and perform the integration using different values of the exponent. The integral is tabulated as a function of  $x_2$  and the values of the integral corresponding to a given  $x_2$  are plotted against the corresponding  $\tau$  for that point. A straight line will result if the rate law correlates the data.

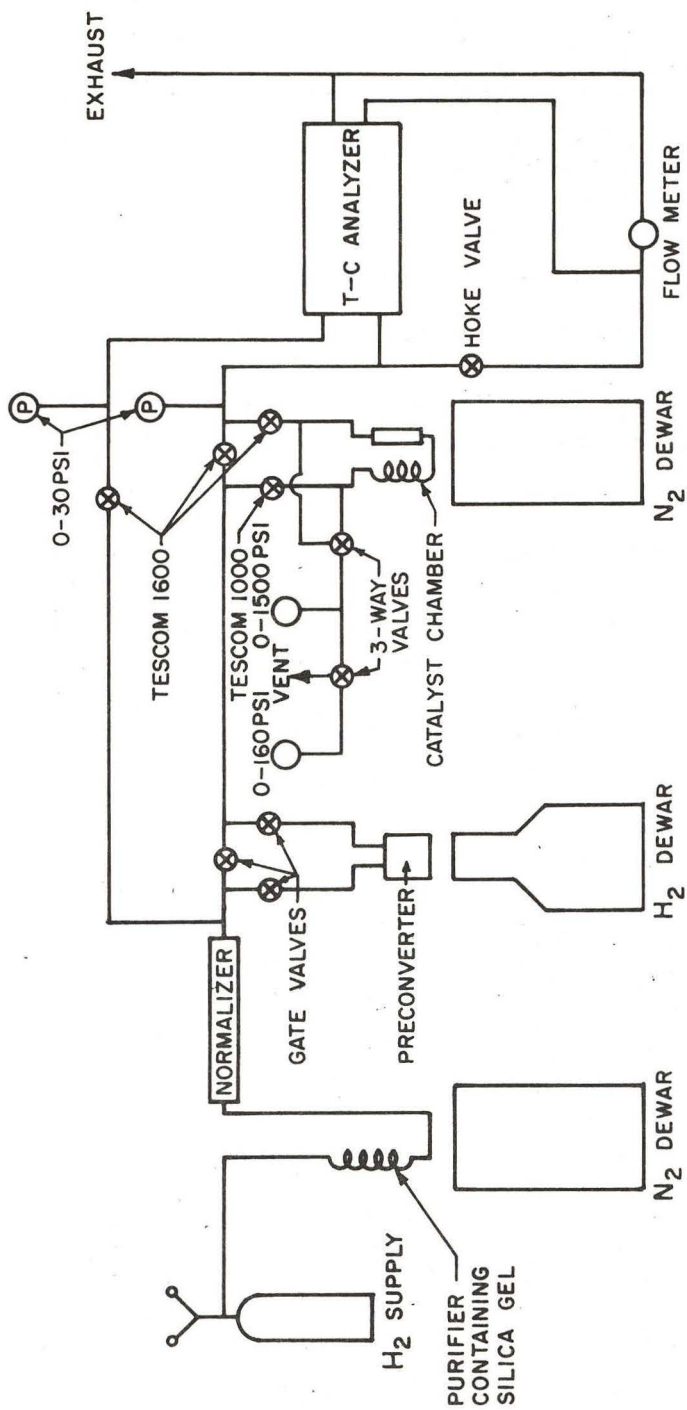
In the above cases the slopes will be of opposite sign for the opposite directions of reaction. However, the

magnitude of the slope (which is equal to  $kc_H$ ) should be equal in both directions. The  $n$ 's should also be the same in both directions.

#### IV. APPARATUS AND PROCEDURE

Data for heterogeneous reaction systems are more easily interpreted if the reactor is isothermal and if conditions are such that mass transfer is not likely to be a rate-controlling factor. Thus a flow system incorporating a temperature-controlled reactor was designed in order to carry out this series of experiments. The apparatus was similar to that used in a previous study [37].

Figure 1 shows a schematic view of the system. Hydrogen was fed from a cylinder to a copper tubing coil, which contained silica gel at 77°K, where moisture and other impurities were removed. The hydrogen stream then passed through a "normalizing" unit, which insured the effluent stream composition to be 25% parahydrogen. The stream was then split; a small amount was fed to the ortho-parahydrogen analyzer to be used as a reference gas, and the remainder became the sample gas. As the reaction was to be run in both directions, i.e., ortho-to-para and para-to-ortho, a parahydrogen feed stream was needed. This was provided by passing the sample stream when required through a large volume catalyst bed, known as the preconverter, at 20°K; the exit stream from this bed consisted of 20°K equilibrium hydrogen--99.8% para. For the ortho-to-para runs, the preconverter was bypassed during the kinetic runs, although the stream was circulated through this unit in order to calibrate the analyzer, as explained below. After the feed stream of hydrogen left this section, it was introduced into the reactor via a Tescom<sup>®</sup> Model #1000 pressure regulator. The pressure was measured both upstream and downstream of the reactor; this was done in order to see if excess



SCHEMATIC OF SYSTEM FOR STUDYING KINETICS OF THE ORTHO-PARAHYDROGEN REACTION

FIGURE 1

pressure drop was present and possibly influencing the reaction. The reactor itself consisted of a five inch length of 1/4" O.D. x 1/8" I.D. copper tube which contained 1.12 g. of Cryenco hydrous ferric oxide gel catalyst. This was immersed in a dewar of liquid nitrogen, in order to provide an isothermal, constant temperature reactor.

The pressure of the hydrogen sample was reduced to analysis pressure after it left the reactor. At this point, a portion of the stream was diverted into the analyzer to be sampled, and then recombined with the main body of the hydrogen to be fed into a wet-test gas flow meter where the total volume of flow was measured. A stopwatch was used in conjunction with the meter to obtain flow rates. All the hydrogen was finally vented to the outside atmosphere for safety reasons.

The conversion of the feed stream was varied by changing its flow rate. The Hoke<sup>®</sup> valve shown in Figure 1 controlled this rate.

The analysis of ortho-parahydrogen was conducted by means of thermal conductivity and was carried out in an apparatus of the type described by Purcell, et.al. [47].

Following is a description of a typical run. Normally the reactor and preconverter were placed in an air bath at 150°C and left overnight with hydrogen gas flowing through them. This procedure activated the catalyst to a fairly reproducible activity.<sup>1</sup> Prior to the run, the reactor was taken from the heater and immersed directly in a bath of

---

<sup>1</sup>Activity is defined here as the STP space velocity which is necessary to convert a stream of 25% parahydrogen to 48% parahydrogen at 77°K and 30 psia.

liquid nitrogen and the preconverter was placed in a dewar containing liquid hydrogen. The valves to and from the reactor were then closed and the bypass valve was opened. The bypass valve to the preconverter was closed and its entrance and exit valves were opened. The sample and reference pressures were adjusted to 6.0 psig and then the recorder zero and span were set. The run was commenced with the opening of the valves to the reactor and the closing of the bypass valve. The total pressure in the reactor was also set at this time. Also, if the reaction was to be ortho-to-para, the preconverter was bypassed. The flow was set and the composition, as read on the recorder, was allowed to stabilize, which usually took a few minutes, and then the flow rate, composition, upstream and downstream pressure were noted. The flow rate was then changed and the system was again allowed to stabilize. The process was repeated until the desired number of data were generated. The span and zero of the recorder were then checked at the termination of the run. Para-to-ortho and ortho-to-para runs were conducted jointly at the same pressure in order to compare the forward and reverse rate constants at constant catalyst activity. The activity at 30 psia was measured for each pair of runs so that, although the activity may have been different for the different pressures, a relative activity could be assigned to each pair of runs. The average time per datum was about five minutes to stabilize and record and most runs took about two hours each to complete.

The room temperature and barometric pressure were recorded during the run. These were needed in order to correct for the vapor pressure of water in calculating the volumes of gas which passed through the wet-test meter.

## V. RESULTS

The experimental data were obtained in the form of a series of space velocity curves, in which the effluent composition, as mole per cent parahydrogen, is plotted against flow rate, in the form of space velocity.<sup>2</sup> A representative pair of space velocity curves is shown in Figure 2 and the curves for the remainder of the runs are presented in Appendix D.

One aspect of the space velocity curves that should be considered is that at zero flow rate (infinite space time) the equilibrium composition of the feed stream is obtained. This fact enables the equilibrium composition ( $x_e$ ), which is used in the rate expressions, to be determined. In the present work, since the space velocity curves become horizontal as they approach zero space velocity, the equilibrium composition was taken to be 0.0001 mole fraction different than the experimental point nearest zero space velocity. This convention was adopted merely for convenience; it enabled the last data point to be retained when plotting the integrated rate expressions. Due to the accuracy limitations of the analytical equipment, the accuracy of four decimal places is unjustified; it is merely the convention that was adopted herein. The reason that concern is expressed over this point is that, in the region of 75°K, the equilibrium composition of hydrogen is a sensitive function of temperature and thus,

---

<sup>2</sup>Space velocity ( $\text{min}^{-1}$ ) is the actual flow rate ( $\text{cm}^3$  hydrogen  $\text{min}^{-1}$ ) per unit bulk volume of catalyst ( $\text{cm}^3$ ).

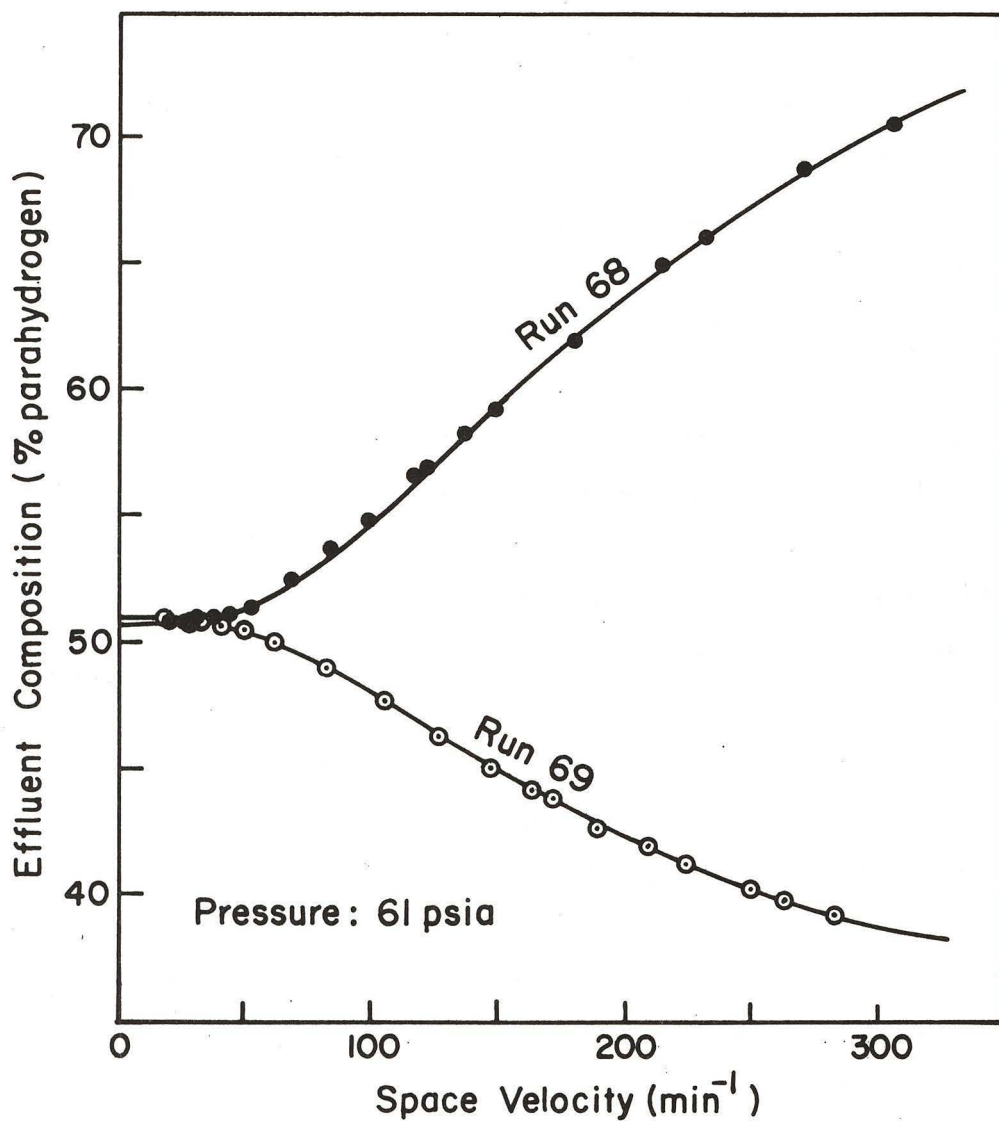


FIGURE 2. Predicted and Observed Space Velocities from Langmuir Rate Equation for Runs 68 and 69

if the reactor were at a temperature even a few-tenths of a degree different from the bath, the equilibrium composition would be different than it would be if the reactor was at actual bath temperature.

Although the runs were conducted with the reactor immersed in a bath of liquid nitrogen, it is apparent from the data that the same equilibrium composition is not achieved for all runs, as would normally be expected. This deviation was noticed during the experimental investigation and steps were taken at that time to ascertain whether or not this was an actual phenomenon or an experimental error. The equilibrium values shown were reproducible; recalibration of the analyzer produced no different results. An explanation of why the equilibrium points fell as they did may be as follows: in the range of approximately 50 to 90°K the equilibrium composition of hydrogen changes about one per cent per degree Kelvin. Therefore, an apparently small change in temperature will produce a noticeable change in composition. There are several ways in which the temperature could change slightly: the bath temperature could vary somewhat due to differences in atmospheric pressure, although calculation showed that these differences were not nearly great enough to account for some of the observed changes in equilibrium composition. Also in all cases the observed compositions are such that the reactor temperature is higher than the bath temperature. The most likely explanation of this is that the feed stream was not completely cooled to bath temperature. Since the specific heat of parahydrogen is higher than that of normal hydrogen, the parahydrogen stream did not cool as much as the normal hydrogen, thus accounting for the relative

positions of the equilibrium compositions of the forward and reverse reactions.

The analysis of the data with regard to rate expressions is presented in the next section. The criteria for a successful correlation have been presented in Section III, but are reviewed here:

1. A straight line should pass through the points when they are plotted in the proper form of coordinates for the integrated rate expression.
2. The two parameters that are obtained from the data should agree in the forward and reverse directions.

If both of these criteria are not met, then the correlation, if it exists, will have value only as an empirical correlation of the data.

Runs 68 and 69, the kinetics at 60 psia, were chosen as the runs against which the various rate laws were tested. This was mainly because the data from this pair of runs seemed to show less deviation from the space velocity curves than some of the data from other runs. Less scatter of these data would hopefully indicate less scatter in the plots of the integrated rate expressions.

## VI. DISCUSSION OF RESULTS

### A. Freundlich Kinetics

The first case to be treated is the Freundlich rate law. This is given by Eq. (31a). According to Trapnell [32] the value of  $n$  in Eq. (31a) must be greater than unity. Consequently, only values of  $n$  greater than one were substituted into the rate expression when the integration was performed.

$$r = k c_H^{1/n} [x^{1/n} - \left(\frac{1}{K_{eq}}\right)^{1/n} (1-x)^{1/n}] \quad (31a)$$

An IBM 709 computer was programmed to perform the integration numerically. Figures 3 and 4 are representative of the plots that were prepared by matching the data with the integrated rate expression. These plots were prepared by integrating the rate expression for a value of  $n = 1.2$ . Similar plots were prepared for values of  $n = 3.0$  and  $10.0$ . The values of  $k$  that were obtained from the slopes of these plots are summarized in Table II.

First of all, it is apparent from the plots that the correlation in all cases is fair. It is slightly better at the higher values of  $n$ . There is some deviation of the data from a straight line at higher contact times, i.e., at lower space velocities. Also, it should be noted that the values of  $k$  in the forward and reverse directions are not equal. Although the percentage deviation between the  $k$ 's for the two directions becomes smaller as  $n$  is increased, it is felt that this deviation is outside the accuracy of the data. The dotted line in Figure 3 shows how the curve would have to appear in order to give the same slope ( $k$ ) as Figure 4. There is a noticeable trend in the deviation

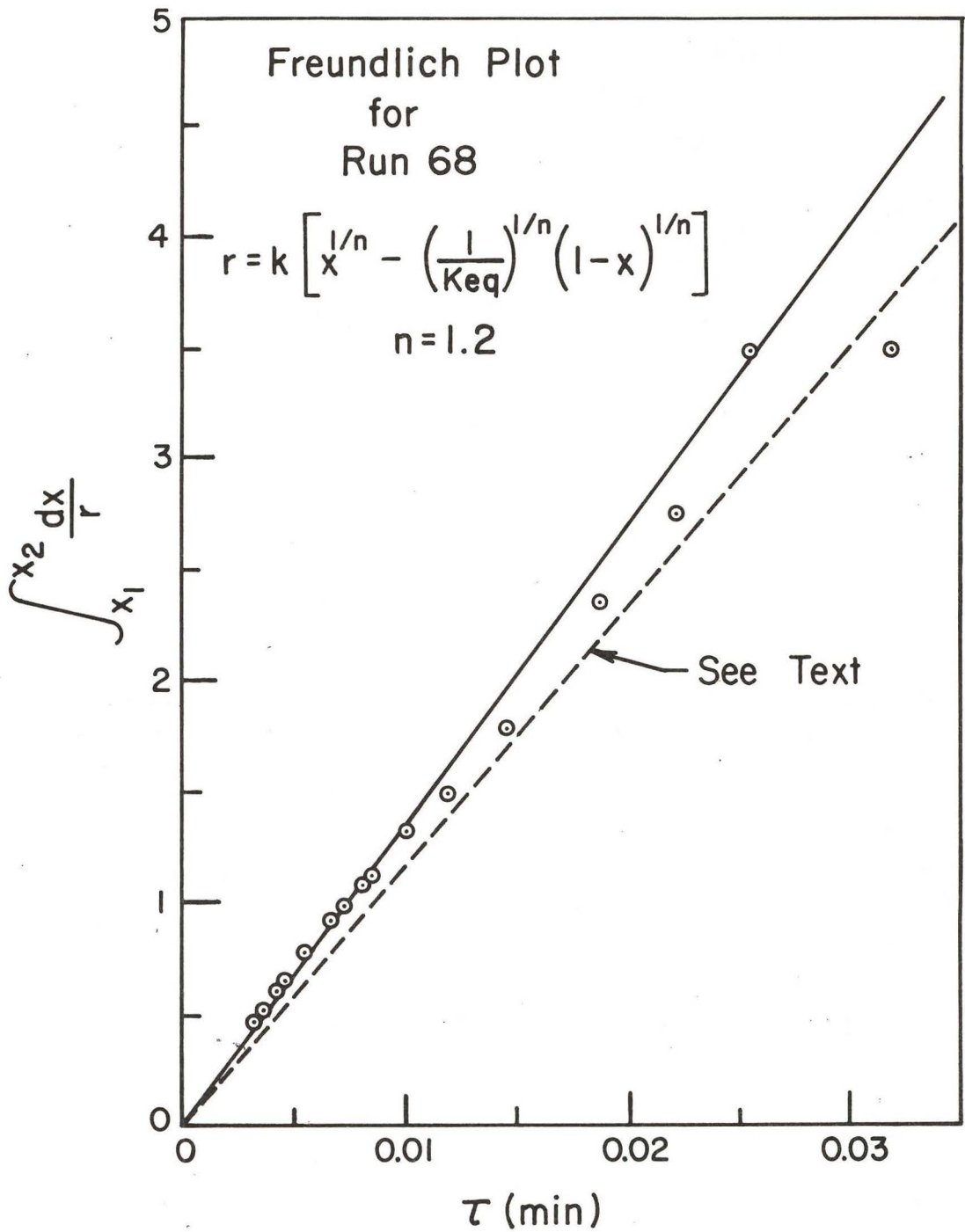


FIGURE 3. Freundlich Plot for Run 68

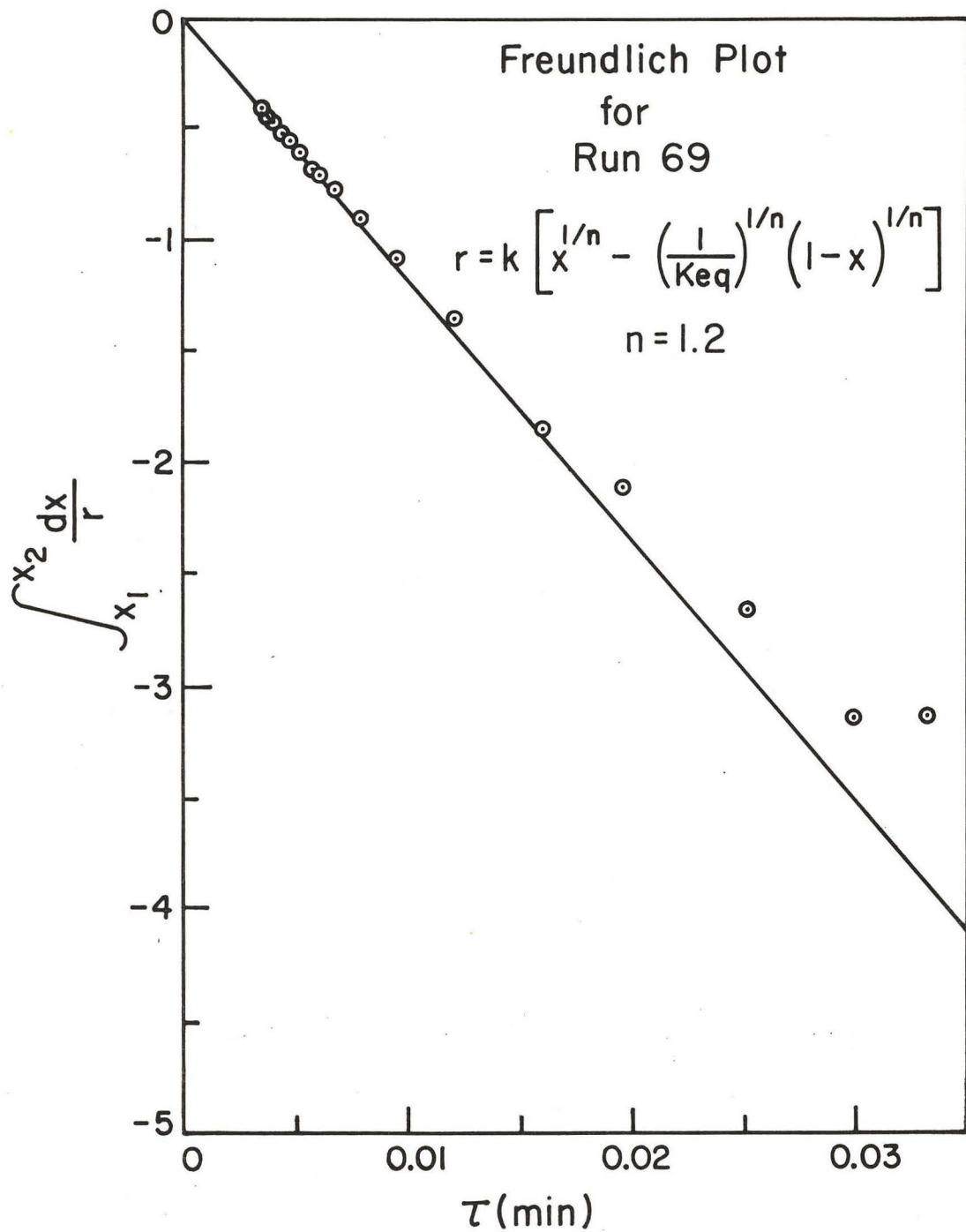


FIGURE 4. Freundlich Plot for Run 69

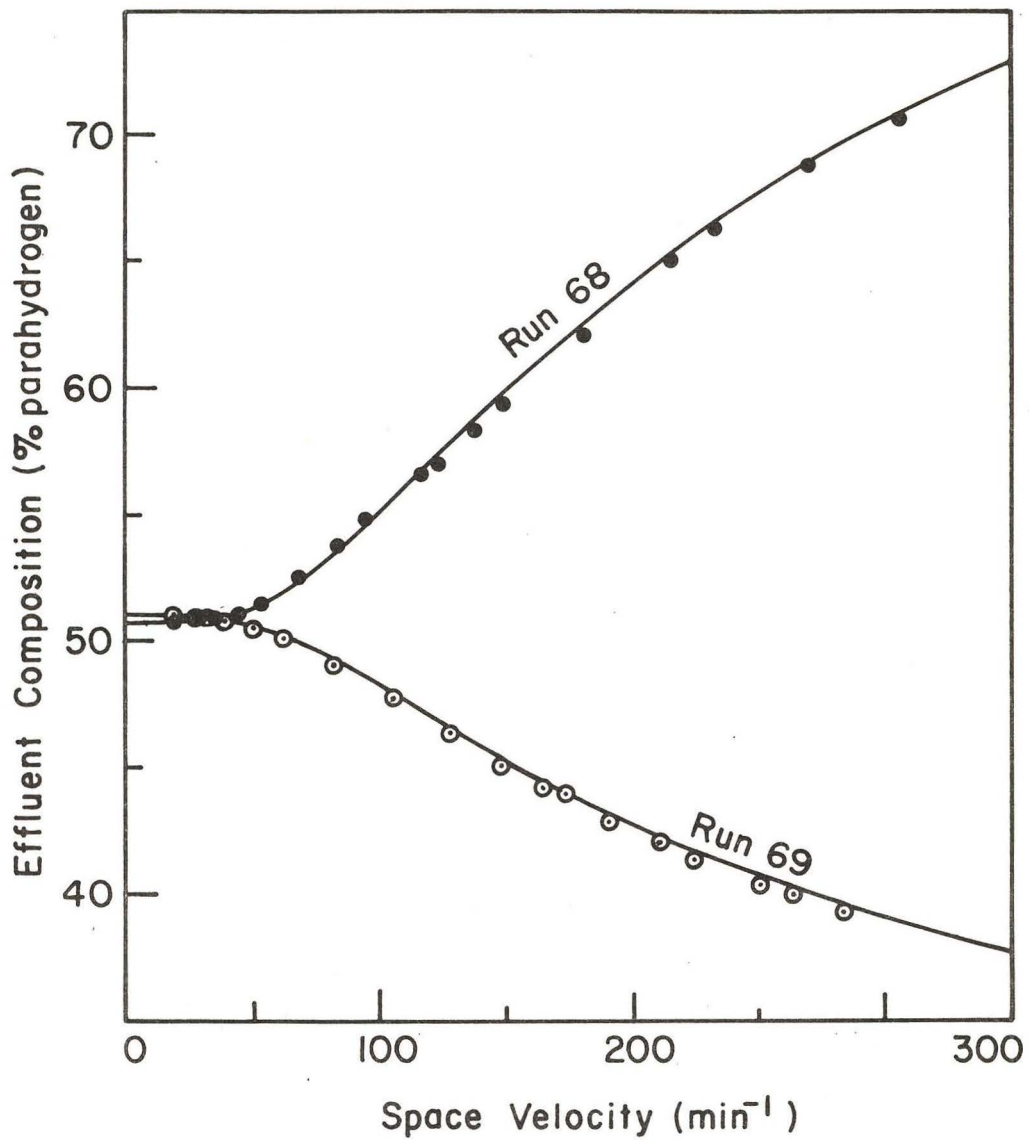


FIGURE 5. Predicted and Observed Space Velocities from Freundlich Rate Equation for Runs 68 and 69

Table II

Freundlich Rate Constants as a Function of  $n$ 

<u>Run</u>	<u>Direction</u>	<u>n</u>	<u>k</u>	<u>k (%)</u>
68	p $\longrightarrow$ o	1.2	136.0	16.4
69	o $\longrightarrow$ p	1.2	116.75	
68	p $\longrightarrow$ o	3.0	223.5	8.8
69	o $\longrightarrow$ p	3.0	205.5	
68	p $\longrightarrow$ o	10.0	621.0	6.15
69	o $\longrightarrow$ p	10.0	585.0	

of the rate constants as  $n$  is increased, i.e., the  $k$ 's approach each other in value at higher values of  $n$ . It is probable that the  $k$ 's will become equal at higher values of  $n$  than were calculated. However, it should be noted that the adsorption data of hydrogen on ferric oxide gel obtained by Clark, et.al. [15], when plotted as a Freundlich isotherm, gave a value of  $n$  of approximately 2.5 (Appendix A). It is assumed that the same value of  $n$  should be obtained from both adsorption and kinetic data. Also, the adsorption rate which leads to a Freundlich isotherm does not account for any effects of the presence of a second specie on the surface. Thus, the theoretical background which was developed in Section III.G is probably not rigorous. In view of this, it is concluded that the Freundlich rate equation probably does not represent the mechanism of the reaction.

However, in order that the equation could be fully checked, the space velocity curves were recalculated using the values of  $k$  and  $n$  that were derived from the data. Figure 5 shows this plot, which was prepared by using values in both directions of  $k = 600$  and  $n = 10$ . As can be seen in Figure 5, the calculated curves pass through the experimental points, even at low space velocities. These lower space velocities represent the points at which the deviation from the straight line (e.g., as in Figures 3 and 4) occurs. Since the calculated curves pass through these points, it is felt that the deviations from the straight line on the integrated rate plots are not as serious as might first be imagined. However, they should not be fully ignored; if less deviation should be noticed for one of the other mechanisms, this fact could serve to further

disqualify the Freundlich expression. It is still possible, if one desires, to use the Freundlich expression (Eq. 31a) as an empirical rate expression to represent the reaction, as advocated by Weller [57]. However, because of the reversible reaction, Eq. (31a) no longer can be easily integrated, as it could if the reaction were irreversible, and so there is actually very little justification for its use.

### B. Modified Temkin Kinetics

The second case to be treated is that of the expression which was modified from the Temkin approach. The rate equation is given by Eq. (23). Again, the integration of Eq. (32a) using Eq. (23) was performed numerically by an IBM 709 computer.

$$r = k \ln \left[ \frac{s(1-x) + x}{s(1-x_e) + x_e} \right] \quad (23)$$

Values of  $s$  were chosen to cover a moderate range, since the value predicted by Sandler's theory [50] is about 2. Figures 6 and 7 show the best plots that were obtained for Runs 68 and 69. These were obtained with a value of  $s = 3.0$ . Although a straight line can be drawn through the data with reasonable justification, it is apparent that the best straight line which passes through the data for Run 69 does not intersect the origin. The  $k$  values which were obtained were 225 for Run 68 and 238 for Run 69. This represents a difference of about five per cent. The fact that the line does not pass through the origin for Run 69 is a deficiency. Also, it has been assumed in the present development that the separation factor is a constant. For a uniform surface this is true but it may not

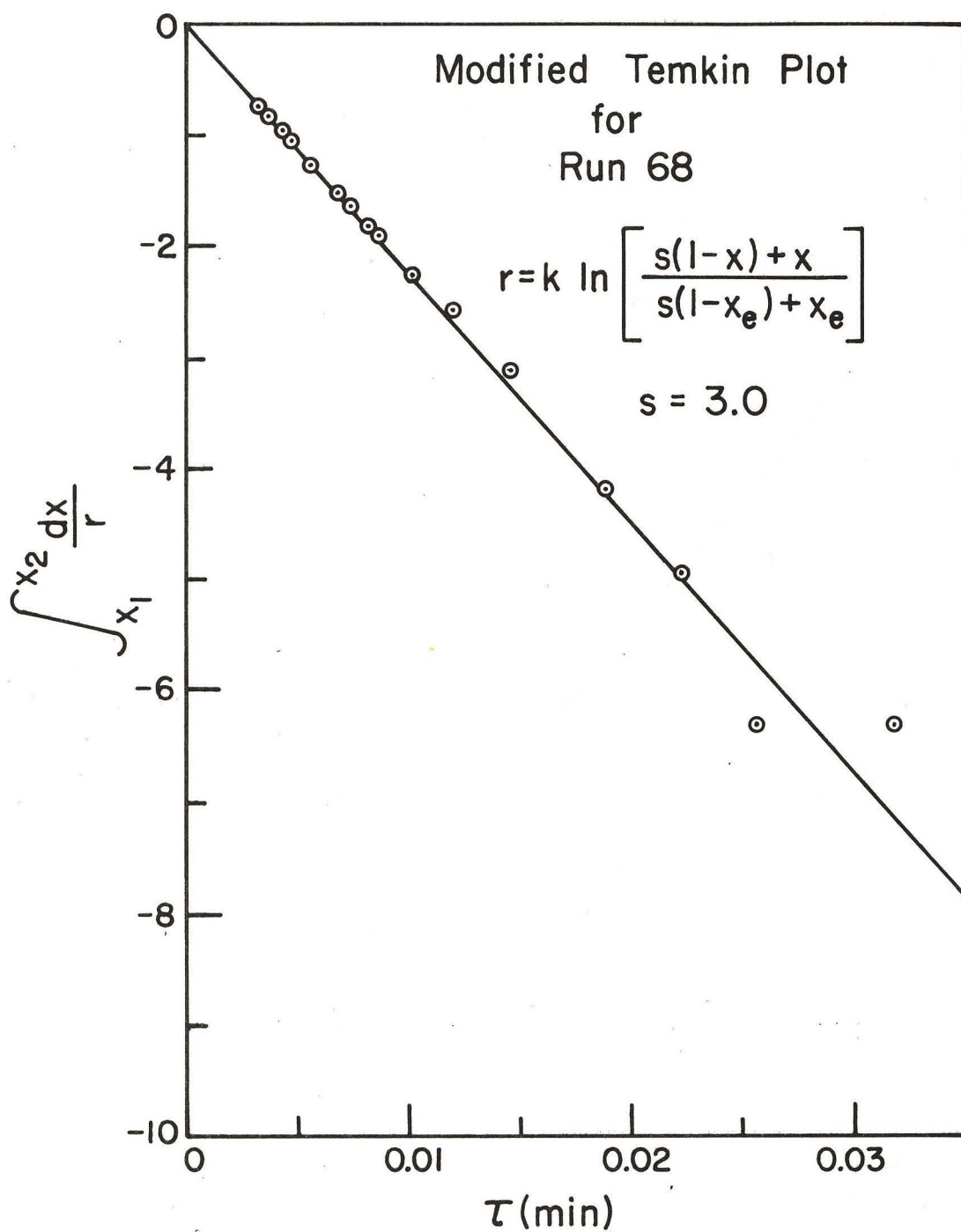


FIGURE 6. Modified Temkin Plot for Run 68

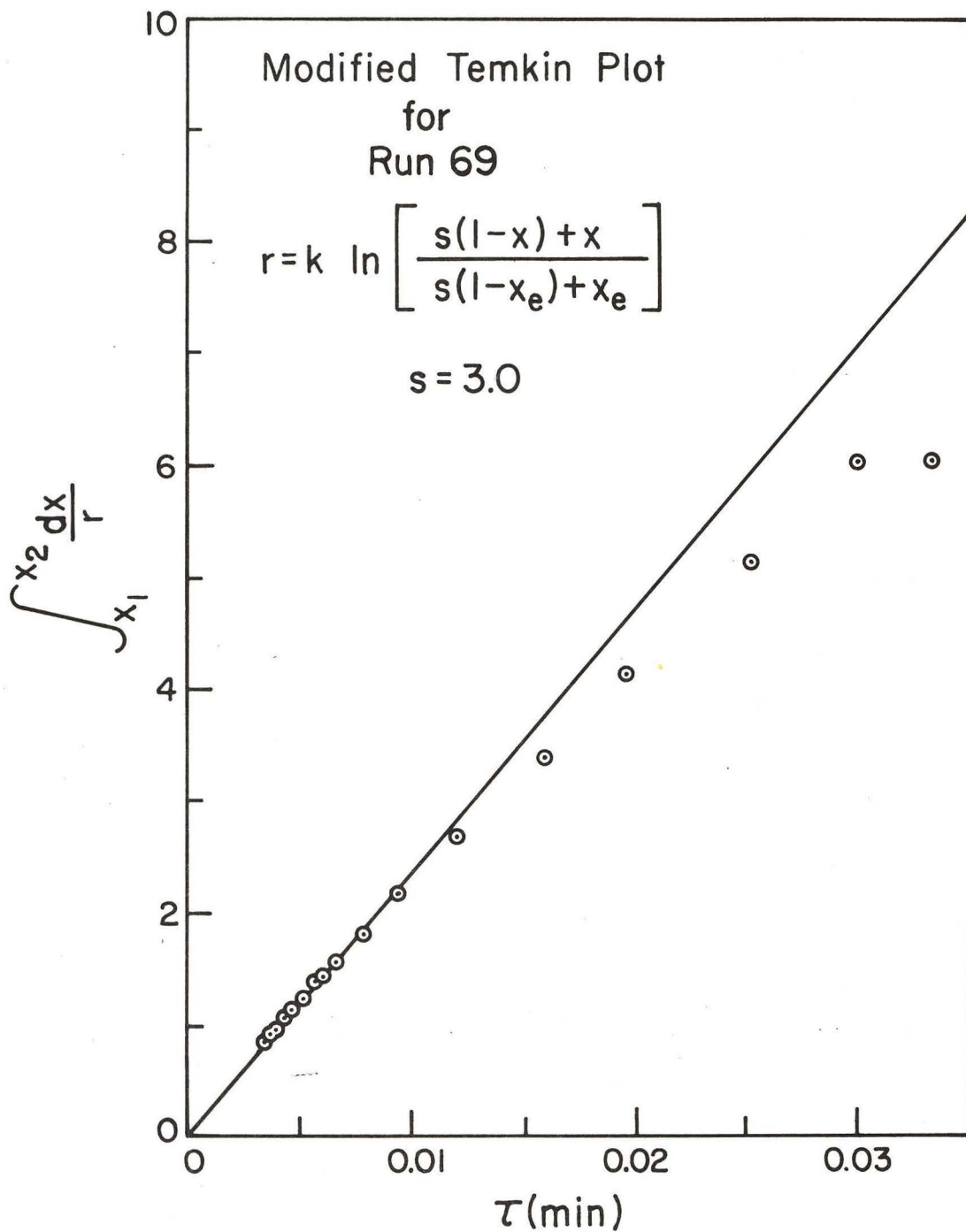


FIGURE 7. Modified Temkin Plot for Run 69

be the case for a non-uniform surface or where interactions occur on the surface (See Appendix B). It is thus concluded that the modified Temkin expression does not represent the reaction.

### C. Elovich Kinetics

Attention is now directed to the third of the four models of rate expressions that are considered in the present work--the rate laws based upon Elovich Kinetics. Eqs. (25a), (27a), and (28a) show these expressions.

$$r = k \left[ \left( \frac{x}{x_e} \right) - \left( \frac{1-x}{1-x_e} \right)^{b_1} \right] \quad (26a)$$

$$r = k \ln \left[ \left( \frac{x}{x_e} \right)^n \left( \frac{1-x_e}{1-x} \right) \right] \quad (27a)$$

$$r = k \left[ \left( \frac{x}{x_e} \right)^{b_2} - \left( \frac{1-x}{1-x_e} \right) \right] \quad (28a)$$

Again, as in the case of Freundlich and modified Temkin kinetics, the integration was performed numerically. In the cases of the Elovich laws, unlike the Freundlich law, there is no theoretical restriction upon the value of  $n$ , other than that it be positive. Hence, values of  $n$  both greater and less than one were tried.

In the case where adsorption of parahydrogen controls, Figure 8 shows the best plot that could be achieved for Run 68. Figure 8 was made for a value of  $n = 1.2$ . Other values tried gave no better correlation than this, and since better representation of the rate were found to exist, it was felt that Elovich kinetics, adsorption of

parahydrogen controlling, is not the mechanism.

The case where desorption of orthohydrogen controls is more difficult to discern. Figures 9 and 10 show the integrated rate plots which appeared to give the best correlation. This occurs for a value of  $n = 2$ . For Run 68, the data deviated to the left of a straight line as  $n$  was increased and deviated to the right as  $n$  was decreased.

The rate constants which were calculated from the slopes of Figures 9 and 10 are not in very good agreement. For Run 68,  $k = 38.2$  and for Run 69,  $k = 41.6$ . The difference here is 8.9%. As with the Freundlich rate constants, the deviation is greater than is expected from the accuracy of the data. Also, as the dotted line in Figure 10 shows, the best straight line that passes through the data for Run 69 does not intersect the origin. Therefore, it must be concluded that the Elovich rate expression with desorption of orthohydrogen controlling probably does not describe the mechanism of the ortho-parahydrogen reaction.

The other case to be considered at this point is Elovich kinetics with surface reaction controlling. Unlike the cases in which adsorption and desorption were assumed controlling, the assumption of non-activated adsorption is not necessary in order to reduce the rate law to a two-parameter equation. This is true because the exponents in Eq. (27) are of the form  $k/(a + b)$ , whereas the single exponents in Eqs. (26) and (28) are  $(-a)$  and  $(b)$  and it was necessary to assume that  $a = 0$  in order to reduce Eqs. (26) and (28) to two-parameter expressions.

Again, there is no theoretical restriction on whether  $n$  should be larger or smaller than unity, so a range of

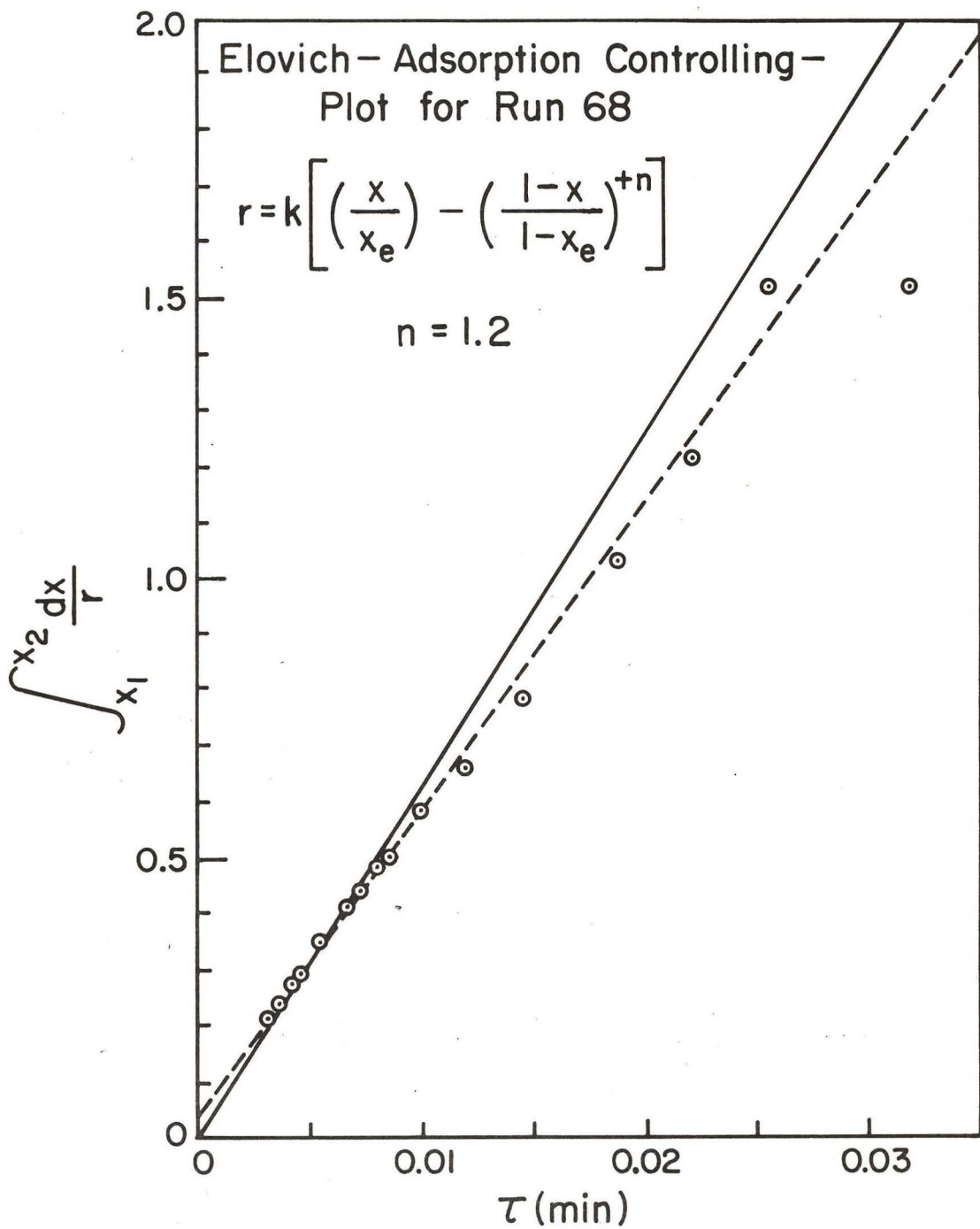


FIGURE 8. Elovich-Adsorption Controlling - Plot for

Run 68

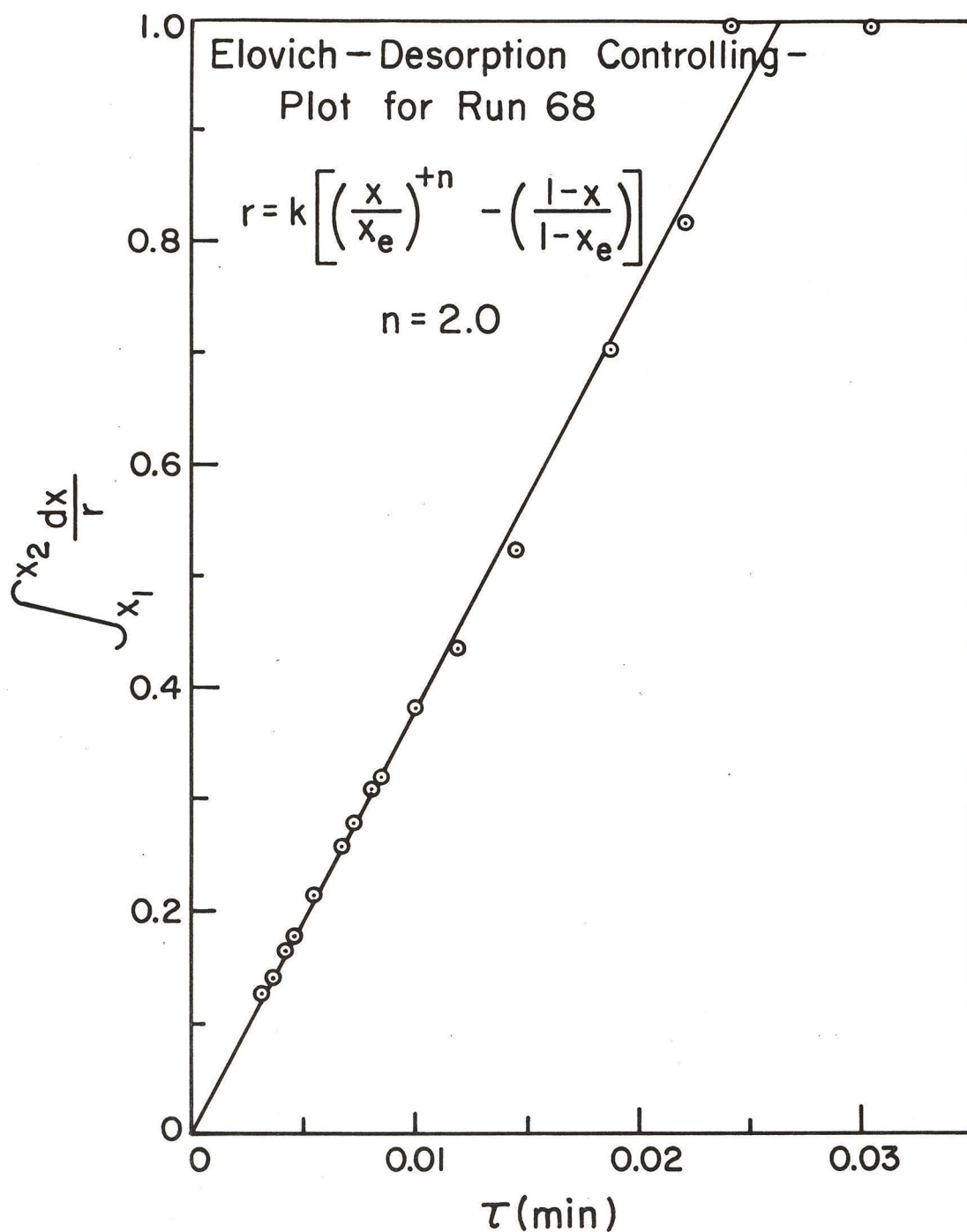


FIGURE 9. Elovich-Desorption Controlling - Plot for

Run 68

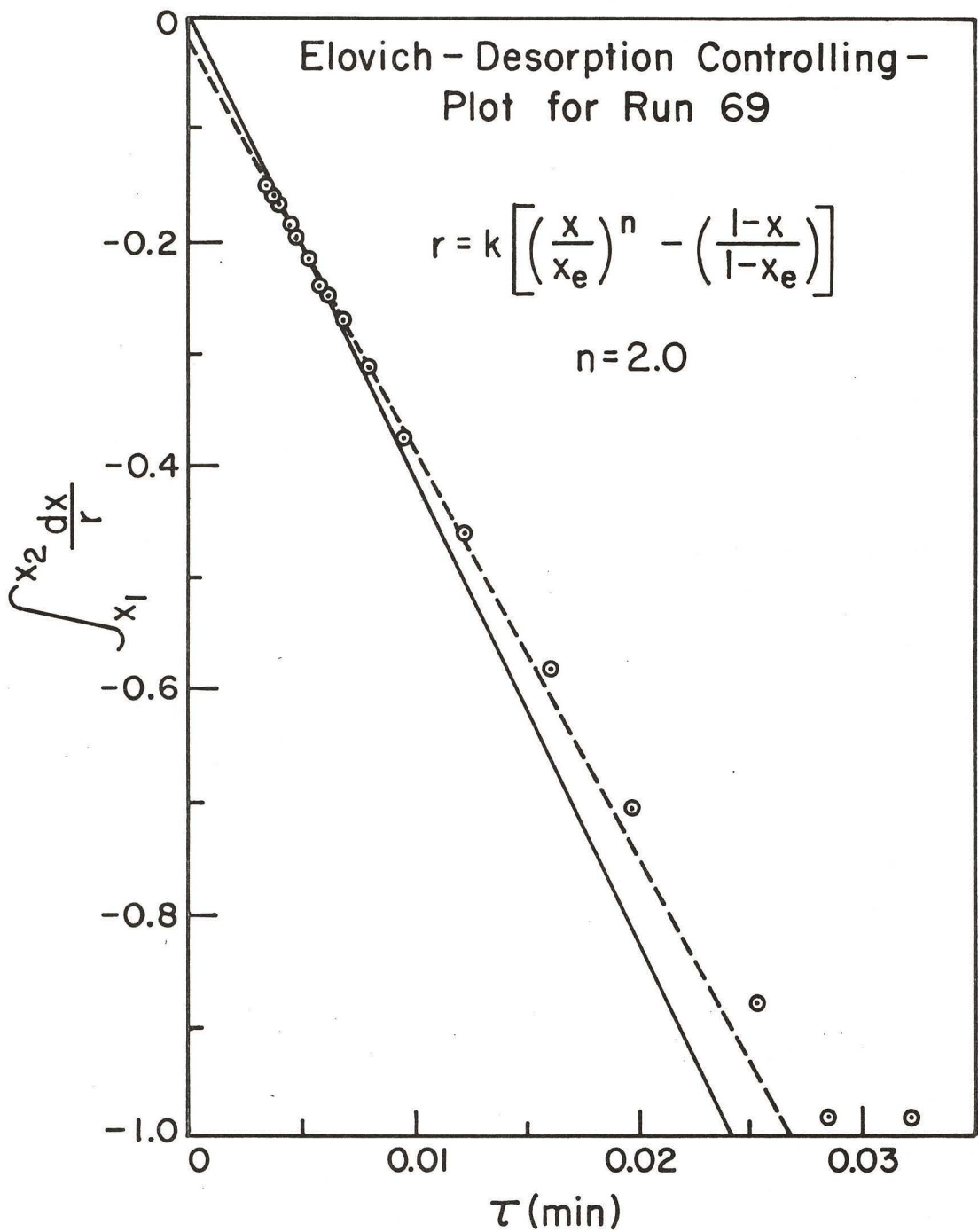


FIGURE 10. Elovich-Desorption Controlling - Plot for

Run 69

values was tried. Plots were made for several values of  $n$  and it was found that, as in the Freundlich case, the rate expression of the integrated rate plot would fit. Trials were made with different values of  $n$  but these did not result in a straight line which passed through the origin.

It was found during the investigation, that particularly for the runs at 30, 61, and 122 psia, the values of  $n$  which gave the best straight line were not those which gave agreement between the  $k$ 's, although the deviation in  $k$ 's was usually less than twenty per cent. For example, the best agreement between the predicted vs actual space velocity curves for the trial runs (68 and 69) came with a value of  $n = 2.0$ . The difference between the forward and reverse rate constants was 15%.

The rate constants that were derived from the data are shown in Table III. There are three columns of rate constants. The first shows the constants as they were obtained directly from the slope of the corresponding rate plot. The second column of rate constants represents the actual  $k$ 's for the particular run. These were obtained by multiplying the values of  $k$  in the first column by  $c_H$ , the total hydrogen concentration. This step must be taken because  $c_H$  appears in the integrated rate equation (See Eq. 32b). The fourth column represents the "intrinsic" rate constants. These are the constants in column three divided by the relative activity of the run. This procedure is necessary because as was shown in Section VI.B, the catalytic activity changed from day to day. The activity was arbitrarily taken as the space velocity at 30 psia and 75°K at which a feed stream of 25% para-hydrogen was

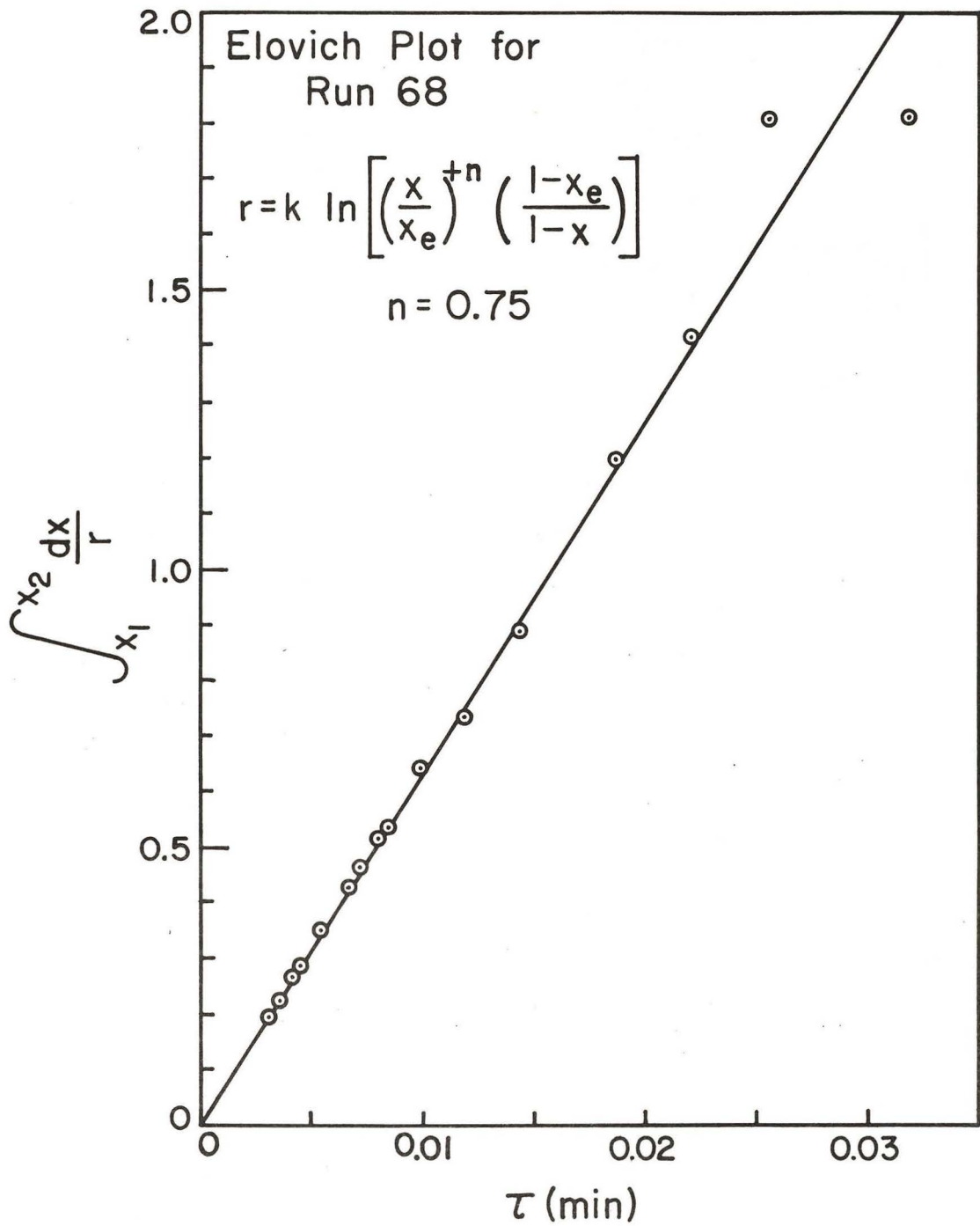


FIGURE 11. Elovich Plot for Run 68

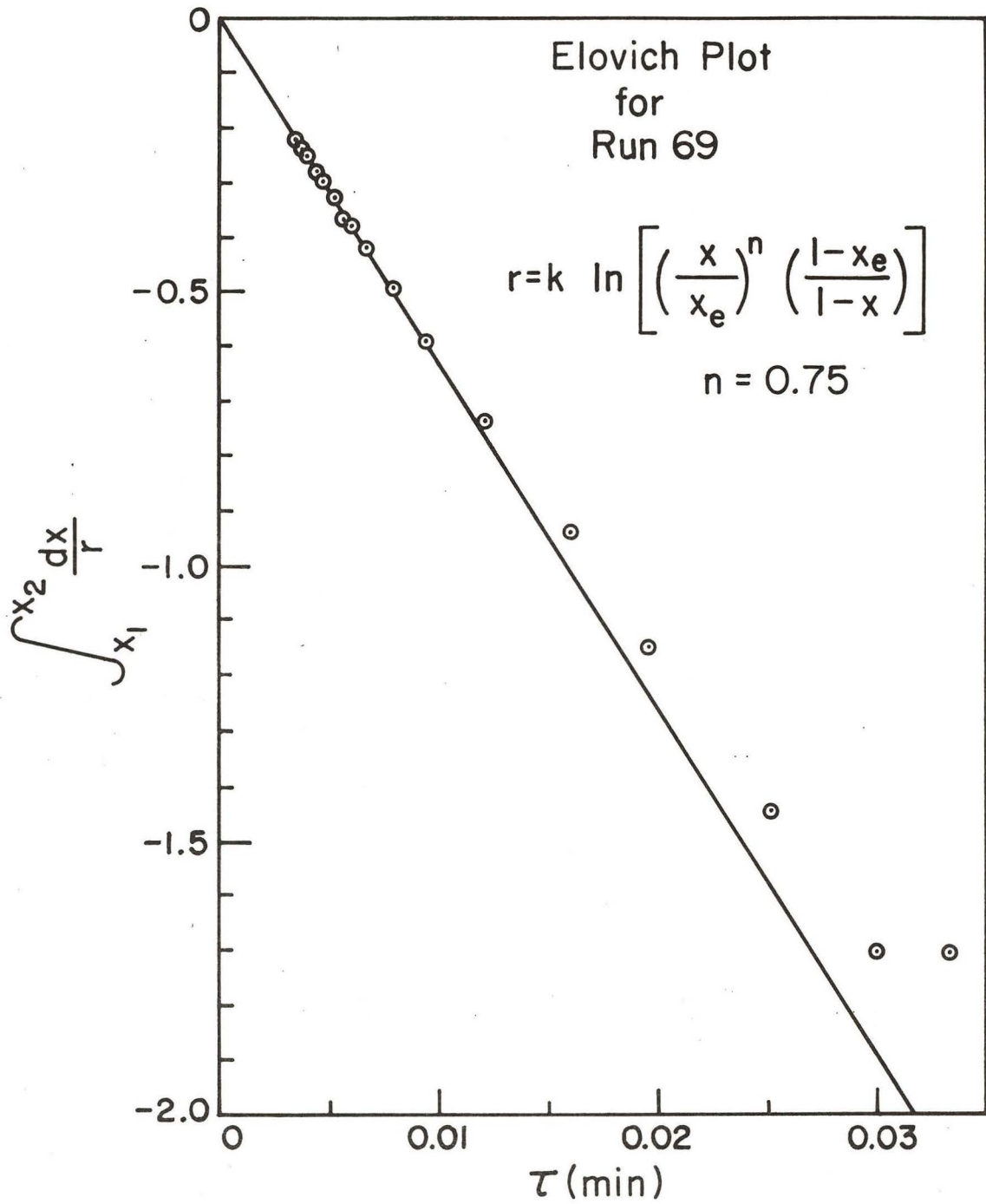


FIGURE 12. Elovich Plot for Run 69

Table III. Elovich Rate Constants

<u>Run</u>	<u>Pressure (psia)</u>	<u>k</u>	<u><math>k c_H</math></u>	<u><math>k c_H / RA</math></u>
60 } 61 }	30	101	4.24	2.5
65 } 66 }	30	103	4.32	2.4
68 } 69 }	61	63	5.36	3.0
70 } 71 }	122	37	6.03	3.3
72 } 73 }	240	18.9	6.28	3.7
76 } 77 }	500	7.4	5.43	5.2
80 } 81 }	1010	3.58	5.23	3.6

Average  $k = 3.4 \text{ g-moles min}^{-1} \text{ cm}^{-3} \text{ catalyst}$ .

converted to a stream containing 48% parahydrogen. The base activity was taken as  $250 \text{ min}^{-1}$ . The relationship between  $k$  and activity may be shown as follows: Eq. (32c) gives the integrated rate expression.

$$k \tau = \int_{x_1}^{x_2} \frac{dx}{\ln \left[ \left( \frac{x}{x_e} \right)^n \left( \frac{1-x_e}{1-x} \right) \right]} \quad (32c)$$

Since, if  $n$  is constant, the integral term remains constant for all runs ( $x_2$  and  $x_1$  are the same), the only quantities that can change are  $k$  and  $\tau$ . But since  $\tau = 1/(\text{space velocity}) = 1/(\text{activity})$ , the relation between  $k$ 's for two different pair of runs is equal to the ratio of the two activities, as shown below.

$$k_1 \tau_1 = k_2 \tau_2 = \int_{x_1}^{x_2} \frac{dx}{r} = \text{constant}$$

Then

$$\frac{k_1}{(\text{SV})_1} = \frac{k_2}{(\text{SV})_2} = \text{constant}$$

Therefore

$$\frac{k_1}{k_2} = \frac{(\text{SV})_1}{(\text{SV})_2} \quad (38)$$

By knowing the rate constant at an activity of  $250 \text{ min}^{-1}$ , if the user knows the activity of his catalyst, he may then calculate the  $k$  for his catalyst by using Eq. (38).

The intrinsic rate constants may be examined for pressure dependence. According to the arguments that were used in developing Eq. (27a), the constants  $k$  and  $n$  should

both be independent of pressure. Figure 13 shows a plot of  $k$  as a function of pressure when  $n = 0.75$ . It can be seen from Figure 13 that  $k$  is not independent of pressure, although at higher pressures the dependence is not as pronounced. At pressures greater than approximately 100 psia, the individual  $k$ 's for the forward and reverse reactions agreed quite well with each other.

Using the values of  $k$  and  $n$  that were obtained from the integrated rate plots, space velocity curves were calculated. These are shown in Figures 30-36, Appendix E. It is apparent that the data are reproduced at least within experimental error at the higher pressures. At the lower pressures, particularly at 30 psia, there is some deviation between the predicted and experimental curves. Although this deviation amounts to, at most, four per cent, this is quite a serious deviation, in view of the excellent agreement between the predicted and experimental curves at higher pressures.

In view of this deviation and the discrepancies which arise from using the Elovich equation for adsorption of a pure component in the presence of a second specie (which is not accounted for), it is felt that the results shown in the present section cannot be given a theoretical interpretation. It is somewhat surprising that the equations which were derived from the above incorrect assumption correlates the data as well as it does. It must at best be regarded as a good empirical representation of the reaction rate.

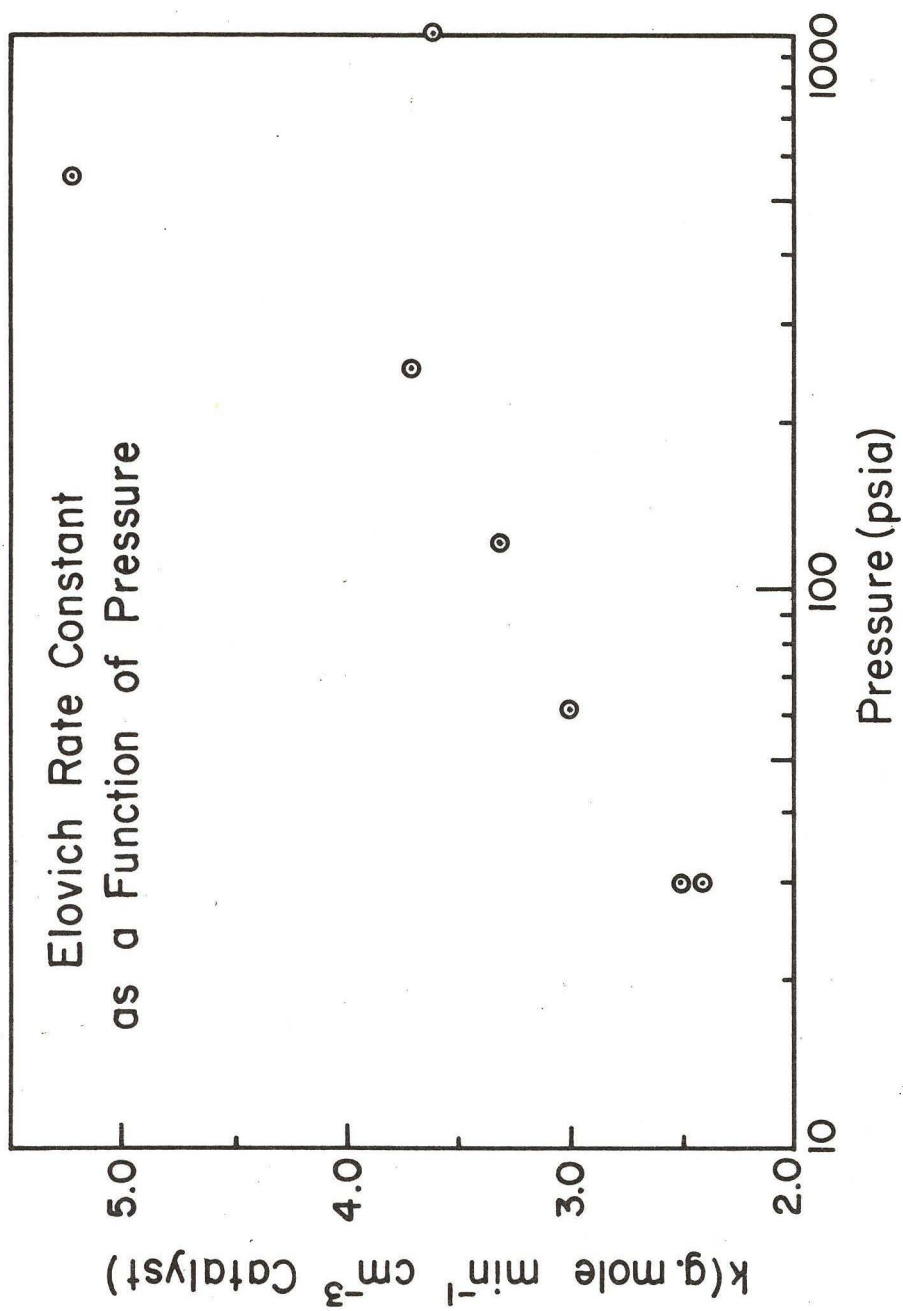


FIGURE 13. Elovich Rate Constant as a Function of Pressure

## D. Langmuir Kinetics

The final case to be treated is that of Langmuir kinetics. The rate equation is shown by Eq. (33c).

$$r = \frac{k c_H (x - x_e)}{1 + k' c_H x} \quad (33c)$$

The coordinates of the integrated rate equations in this instance are  $\ln[(x_2 - x_e)/(x_1 - x_e)]/(x_2 - x_1)$  and  $\tau/(x_2 - x_1)$ . Hence, plots for the Langmuir mechanism may be prepared directly from the data without the need for numerical integration with trial parameters. Langmuir plots for the trial runs (68 and 69) are shown in Figures 14 and 15. It is apparent that the correlation here is quite good, certainly no worse than with the Elovich equations and perhaps slightly better than with the Freundlich equation (compare Figure 4 with Figure 15). On this basis plots were prepared for the other runs in the series and a program was written which enabled the computer to calculate the values of  $k$  and  $k'$  for these runs. These values are tabulated in Table IV. The plots are shown in Appendix F. These values are corrected for catalytic activity as was done with the parameters in the Elovich model.

The corrections for activity are somewhat more difficult to derive in this case than for the Elovich case. The integrated rate expression appears as in Eq. (32d).

$$k \tau = \int_{x_1}^{x_2} \frac{(1 + k' c_H x) dx}{(x - x_e)} \quad (32d)$$

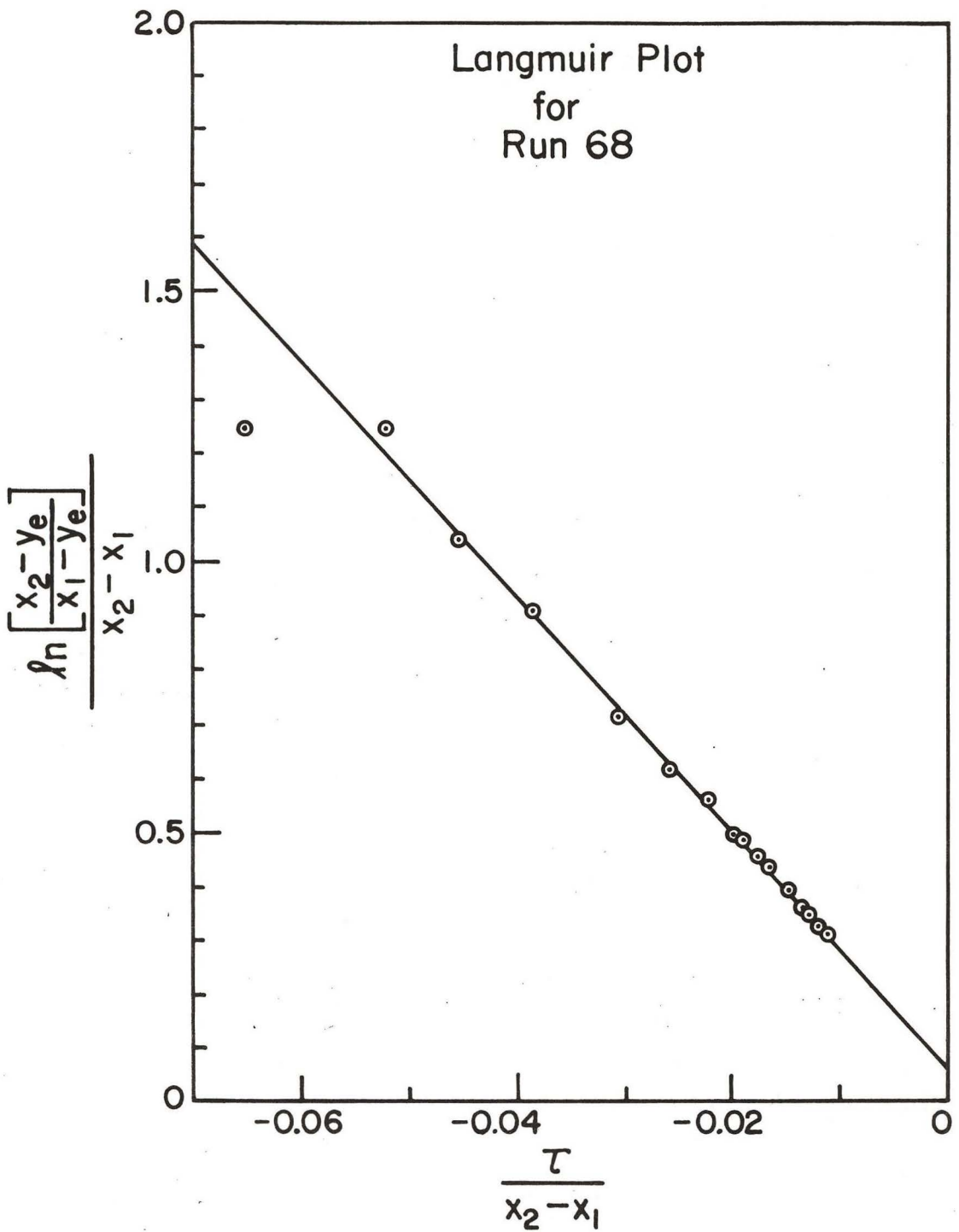


FIGURE 14. Langmuir Plot for Run 68

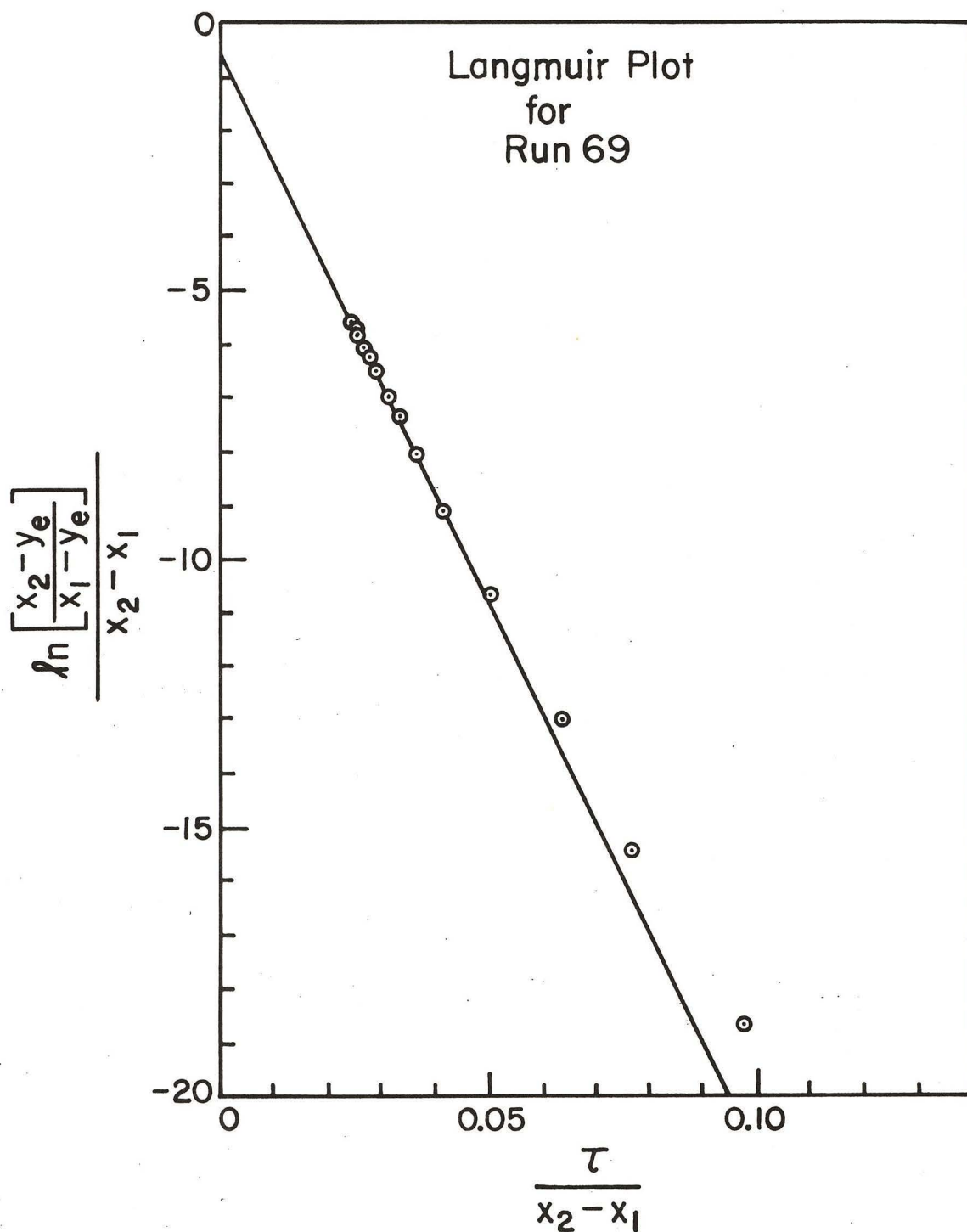


FIGURE 15. Langmuir Plot for Run 69

For the activity runs, the limits  $x_1$  and  $x_2$  are the same. The simplest assumption that can be made is that  $k'$  does not change with activity, and if this is so the integral on the right side of Eq. (32d) is constant for all activities. There results:

$$k \kappa = \frac{k}{SV} = \text{constant}$$

or

$$k = (\text{constant})(\text{activity}) \quad (38a)$$

since the activity is the space velocity for a given conversion. Thus, one may calculate the values of  $k$  for a given activity merely by dividing by the relative activity. This is the procedure that was followed in constructing Table IV and is analogous to the procedure that was used in Section VI.C., wherein  $n$  was assumed to be constant and only the  $k$  was assumed to change with activity. However, rigorously it is probably not correct in either the Langmuir or Elovich models to account for activity corrections on the basis of only one constant. The factors which influence catalytic activity have not yet been expressly pinpointed [3] and it is safe to say that probably all six constants in the mechanism equations (Eqs. 4, 5, and 6) will change with activity. Since the constants  $k$  and  $k'$  in Eq. (33c) and  $k$  and  $n$  in Eq. (27a) depend upon the six individual constants, it is reasonable to expect that both constants in the Langmuir and Elovich models will change with activity. However, there is no method at present of predicting a priori how these constants will change with changing activity, and since only one activity measurement was made, at most only one constant could be measured, and

Table IV. Constants for Langmuir Rate Expressions

## A. Ortho-to-parahydrogen conversion

<u>Run</u>	<u>Pressure (psia)</u>	<u>k (min<sup>-1</sup>)</u>	<u>k' (cm<sup>3</sup> g-mole<sup>-1</sup>)</u>
60	30	516	23.3
66	30	396	8.45
69	61	300	11.7
71	122	195	8.45
73	240	90.7	2.82
77	500	41.1	2.17
81	1010	18.5	0.90

## B. Para-to-orthohydrogen conversion

61	30	356	-5.48
65	30	317	-9.82
68	61	151	-6.45
70	122	85.0	-3.43
72	240	54.0	-1.32
76	500	19.0	-0.69
80	1010	9.39	-0.33

C. Ortho-to-parahydrogen conversion  
over smaller mesh catalyst

82	30	523	19.0
83	100	135	14.8
85	300	-161	-24.7

thus the corrections suggested by Eq. (38) were used. The above statements may help to explain somewhat the scatter in the variation of the constants  $k$  and  $n$  in the Elovich model and  $k$  and  $k'$  in the Langmuir model with pressure.

It is apparent that, despite the good agreement between the rate law and the data, the rate constants for the Langmuir model do not meet the criteria that have previously been established for a rate law to be a valid explanation of the mechanism, namely, equality of corresponding constants for both reaction. Figure 2 and Figures 24-29, Appendix D, show that, using the value for  $k$  and  $k'$  that have been obtained from the data, the calculated space velocity curves, which are the lines in Figure 2 and Figures 24-29, Appendix D, correspond very well to the experimental data. But the inequality in the values of the  $k$ 's and  $(k')$ 's and the difference in sign between the  $(k')$ 's for the forward and reverse reactions are phenomena that the simple Langmuir theory does not predict. Hence, modifications of the theory seem to be indicated by the experimental results.

One of the likely explanations of the deviation from theory seems likely to result from accounting for surface interactions and varying heat of adsorption with surface coverage, such as is indicated in Appendix A.4 and used in Section III.G. The approach is similar to that used in the development of Eq. (23), except that here the exponential terms in  $\theta_o$  and  $\theta_p$  will be first suppressed, whereas before the linear terms in  $\theta_o$  and  $\theta_p$  were first suppressed and added later. The rate equations are given by Eqs. (18), (3a), and (19).

$$r_{ad} = k_1 c_p (1 - \theta_o - \theta_p) e^{-a_1 \theta_p - a_2 \theta_o} - k_2 \theta_p e^{b_1 \theta_p + b_2 \theta_o} \quad (18)$$

$$r = k_3 \theta_p - k_4 \theta_o \quad (3a)$$

$$r_{de} = k_5 \theta_o e^{b_5 \theta_o + b_6 \theta_p} - k_6 c_o (1 - \theta_o - \theta_p) e^{-a_5 \theta_o - a_6 \theta_p} \quad (19)$$

If the surface reaction is assumed to be rate-controlling and it is further assumed that  $a_1 = a_2$ ,  $b_1 = b_2$ ,  $a_5 = a_6$ , and  $b_5 = b_6$ , (this implies that either an orthohydrogen or parahydrogen molecule adsorbed on a site will have the same heat of adsorption for that particular site), one achieves the rate equation

$$r = \frac{\frac{k^* c_H}{A + D c_H} (x - x_e)}{1 + \frac{(B - D) c_H}{A + D c_H} x} \quad (33a)$$

where now

$$k^* = k_1 k_3 k_5 \exp [(b_6 - a_1) (\theta_o + \theta_p)]$$

$$A = k_2 k_5 \exp [(b_6 + b_1) (\theta_o + \theta_p)]$$

$$B = k_1 k_5 \exp [(b_6 - a_1) (\theta_o + \theta_p)]$$

$$D = k_2 k_6 \exp [(b_1 - a_6) (\theta_o + \theta_p)]$$

The reason for the above equalization of the appropriate a's and b's is now apparent--all of the exponential terms contain the variable  $(\theta_o + \theta_p)$ , which is equal to the total fraction of surface that is covered. That the total

fraction covered is not constant is shown by the subsequent development.

The total fraction of surface that is covered at equilibrium composition of hydrogen is given by Eq. (39)

$$\theta_H = \frac{K_H c_H}{1 + K_H c_H} = \frac{K_H (c_{oe} + c_{pe})}{1 + K_H (c_{oe} + c_{pe})} \quad (39)$$

where

$K_H$  = hydrogen adsorption equilibrium constant  
(See Appendix A).

$$\theta_H = \theta_{oe} + \theta_{pe}.$$

For any other composition, the total coverage is postulated to change. If this change in coverage is designated as  $\delta\theta_H$ , then the relation between  $\delta\theta_H$  and the hydrogen coverage is given by Eq. (40).

$$\theta_o + \theta_p = \theta_H + \delta\theta_H \quad (40)$$

$\delta\theta_H$  can be positive, negative, or zero. The present task is to see if (and how)  $\delta\theta_H$  changes with gas phase composition. If ortho- and parahydrogen both obey a Langmuir adsorption isotherm, then it can be shown (Appendix A) that the total hydrogen isotherm is also a Langmuir isotherm, and that the adsorption constant  $K_H$  is given by Eq. (41).

$$K_H = K_p [s(1-x_e) + x_e] \quad (41)$$

where

$K_H$  = parahydrogen adsorption constant.

$s$  = separation factor.

For non-equilibrium adsorption, then, the coverage is given by Eq. (42).

$$\theta_o + \theta_p = \frac{K_p c_H [s(1-x) + x]}{1 + K_p c_H [s(1-x) + x]} \quad (42)$$

Eq. (41) is substituted into Eq. (39) and the result is combined with Eqs. (40) and (42) to yield Eq. (43), which gives  $\int \theta_H$  in terms of gas phase composition.

$$\int \theta_H = \frac{K_p c_H (s - 1) (x_e - x)}{1 + K_p c_H s [2 - (x + x_e)] + (x + x_e)} + K_p^2 c_H^2 [s(1-x) + x] [x(1-x_e) + x_e] \quad (43)$$

No matter whether  $x$  is greater or less than  $x_e$ , the denominator of Eq. (43) does not change sign. However, if  $x$  is smaller than  $x_e$ , the numerator of Eq. (43) is positive and hence,  $\int \theta_H$  is positive; conversely, if  $x$  is larger than  $x_e$ , the numerator is negative and  $\int \theta_H$  is consequently negative.

In the present series of runs, for the reaction  $o\text{-H}_2 \longrightarrow p\text{-H}_2$ ,  $x$  is less than  $x_e$  and consequently  $\int \theta_H$  is positive for the forward reaction. In the reverse reaction  $x$  is always greater than  $x_e$  and thus  $\int \theta_H$  is negative for this direction.

To return to the reaction mechanism, the experimental properties of the constants  $k$  and  $k'$  are listed in Table V. Also listed in Table V are the properties that must be exhibited by the parameters  $k^*$ ,  $A$ ,  $B$ , and  $D$  in order to achieve the observed results. If these constants are

Table V. Properties of Constants  $k$  and  $k'$ 

A. Observed properties of  $k$  and  $k'$ .

$$k = \frac{k^*}{A + Dc_H} \quad (a)$$

$$k' = \frac{B-D}{A + Dc_H} \quad (b)$$

$$\begin{array}{ccc} \underline{o \rightarrow p} & & \underline{p \rightarrow o} \\ k & \text{is greater than} & k \end{array} \quad (c)$$

$$\begin{array}{ccc} |k'| & \text{is greater than} & |k'| \end{array} \quad (d)$$

$$k' \text{ is positive} \quad \quad \quad k' \text{ is negative} \quad (e)$$

B. Properties of  $k^*$ ,  $A$ ,  $B$ , and  $D$  which yield above results.

$$\begin{array}{ccc} \underline{o \rightarrow p} & & \underline{p \rightarrow o} \\ k^* & \text{is greater than} & k^* \end{array} \quad (f)$$

$$B > D \quad \quad \quad D > B \quad (g)$$

$$A + Dc_H \quad \text{is less than} \quad A + Dc_H \quad (h)$$

$$\begin{array}{ccc} |B-D| & \text{is greater than} & |B-D| \end{array} \quad (i)$$

rearranged in terms of  $\delta\theta_H$ , the forms are given by Eqs. (44) through (47).

$$k^* = k_o^* e^{\beta \delta\theta_H} \quad (44)$$

$$A = A_o e^{\gamma \delta\theta_H} \quad (45)$$

$$B = B_o e^{\beta \delta\theta_H} \quad (46)$$

$$D = D_o e^{\alpha \delta\theta_H} \quad (47)$$

where

$$\gamma = b_1 + b_6$$

$$\beta = b_6 - a_1$$

$$\alpha = b_1 - a_6$$

The quantities  $\alpha$  and  $\beta$  can be either positive or negative, depending on the magnitudes of the quantities involved. There appears to be no way at present to predict which sign these quantities should take. However, if  $\alpha$  is negative and  $\beta$  is positive, then Table VI shows that the criteria that are outlined in Table V for a prediction of the experimental results are met.

The preceding development shows that if certain assumptions are accepted, namely those relating surface interactions and energy to the amount of hydrogen adsorbed, then the use of the Langmuir-Hinshelwood model as a representation of the ortho-parahydrogen reaction is justified. It should be pointed out that for the Langmuir rate equation, if either a two- or three-step-controlling mechanism is assumed, then the methods which were outlined above are much more difficult, and perhaps impossible to apply

Table VI.

Behavior of  $k^*$ , A, B, and D with Changes in  $\delta\theta_H$ .

$$k^* = k_o^* \exp(\beta \delta\theta_H) \quad (a)$$

$$A = A_o \exp(\gamma \delta\theta_H) \quad (b)$$

$$B = B_o \exp(\beta \delta\theta_H) \quad (c)$$

$$D = D_o \exp(\alpha \delta\theta_H) \quad (d)$$

Assume  $\beta$  and  $\gamma$  are positive and  $\alpha$  is negative.

$$\begin{array}{ccc} \underline{o \rightarrow p} & & \underline{p \rightarrow o} \\ \delta\theta_H \text{ is positive} & & \delta\theta_H \text{ is negative} \\ \text{(These are independent of mechanism)} & & \end{array} \quad (e)$$

Then

$$k^* \text{ is greater than } k^* \quad (f)$$

$$A \text{ is greater than } A \quad (g)$$

$$B \text{ is greater than } B \quad (h)$$

$$D \text{ is less than } D \quad (i)$$

At this stage, the terms (B-D) and  $(A+Dc_H)$  can be either greater or smaller for one direction compared to the other. However, if  $\delta\theta_H = 0$ , the simple Langmuir law is obtained. Hutchinson [36] showed that, for surface reaction controlling, the terms B and D are essentially the same as the adsorption constants for para- and orthohydrogen, respectively. Under these conditions,  $D > B$  due to the separation factor, as he showed [36]. Thus, it is probable that  $D_o > B_o$  in the present case.

The following statements summarize the justification of statements (f), (g), (h), and (i), Table V, by statements outlined in Table VI:

1. The requirement of statement (f) in Table V is met directly by the result of statement (f) in Table VI.
2. Since  $D_o$  is probably greater than  $B_o$ , statement (g) of Table V can be met without contradiction by statements (h) and (i) of Table VI.
3. If  $|D_{o \rightarrow p} - D_{p \rightarrow o}|$  is greater than  $|A_{o \rightarrow p} - A_{p \rightarrow o}|$ , then the requirement presented by statement (h), Table V, is met.

Table VI (Continued)

4. If  $\left| B_{o \rightarrow p} - B_{p \rightarrow o} \right|$  is less than  $\left| D_{o \rightarrow p} - D_{p \rightarrow o} \right|$ ,  
 then the requirement of statement (i), Table V,  
 is satisfied.

Statements 3 and 4 (above) will be true if  $|d|$  is greater than  $\nu$  and  $B_o$  is less than  $D_o$ . It has already been shown that  $D_o$  is probably greater than  $B_o$  and there is no way at present of predicting relative magnitudes of the exponential terms. See text for amplification of this latter point.

because of the presence of additive terms in the formation of the constants A, B, and D.

It should also be noted that, during the course of the investigation, it was thought that the deviation from the straight line of the points at low space velocities could be accounted for by pore diffusion effects. The reason for this thought is that, although the previous investigators who had studied pore diffusion in the ortho-parahydrogen reaction [cf., 2, 25, 56, 57] had found no pore diffusion effects, in some cases they were working with less active catalysts than the present one and all of their results were based upon a first-order rate law. As is shown in Appendix C, for a first order rate law, pore diffusion affects the value of the rate constant only by lowering it at a constant value. In the case of a non-first-order reaction, the rate constant with pore diffusion effects is a function of the reactant concentration. The result of this effect is that the reaction order is reduced, as shown in Appendix C. The Langmuir equation is not a first-order expression, so that it falls in the latter category. The idea of using a smaller mesh catalyst to check pore diffusion effects is still valid for the example of a non-first-order reaction. Thus, Runs, 82, 83, and 85 were conducted using a 50-80 mesh catalyst. (A 30-50 mesh catalyst was used in the other runs). However, it is apparent from Table IV that the rate constants for the smaller particle catalyst are quite in line with those for the larger particle catalyst at comparable pressures, except for Run 85. The case of Run 85 is difficult to explain. It is seen from the integrated rate plot (Figure 51, Appendix F) that the magnitude of the intercept is

much higher than that of any of the other runs. This fact affects the values of  $k$  and  $k'$  both to the extent that they are negative numbers as calculated from the slope and intercept (Eqs. 36 and 37). Physically,  $k'$  could be negative, but it is unrealistic to talk about a negative  $k$ . There was a slight change in equipment arrangement in Runs 82, 83, and 85 in that a span on the recorder of approximately twice that that was used in the other runs was used for the latter three runs. It was hoped that this procedure would improve the accuracy of the data, but one effect that was noticed during the runs was that the equilibrium point was harder to establish here than in the rest of the runs. It is suspected that this may have had some influence on the data. Runs 82 and 83 may be alright; the data, as was previously mentioned, are in line with the data from the larger mesh size catalyst pellets. Also, the integrated plots for these runs showed the same deviation effects as for the runs with the larger catalyst particles. In a recent publication Roberts and Satterfield [49] showed how effectiveness factors (Appendix C) could be calculated for a rate expression of the Langmuir-Hinshelwood type. These calculations were performed (Appendix C) and the results of these, together with the above considerations, showed that pore diffusion was probably not a major rate-influencing factor.

A final justification of the use of the Langmuir model is seen when the constants  $k$  and  $k'$  are tested for pressure dependence. According to statements following Eq. (33) both constants should be inversely dependent upon pressure. They are of the form

$$k = \frac{\rho}{A + Dc_H} \quad (48)$$

where

$$K = k \text{ or } k'.$$

$$\rho = k^* \text{ or } (B-D).$$

Eq. (48) may be rearranged to the form shown by Eq. (49).

$$\frac{1}{K} = \frac{D}{\rho} c_H + \frac{A}{\rho} \quad (49)$$

Thus, a plot of  $1/K$  vs.  $c_H$  should yield a straight line. Plots of  $k$  vs  $c_H$  and  $k'$  vs  $c_H$  were prepared. Figures 16 and 17 show these plots. It is apparent that Eq. (49) predicts the behavior of  $k$  and  $k'$  quite well. There is some scatter in the data, particularly in the  $(k')$ 's, but the overall trend is apparent. Eqs. (50) and (51) give the relationship between  $k$ ,  $k'$ , and  $c_H$  for the forward reaction.

$$k = \frac{1}{0.0318c_H + 0.001} \quad (50)$$

$$k' = \frac{1}{0.70c_H + 0.02} \quad (51)$$

and Eqs. (52) and (53) show the similar relationships for the reverse reaction.

$$k = \frac{1}{0.0712c_H + 0.001} \quad (52)$$

$$k' = \frac{-1}{2.16c_H - 0.04} \quad (53)$$

The constants  $A$ ,  $D$ , and  $\rho$  in Eq. (49) cannot be determined explicitly because there are only two independent relationships from which to determine them.

#### E. First Order Kinetics

Since a first-order rate law was found by many investigators to represent the rate of ortho-parahydrogen

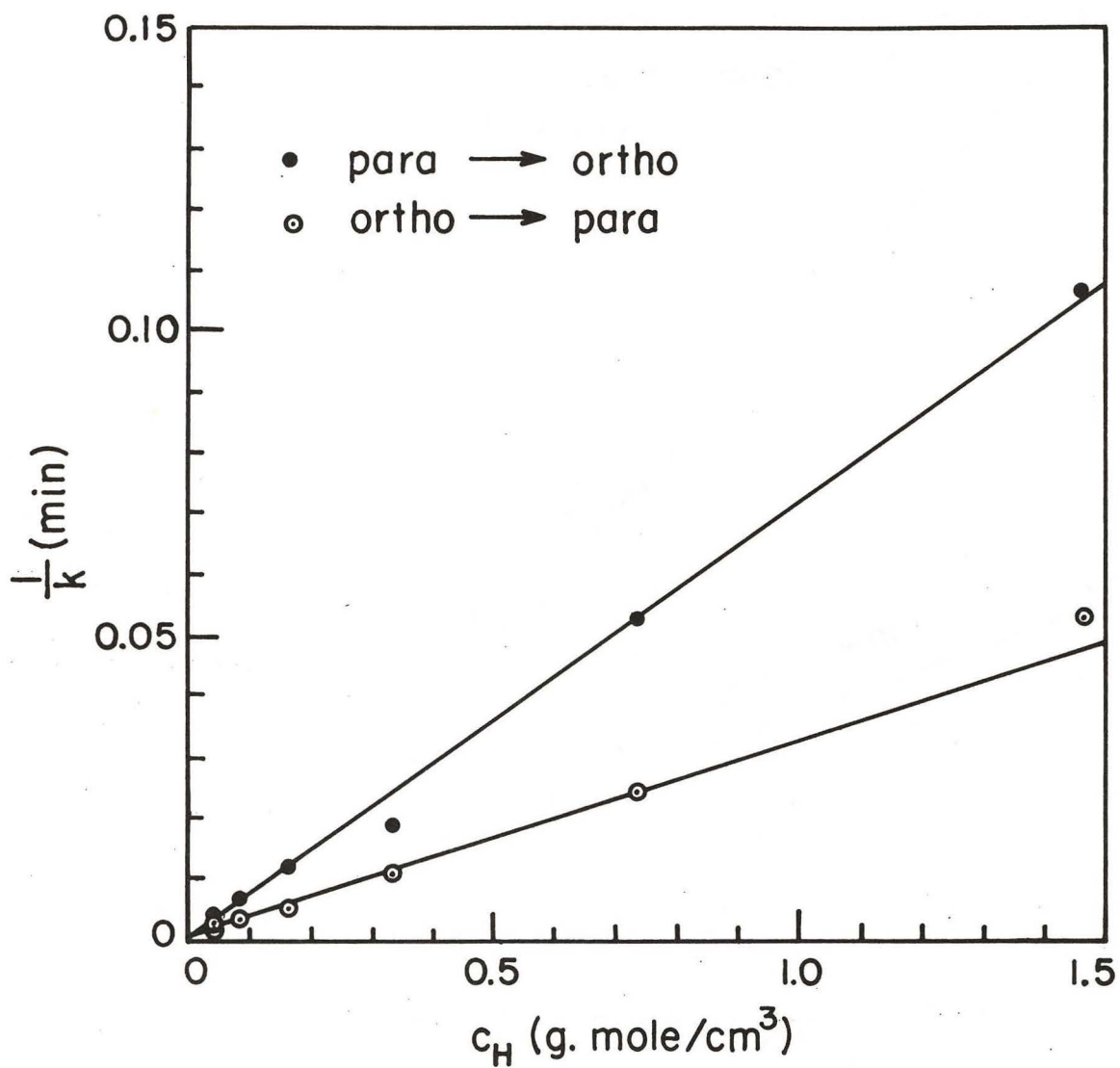


FIGURE 16. Rate Constant  $k$  as a Function of Pressure

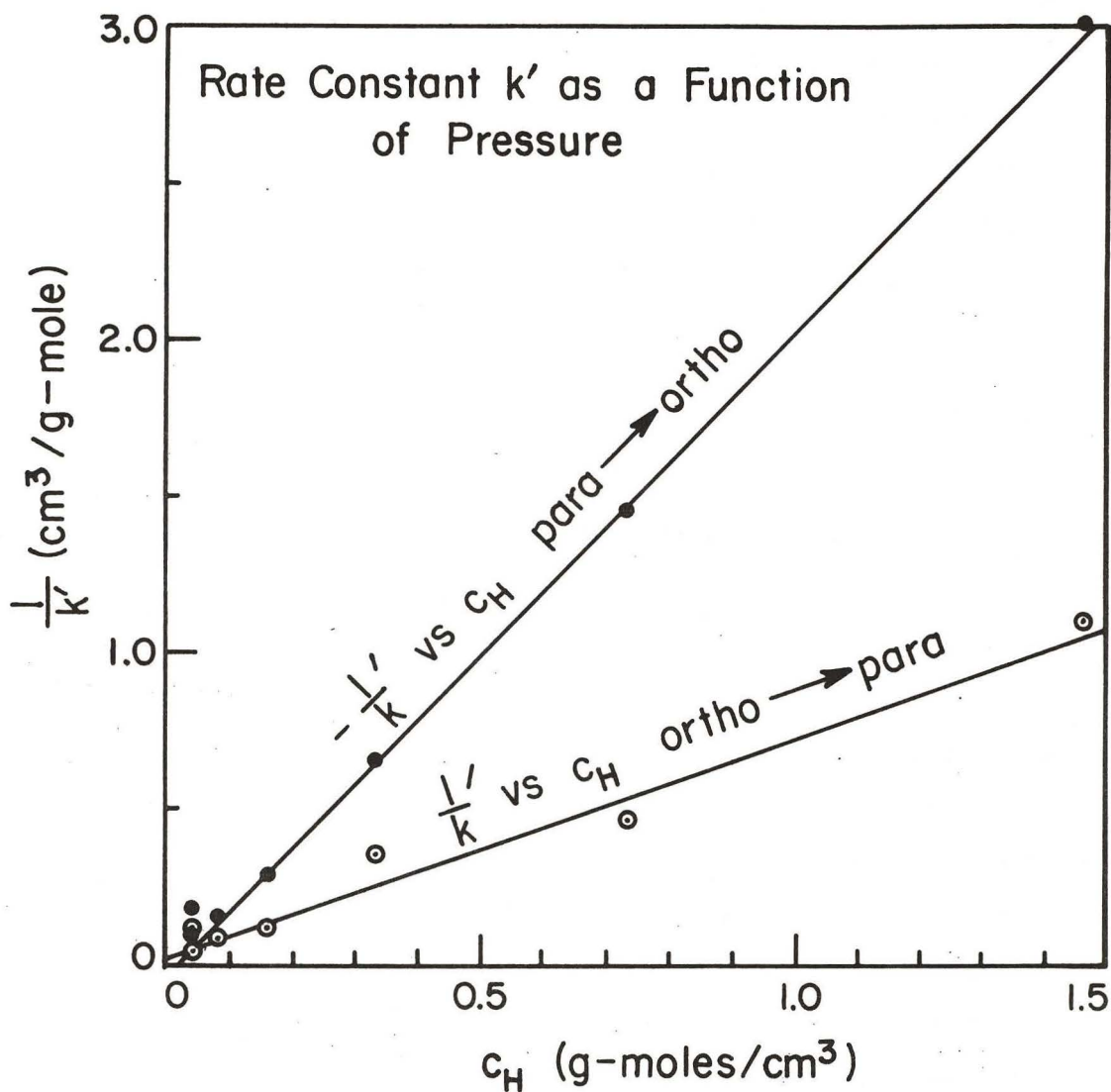


FIGURE 17. Rate Constant  $k'$  as a Function of Pressure

conversion, it should be mentioned here. As was pointed out in Section III.C., a first order rate law will be obtained from the Langmuir rate expression if  $k' = 0$ . If  $k'$  does equal zero, then the line on the Langmuir plots should pass through the origin. It is obvious that such is not the case for the present data. However, in order to remove any lingering doubt about the non-validity of first-order kinetics, first-order rate plots were made. The first-order rate equation is given by Eq. (1).

$$r = k(c_p - c_{pe}) = kc_H(x - x_e) \quad (1)$$

The integrated form is given by Eq. (54)

$$-k\tau = \ln(x_2 - x_e) - \ln(x_1 - x_e) \quad (54)$$

Thus, a plot of  $\ln(x_2 - x_e)$  vs  $\tau$  will give a straight line of slope  $(-k)$  and intercept  $\ln(x_1 - x_e)$  if first order kinetics are valid. Figures 18 and 19 show the first-order plots for Runs 68 and 69. The correlations appear to be fairly good, although the rate constants in both directions do not agree too well. The values of the constants are  $k=261$  for Run 68 and  $k=230$  for Run 69. This represents a 13.4% difference. These values of  $k$  were used to calculate space velocity curves (Figure 20). A glance at Figure 20 shows that the first-order expression does not predict the actual values very well, certainly not as accurately as the Langmuir expression. It is therefore concluded that a first-order rate law does not represent the rate of the ortho-parahydrogen reaction over a hydrous ferric oxide catalyst.

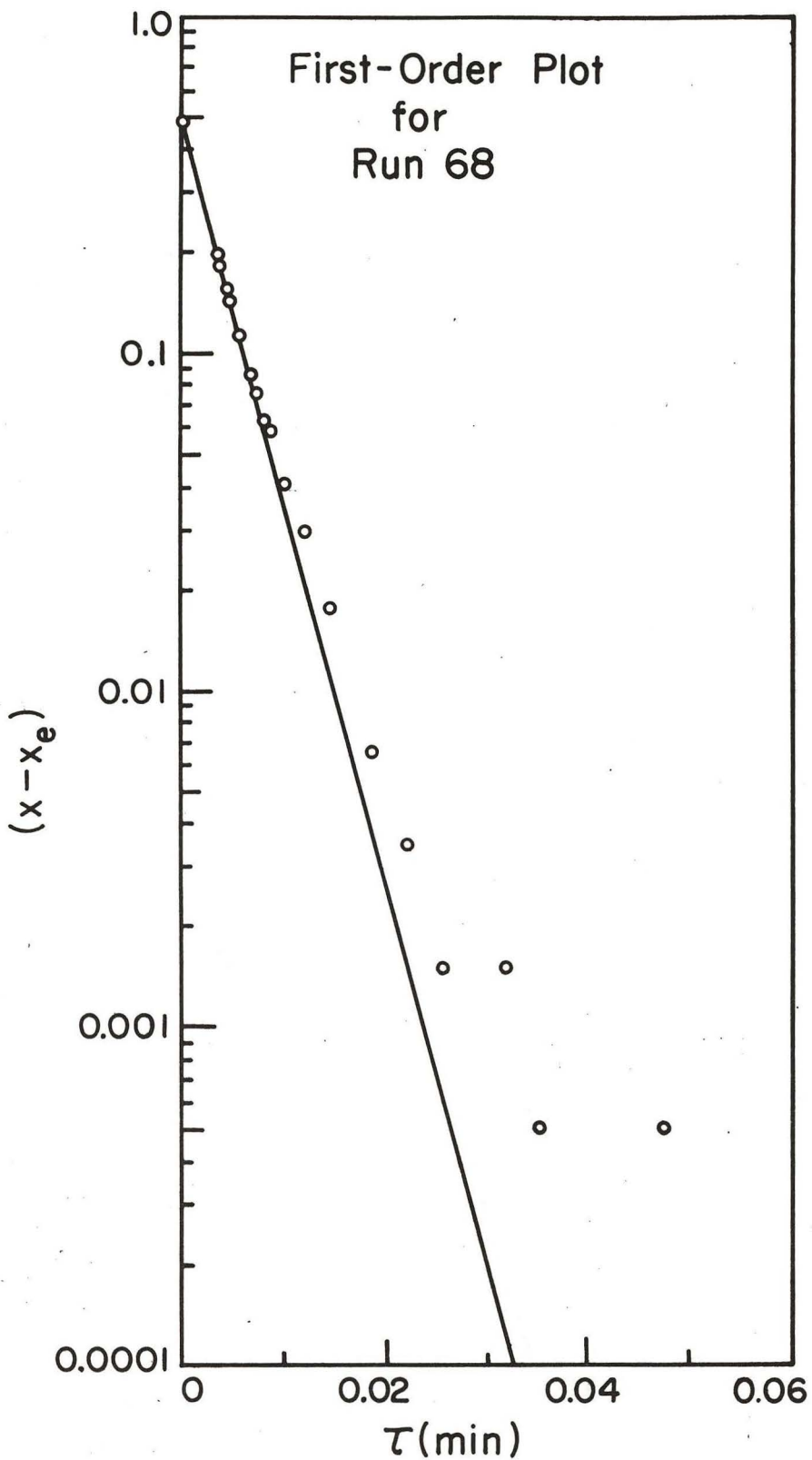


FIGURE 18. First-Order Plot for Run 68

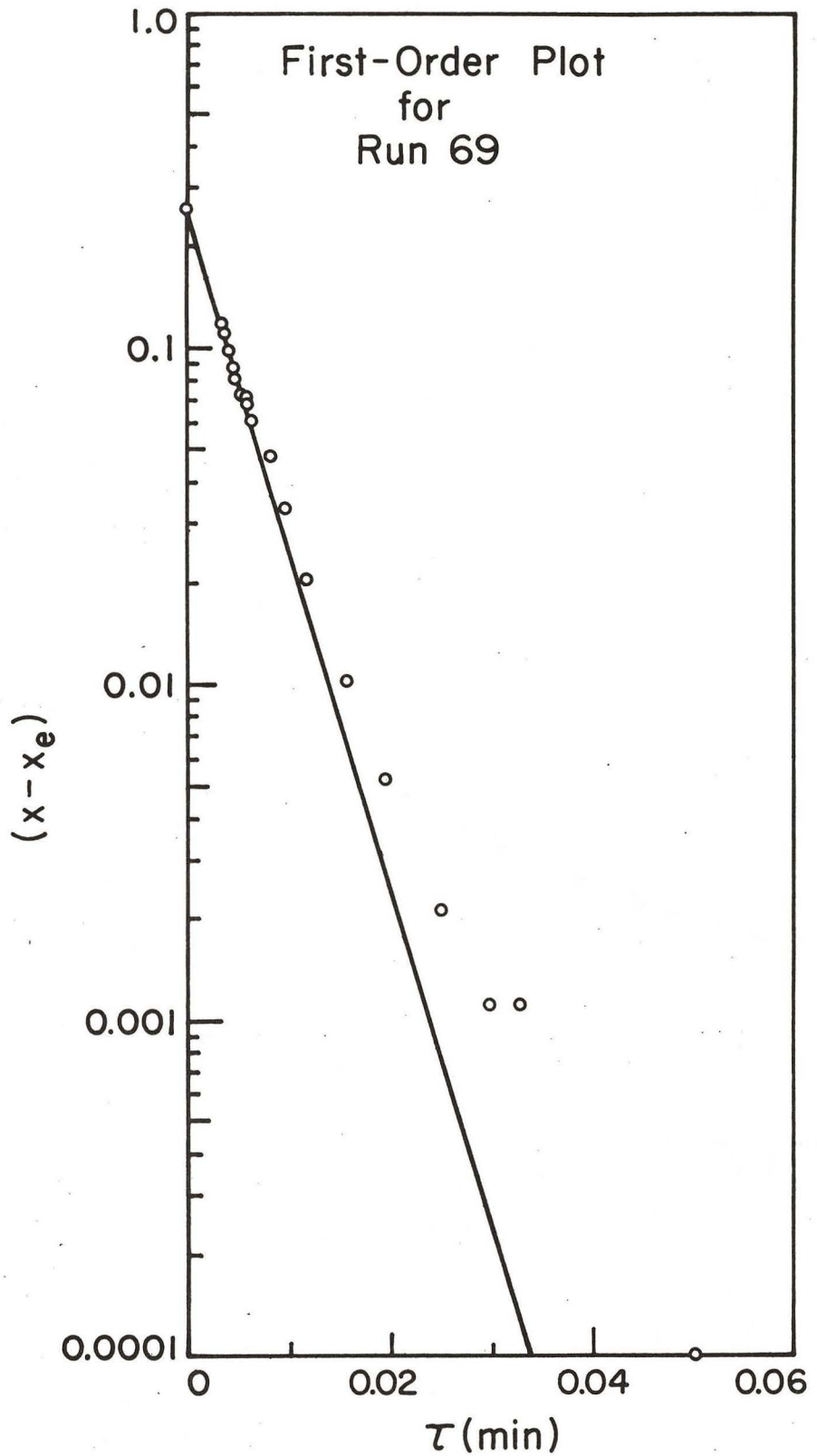


FIGURE 19. First-Order Plot for Run 69

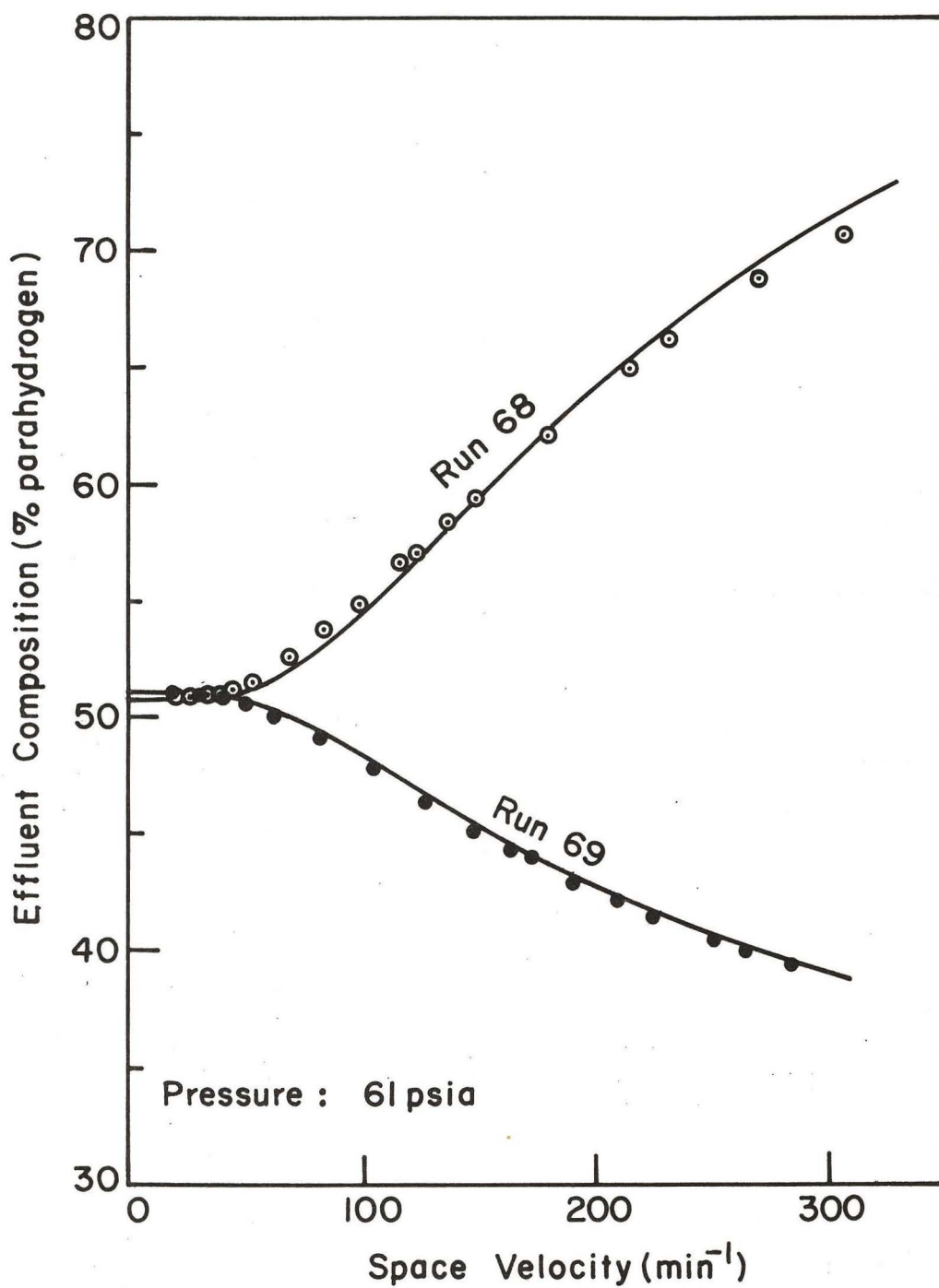


FIGURE 20. First-Order Space Velocity Curves for Runs 68 and 69

## VII. CONCLUSIONS

### A. Comparison of Models

Four different reaction rate laws have been derived from different sets of assumptions. Data for the ortho-parahydrogen shift reaction in both directions at 76°K and at pressures of 30 to 1010 psia have been compared with these laws. It was found that none of the models could be considered as being a satisfactory theoretical explanation for the reaction rate. However, two of them were found to give a better representation of the data than the other two.

The first rate equation is of the Langmuir-Hinshelwood type, as shown.

$$r = \frac{k c_H (x - x_e)}{1 + k' c_H x}$$

This equation may be used to describe the reaction in either direction. However, the rate constants  $k$  and  $k'$  were found to differ for the opposite reactions. For the forward (ortho-to-para) reaction, the constants  $k$  and  $k'$  are given by

$$k = \frac{1}{0.0318 c_H + 0.001} \quad \text{min}^{-1}$$
$$k' = \frac{1}{0.70 c_H + 0.02} \quad \text{cm}^3 \text{ g-mole}^{-1}$$

and  $k$  and  $k'$  may be found for the reverse reaction by

$$k = \frac{1}{0.0712 c_H + 0.001} \quad \text{min}^{-1}$$
$$k' = \frac{-1}{2.16 c_H - 0.04} \quad \text{cm}^3 \text{ g-mole}^{-1}$$

where  $c_H = \text{g-moles cm}^{-3}$ . The difference in the  $k$  and  $k'$  values for the forward and reverse reactions can be qualitatively explained by the assumption of a non-uniform heat of adsorption.

It was also found that the reaction rate could be correlated by a relation which was derived using the Elovich equation for rates of adsorption.

$$r = k \ln \left[ \left( \frac{x}{x_e} \right)^n \left( \frac{1-x_e}{1-x} \right) \right]$$

where  $k = 3.5 \text{ g-moles min}^{-1} \text{ cm}^{-3}$  and  $n = 0.75$ . This equation is valid in both directions, but appears to break down at pressures below approximately 100 psia. Since the use of the Elovich equation in the present case is somewhat open to question, due to the fact that hindering effects between species on the surface are not taken into account, this equation must be regarded as being primarily an empirical one.

A third rate equation that was developed was the Freundlich equation

$$r = k c_H^m \left[ x^{1/n} - \left( \frac{1}{K_{eq}} \right)^{1/n} (1-x)^{1/n} \right]$$

This same equation resulted regardless of which step was assumed rate-controlling. The data were not as well correlated by this equation as by the above two, so that the Freundlich equation is not felt to be useful for the present reaction.

The fourth equation that was derived followed an approach that was suggested by the work of Temkin.

$$r = k \ln \left[ \frac{s(1-x) + x}{s(1-x_e) + x_e} \right]$$

This equation did not correlate the rate data as well as any of the previous three and, in view of the somewhat simplified assumptions regarding the separation factor that were used, this equation is not recommended as a means of describing the ortho-parahydrogen shift reaction.

For design purposes, the Langmuir rate equations are preferred, due to their relative simplicity in handling. It appears though that further understanding of the adsorption process is necessary before a complete model of the reaction can be constructed.

#### B. Significance of Project

The project was undertaken in order to learn more about catalytic reactions and to develop a model for the ortho-parahydrogen shift reaction. In order to accomplish these aims mechanisms based upon four different adsorption rate laws were derived and compared against the data. The results showed that none of the models was entirely satisfactory as a representation of the reaction. When non-uniform heat of adsorption effects were assumed, the deviation from the Langmuir model could be explained under certain conditions. These conditions required that the heat of adsorption vary linearly with total hydrogen surface coverage and that changes in the total coverage be caused only by changes in gas-phase composition. To the author's knowledge, no such accounting for deviation from the Langmuir model has previously been reported, although models

in which a non-uniform heat of adsorption is postulated have been proposed before (the ammonia synthesis reaction is a well-known example).

The technique of using a change in surface coverage ( $\int \theta_H$ ) appears not to have been used prior to this time, although this approach admittedly might be restricted to the ortho-parahydrogen reaction. One of the weaknesses of this model is that there are no data at present which allow a priori the prediction of the signs of the coefficients of  $\int \theta_H$ . The ultimate goal of any theory is the prediction of results, rather than the relying of data to predict fundamental quantities which might be contained in a theory.

The results of the present work do not support rigorously any of the existing kinetic models. Although it seems from the data that surface reaction is the rate-controlling step, the formulas which were derived from the Langmuir and Elovich adsorption rate equations must be regarded as more or less empirical correlations due to the inaccuracies in the assumptions upon which these two adsorption models are based. However, the results have shown that at pressures above approximately 100 psia, the Elovich-based equation is a good representation of the reaction in both directions and that at all pressures, a Langmuir-Hinshelwood equation can be written for the reaction in either direction. The Langmuir equations are preferred chiefly because they are easier to work with.

## VIII. RECOMMENDATIONS FOR FURTHER WORK

During the period in which the present work was undertaken, several relevant and interesting problems arose. Some of these were solved and the results are contained herein; others showed that much more thought and experimentation than were felt to be inside the scope of the present work were required.

One of the most important and significant items that requires attention is a study of the adsorption process, particularly in reference to hydrogen on ferric oxide. There are two experiments that can be suggested. The first is the obtaining of adsorption isotherms. Although Clark, et.al. [15] have obtained some data for hydrogen adsorption on an iron catalyst, the pressure range of their data is limited to about 200 psia. Adsorption data are needed up to a pressure of at least 1000 psia in order that comparison with the present kinetic data may be made. Also in such an experiment, it would be well to obtain separate isotherms for ortho- and parahydrogen. These could be compared with the total hydrogen isotherm in a manner suggested in Appendix A. It is realized that the presence of a reaction complicates this type of work but one approach might be to adsorb hydrogen on a substance (such as nickel) which does adsorb hydrogen but does not promote the shift reaction. The use of such an adsorbent would allow the researcher to introduce different compositions of hydrogen into the chamber and see what effect a change in composition has on the total amount adsorbed. If orthohydrogen is more strongly adsorbed than parahydrogen (which case the evidence seems to support (See Appendix A)), a change

in composition of the gas should affect the amount that can be adsorbed.

A second adsorption experiment would be the measurement of rates of adsorption. It is apparent from the present work that not enough is known about this phase of kinetics to be able to build a satisfactory reaction model. Ortho-parahydrogen adsorption would be a particularly interesting system to study because it provides an ideal one for examining rates of adsorption of mixtures. Perhaps experiments similar to the one suggested above (adsorption without reaction) could be devised.

Much more knowledge of rates of adsorption of mixtures is required in order to better understand catalytic rate processes. There has been very little work done in this area and the data that are available are confusing and contradictory [44]. There is no end to systems which might be investigated along this line, although there are some which would obviously be more practical for experimental purposes than others. Perhaps a long term project involving several systems should be undertaken. Much valuable information could be obtained from such a project.

As far as ortho-parahydrogen kinetics are concerned, one or two projects might be considered. Probably the more important would be the investigation of the kinetics over the new, more active catalysts that have recently been developed [14, 15, 50]. It may be that these catalysts are active enough that diffusion effects may become significant [14]. This would provide a point from which to investigate pore diffusion effects, particularly with the involvement of a Langmuir-Hinshelwood type rate expression (See Appendix C). Of this, more will be said below.

The second ortho-parahydrogen shift study that might be made, although in view of the conclusions that are contained herein this is probably of not too great importance, would be a temperature study of the reaction in both directions. An apparatus similar to that reported by Hutchinson, et.al. [37] could be built for this purpose.

It was mentioned above that pore diffusion effects for non-integral-order reactions could be studied. Some work has been done in this area [49] but more work seems to be indicated. The ortho-parahydrogen reaction would appear to be an ideal one for this study, since a Langmuir type expression does fit the reaction. It may be likely that the newly developed catalysts would provide an ideal vehicle for such a study, as present evidence suggests that pore diffusion effects are present [14].

While the present theoretical approach was being developed, it became increasingly apparent to the author that perhaps the present approach to catalytic kinetics is somewhat lacking. There is no quarrel with the postulation that adsorption and desorption are involved (nor diffusion, for that matter) but as the experimental data showed, none of the existing approaches proved entirely adequate as a means of building a catalytic model. Of course this topic has been argued previously (cf., Boudart [7] and Weller [59]), but the author cannot agree entirely with either of these writers' approaches. He agrees with Weller [59] that the Langmuir approach leaves much to be desired as the basis for a catalytic model but does not agree that simply taking the data and fitting them to some empirical curve is a desired method. The present work showed that models based on Freundlich or Temkin adsorption mechanisms do not

appear to work even as well as one based on the Langmuir adsorption mechanism, which itself had to be regarded more or less as an empirical correlation in view of the present results. The phenomenon of non-uniform heat of adsorption is one topic that appears to be promising as a means of better explaining the physical situation. Perhaps an entirely new approach to the topic is needed. A parallel which might be drawn is the introduction of the "penetration theory" as an alternate for the old "two-film theory" in interphase mass transfer. It seems to the author that the time is about ripe for new advances in the theory of kinetics to be made.

## IX. NOTATION

A	= constant in Eq. 33.
a	= $\alpha/RT$ , coefficient of surface effect on activation energy of adsorption.
B	= constant in Eq. 33.
b	= $\beta/RT$ , coefficient of surface effect on activation energy of desorption.
c	= concentration, g-moles $\text{cm}^{-3}$ .
D	= constant in Eq. 33.
d	= differential operator.
F	= total feed rate, $\text{cm}^3 \text{min}^{-1}$ .
I	= intercept on Langmuir plot.
K	= equilibrium constant.
k	= reaction rate constant, $\text{min}^{-1}$ or $\text{g-mole min}^{-1} \text{cm}^{-3}$ catalyst.
m	= constant.
n	= constant.
p	= partial pressure, atm.
R	= gas constant, $1.998 \text{ cal g-mole}^{-1} \text{ }^\circ\text{K}^{-1}$ .
r	= reaction rate, $\text{g-mole min}^{-1} \text{cm}^{-3}$ catalyst.
S	= slope on Langmuir plot
SV	= space velocity, $\text{min}^{-1}$ .
s	= separation factor.
T	= temperature, $^\circ\text{K}$ .
V	= volume, $\text{cm}^3$ .
x	= mole fraction parahydrogen

### GREEK

$\alpha$	= coefficient of surface effect on activation energy of adsorption, cal.
$\Delta$	= constant in Eq. 47.
$\beta$	= coefficient of surface effect on activation energy of desorption, cal.

$\beta$	= constant in Eq. 44.
$\gamma$	= constant in Eq. 45.
$\delta$	= change in state.
$K$	= constant in Eq. 48.
$\rho$	= constant in Eq. 48.
$\theta$	= fraction of surface occupied by adsorbed specie.
$\tau$	= space time, min.

### SUBSCRIPTS

A	= ammonia.
ad	= adsorption or adsorbed.
b	= reverse direction, Eq. A.
des	= desorption or desorbed.
e,eq	= equilibrium.
f	= forward direction, Eq. A.
H	= hydrogen.
o	= orthohydrogen.
p	= parahydrogen.
s	= surface.
r	= first-order reaction.
r	= reactor volume.
$\alpha$	= adsorption controlling, Eq. 26.
$\delta$	= desorption controlling, Eq. 28.

## X. BIBLIOGRAPHY

1. Barrick, P.L., L.F. Brown, "Literature Survey of Orthohydrogen and Parahydrogen Research," University of Colorado, Technical Documentary Report APL-TDR-64-81, August 1964.
2. Barrick, P.L., L.F. Brown, H.L. Hutchinson, "Kinetics and Diffusion Study of the Para-Ortho Shift of Hydrogen," University of Colorado, Technical Documentary Report APL-TDR-64-77, September 1964.
3. Barrick, P.L., L.F. Brown, H.L. Hutchinson, R.L. Cruse, Adv. Cryo. Eng., 10, 181 (1965).
4. Bokhoven, C., C. van Heerden, R. Westrik, P. Zweitering, in Emmett, P.H., ed., "Catalysis," III, Reinhold, New York, 265 (1955).
5. Bonhoeffer, K.F., P. Harteck, Naturwiss., 17, 182 (1929).
6. \_\_\_\_\_, Z. physik. Chem., B4, 113 (1929).
7. Boudart, M., A.I.Ch.E. J., 2, 62 (1956).
8. Brown, L.F., Personal Communication.
9. Brunauer, S., K.S. Love, R.G. Keenan, J. Am. Chem. Soc., 64, 751 (1942).
10. Buyanov, R.A., Kinetika i Kataliz, 1, No. 2, 306 (1960).
11. Ibid., 1, No. 3 (1960).
12. Ibid., 1, No. 4 (1960).
13. Chapin, D.S., H. L. Johnston, J. Am. Chem. Soc., 79, 2406 (1957).
14. Clark, R.G., J.F. Kucirka, A. Jambhekar, G.E. Schmauch, "Investigation of the Para-Ortho Shift of Hydrogen," Air Products and Chemicals, Inc., Summary Technical Report ASD-TDR 62-833, Part I, July 1962.

15. Ibid., Part II, October 1963.
16. Cunningham, C.M., H.L. Johnston, J. Am. Chem. Soc., 80, 2377 (1958).
17. Denbigh, K.G., "Chemical Equilibrium," Cambridge, 158 (1961).
18. \_\_\_\_\_, "Chemical Reactor Theory," Cambridge, 39 (1965).
19. Dennison, D.M., Proc. Roy. Soc. Ser. A (London), 115, 483 (1927).
20. Farkas, A., Z. physik. Chem., B10, 419 (1930).
21. Farkas, A., H. Sachsse, Z. physik. Chem., B23, 1 (1933).
22. Ibid., p. 19.
23. Frankenburg, W.G., in Emmett, P.H., ed., "Catalysis," III, Reinhold, New York, 171 (1955).
24. Ibid., p. 186.
25. Geddes, D.D., M.S. Thesis, University of Colorado (1963).
26. Gould, A.J., W. Bleakney, H.S. Taylor, J. Chem. Phys., 2, 362 (1934).
27. Harrison, L.G., C.A. McDowell, Proc. Roy. Soc. (London) Ser. A., 220, 77 (1953).
28. Ibid., 228, 66 (1955).
29. Hayward, D.O., B.M.W. Trapnell, "Chemisorption," 2nd ed., Butterworths, Washington, Ch. 3 (1964).
30. Ibid., Ch. 4.
31. Ibid., Ch. 5.
32. Ibid., p. 170.
33. Heisenberg, W., Z. Physik., 41, 239 (1927).

34. Hougen, O.A., K.M. Watson, Ind. Eng. Chem., 35, 529 (1943).
35. Hund, F., Z. Physik., 42, 93 (1927).
36. Hutchinson, H.L., M.S. Thesis, University of Colorado (1964).
37. Hutchinson, H.L., P.L. Barrick, L.F. Brown, Adv. Cryo. Eng., 10, 190 (1965).
38. Johnson, V.J., ed., "Properties of Materials at Low Temperature," Phase I, Nat. Bur. Standards Report, Ch. 4.002, December 1959.
39. Kalckar, F. E. Teller, Proc. Roy. Soc., A150, 520 (1935).
40. Keeler, R.N., D.H. Weitzel, J.H. Blake, M. Konecnik, Adv. Cryo. Eng., 5, 511 (1960).
41. Levenspiel, O.A., "Chemical Reaction Engineering," John Wiley and Sons, New York, 101 (1962).
42. Ibid., p. 107.
43. Ibid., p. 431.
44. Low, M.J.D., Chem. Rev., 60, 267 (1960).
45. McLennan, J.C., J.H. McLeod, Nature, 123, 160 (1929).
46. Ozaki, A., H.S. Taylor, M. Boudart, Proc. Roy. Soc., A258, 47 (1960).
47. Purcell, J.R., J.W. Draper, D.H. Weitzel, Adv. Cryo. Eng., 3, 191 (1960).
48. Rideal, E.K., Proc. Camb. Phil. Soc., 35, 130 (1939).
49. Roberts, G.W., C.N. Satterfield, Ind. Eng. Chem. Fundamentals, 4, 288 (1965).
50. Sandler, Y.L., J. Phys. Chem., 58, 58 (1954).
51. Schmauch, G.E., A. H. Singleton, Ind. Eng. Chem., 56, 20 (1964).

52. Smith, J.M., "Chemical Engineering Kinetics," McGraw-Hill, New York, 94 (1956).
53. Ibid., p. 248.
54. Temkin, M., V. Pyzhev, Acta. Physicochim. USSR, 12, 327 (1940).
55. Trapnell, B.M.W., in Emmett, P.H., ed., "Catalysis," III, Reinhold, New York, 1 (1955).
56. Wakao, N., P.W. Selwood, J.M. Smith, A.I.Ch.E. J., 8, 478 (1962).
57. Weitzel, D.H., J.H. Blake, M. Konecnik, Adv. Cryo. Eng., 4, 286 (1960).
58. Weller, S., A.I.Ch.E. J., 2, 59 (1956).
59. Wigner, E., Z. physik. Chem., B23, 28 (1933).
60. Yang, K.H., O.A. Hougen, Ind. Eng. Chem., 35, 529 (1943).

XI. APPENDICES

## APPENDIX A

### Adsorption Phenomena

#### 1. Adsorption

There are two general types of adsorption that are commonly accepted today. These are physical adsorption and chemical or chemisorption. Physical adsorption is characterized by the formation of van der Waal-type bonds and low heats of adsorption (2-3 kcal/mole, at most). Chemisorption, on the other hand, is generally thought of as possessing chemical type bonds and consequently, high (on the order of 20-30 kcal/mole) heats of adsorption. In addition, multiple layers of adsorbed molecules are possible under conditions of physical adsorption while only monolayer adsorption is possible in chemical adsorption. For monolayer adsorption, the following development is valid regardless of whether physical or chemical adsorption is occurring. The development follows that of Trapnell [7], although it is not original with him (cf., 13,18).

For a gas at pressure  $p$  and temperature  $T$ , the number of molecules striking one square centimeter of surface per second is  $p/\sqrt{2\pi mk_B T}$ , where  $m$  is the mass of one molecule and  $k_B$  is the Boltzmann constant. However, not all of the molecules which strike a catalytic surface will necessarily be adsorbed. If  $s$  is defined as the fraction of molecules striking the surface that are adsorbed, then the rate of adsorption,  $u$  (molecules adsorbed per  $\text{cm}^2$  per second) is

$$u = \frac{sp}{\sqrt{2\pi mk_B T}} \quad (1)$$

Generally,  $s$  is not equal to unity. One or more of the following factors may affect  $s$  and cause it to be less than unity.

1. Activation energy. For an activated adsorption process the molecules must possess the necessary activation energy in order to be adsorbed.
2. Steric factor. The molecules must also possess the particular configuration of the "activated complex" in order to be adsorbed.
3. Efficiency of energy transfer. Once the molecule strikes the surface, it must lose the amount of energy which exceeds its thermal energy. Otherwise it will "bounce off" the surface after a period of one molecular vibration.
4. Surface heterogeneity. The activity will not, in general, be uniform over the surface and this fact will affect the sticking probability.
5. Collision with an occupied site. Although this does not preclude adsorption, there is a possibility that a molecule colliding with an occupied site will desorb before it can migrate to an unoccupied site.

If the above factors are taken into account, the sticking factor  $s$  may be represented as

$$s = \sigma f(\theta) e^{-E/RT} \quad (2)$$

where

$\sigma$  = condensation coefficient.

$f(\theta)$  = function of surface coverage,  $\theta$ .

$E$  = activation energy, cal g-mole<sup>-1</sup>.

$R$  = gas constant, cal g-mole<sup>-1</sup> °K<sup>-1</sup>.

Generally,  $s$  is not equal to unity. One or more of the following factors may affect  $s$  and cause it to be less than unity.

1. Activation energy. For an activated adsorption process the molecules must possess the necessary activation energy in order to be adsorbed.
2. Steric factor. The molecules must also possess the particular configuration of the "activated complex" in order to be adsorbed.
3. Efficiency of energy transfer. Once the molecule strikes the surface, it must lose the amount of energy which exceeds its thermal energy. Otherwise it will "bounce off" the surface after a period of one molecular vibration.
4. Surface heterogeneity. The activity will not, in general, be uniform over the surface and this fact will affect the sticking probability.
5. Collision with an occupied site. Although this does not preclude adsorption, there is a possibility that a molecule colliding with an occupied site will desorb before it can migrate to an unoccupied site.

If the above factors are taken into account, the sticking factor  $s$  may be represented as

$$s = \sigma f(\theta) e^{-E/RT} \quad (2)$$

where

$\sigma$  = condensation coefficient.

$f(\theta)$  = function of surface coverage,  $\theta$ .

$E$  = activation energy, cal g-mole<sup>-1</sup>.

$R$  = gas constant, cal g-mole<sup>-1</sup> °K<sup>-1</sup>.

However, it should be noted that both  $\sigma$  and  $E$  can be functions of  $\theta$ , the fraction of surface that is occupied by adsorbed molecules.

Substitution of Eq. (2) into Eq. (1) yields

$$u = \frac{\sigma(\theta) p}{\sqrt{2\pi m k_B T}} f(\theta) e^{-E(\theta)/RT} \quad (3)$$

An exact solution of Eq. (3) may be obtained by dividing the surface into elements  $ds$  over which the above five factors are the same and integrating over the surface.

$$u = \frac{p}{\sqrt{2\pi m k_B T}} \int_S \sigma_s f(\theta_s) e^{-E_s/RT} ds \quad (4)$$

However, in general the relationship between  $T_s$ ,  $\theta_s$  and  $E_s$  is not known and therefore Eq. (4) cannot be integrated. Therefore, it will now be shown that different sets of assumptions applied to Eq. (3) will lead to different adsorption rates.

First, the term  $f(\theta)$  is considered. For the ortho-parahydrogen reaction, it is probable that there is adsorption of one molecule on a single site. There is a chance that dissociation could occur but it is not likely in the present case, as was shown in Sections II and III. For single molecule adsorption it is assumed that adsorption takes place only on unoccupied sites. Under these conditions

$$f(\theta) = 1 - \theta \quad (5)$$

Substitution of Eq. (5) into Eq. (3) yields

$$u = \frac{\sigma(\theta) p}{\sqrt{2\pi} m k_B T} (1-\theta) e^{-E(\theta)/RT} \quad (6)$$

Now, for a uniform surface,  $\sigma$  and  $E$  are constants. Eq. (6) then becomes

$$\begin{aligned} u &= \frac{\sigma e^{-E/RT}}{\sqrt{2\pi} m k_B T} p (1-\theta) \\ &= k_a p (1-\theta) \end{aligned} \quad (7)$$

where

$$k_a = \text{adsorption rate constant, molecules cm}^{-2} \text{ sec}^{-1} \text{ atm}^{-1}.$$

For a non-uniform surface there are several sets of assumptions that may be used. One of the more successful is the assumption that  $E$  varies linearly with surface coverage and that  $\sigma$  remains approximately constant. Under these conditions Eq. (6) becomes (if  $E = E_0 + \alpha \theta$ )

$$\begin{aligned} u &= \frac{\sigma p}{\sqrt{2\pi} m k_B T} (1-\theta) e^{-(E_0 + \alpha \theta)/RT} \\ &= k_a' p (1-\theta) e^{-\alpha \theta/RT} \end{aligned} \quad (8)$$

If  $\theta$  is not close to unity, the variation in  $(1-\theta)$  is small in comparison to the variation in  $\exp(-\alpha \theta/RT)$ . Thus, Eq. (8) becomes

$$u = k_a'' p e^{-\alpha \theta/RT} \quad (9)$$

which is a form of the Elovich equation [3,15,17].

Eqs. (7) and (9) will be used later in developing adsorption isotherms and reaction rate equations.

## 2. Desorption

Under conditions which are similar to those that are described above for adsorption, the rate of desorption may be written as [8]

$$u' = K_d(\theta) f'(\theta) e^{-E'(\theta)/RT} \quad (10)$$

It should be noted here that the activation energy of desorption  $E'$  is related to the activation energy of adsorption  $E$  and the heat of adsorption  $q_a$  by the relation

$$E' = E + q_a \quad (11)$$

Since adsorption is always an exothermic process, it follows that  $E'$  will always be positive, even for non-activated adsorption ( $E = 0$ ).

As above, for a molecule desorbing from a single site, the rate of desorption is proportional to the amount adsorbed and thus

$$f'(\theta) = \theta \quad (12)$$

Eq. (12) thus becomes

$$u' = K_d(\theta) \theta e^{-E'(\theta)/RT} \quad (13)$$

For a uniform surface,  $K_d$  and  $E'$  are constant and Eq. (13) becomes

$$u' = k_d \theta \quad (14)$$

For a non-uniform surface of the type described in the previous section  $E' = E'_0 - \beta \theta$  and  $K_d(\theta)$  is approximately constant. Thus Eq. (13) becomes

$$u' = k'_d \theta e^{\beta \theta / RT} \quad (15)$$

Now, if  $\theta$  is not close to zero, the variation of  $u'$  with  $\theta$  is small compared to the variation with  $\exp(\beta \theta / RT)$ . Thus, Eq. (15) reduces to

$$u' = k''_d e^{\beta \theta / RT} \quad (16)$$

Eqs. (14) and (16) are the important results of this section.

### 3. Adsorption Isotherms

Individual rates of adsorption and desorption are very frequently immeasurable. Consequently, the equations developed in the previous two sections are of limited value in themselves. However, although the rates of adsorption cannot be measured, the total amounts adsorbed can be measured. The total amounts adsorbed are taken to be the amounts adsorbed when the system is in adsorption-desorption equilibrium.

At equilibrium the rates of adsorption and desorption are equal. Thus  $u = u'$ . If now the appropriate equations are combined, some interesting and extremely useful results are obtained [9].

Eqs. (7) and (14) were both derived from the same set of assumptions. Thus they can be combined to yield the adsorption isotherm for a uniform surface. If this

combination is made, the results are as follows:

$$k_a p (1-\theta) = k_d \theta \quad (17)$$

which may be rearranged to give

$$\theta = \frac{K_a p}{1 + K_a p} \quad (18)$$

where

$$K_a = k_a/k_d = \text{adsorption equilibrium constant, atm}^{-1}.$$

Eq. (18) is the well-known Langmuir adsorption isotherm [12].

Eqs. (9) and (16) were derived from the same set of assumptions and therefore may be treated in a manner similar to that in the preceding paragraph. The main steps are shown in Eqs. (19) and (20):

$$k_a'' p e^{-\alpha \theta/RT} = k_d'' e^{\beta \theta/RT} \quad (19)$$

which may be rearranged to give

$$\theta = K'_a \ln A_o p \quad (20)$$

where

$$K'_a = RT/(\beta + \alpha).$$

$$A_o = k_a''/k_d''.$$

Eq. (20) is known as the Temkin isotherm [5]. In passing it should be noted that Eq. (9) was derived with the assumption that  $\theta$  was not very close to unity in value, while Eq. (16) was derived under the assumption that  $\theta$  was not close to zero. These two assumptions, when used

simultaneously, lead to the fact that the Temkin isotherm, Eq. (20), is strictly valid only under conditions which Trapnell calls "the middle range of coverage." This may be a serious physical limitation on the Temkin isotherm in some cases, but if the assumption of middle range of coverage is not made, the equations are extremely difficult to work with, as far as the treatment of experimental data is concerned. Also, many adsorption data have been found to be well-correlated by the Temkin isotherm.

A third isotherm may be developed by starting with a different assumption from that which led to the Langmuir and Temkin isotherms. It is recalled that the Langmuir isotherm was developed under the assumption of a uniform surface while the Temkin isotherm arose from the assumption of a linear variation of activation energy with surface coverage. Since the activation energies of adsorption and desorption are related to the heat of adsorption as shown by Eq. (11), it follows that the heat of adsorption will vary with surface coverage in the same manner as the activation energy. In fact, starting with heat of adsorption as his criterion instead of activation energy, Trapnell derives the Temkin isotherm by assuming a linear variation of heat of adsorption with surface coverage [9].

If now, the assumption of a logarithmic variation in heat of adsorption with surface coverage is made, a different adsorption isotherm will arise. The surface is divided into a series of areas, each of which obeys the Langmuir isotherm. If these areas are designated by the subscript  $i$ , the amount adsorbed on each area is

$$\theta_i = \frac{K_i p_i}{1 + K_i p_i} \quad (21)$$

The total amount adsorbed is then

$$\theta = \sum n_i \theta_i \quad (22)$$

where

$$n_i = \text{number of areas of type } i.$$

If now the  $K_i$  values are close enough together to form a continuous distribution, Eq. (22) may be replaced by an integral

$$\theta = \int n_i \theta_i di \quad (23)$$

The assumption is now made that the variation in surface is strictly due to  $q$ , the heat of adsorption. If this is true, Eq. (23) may be expressed as

$$\theta = \int n_q \theta_q dq \quad (24)$$

or

$$\theta = \int_0^{\infty} n_q \frac{K_q p}{1 + K_q p} dq \quad (25)$$

Now,  $K_q$  is exponentially determined by  $q$ , as shown by thermodynamics (cf., Denbigh [2]).

$$K_q = K_o e^{-q/RT} \quad (26)$$

If, now,  $n_q$  is of the form

$$n_q = n_o e^{q/q_m} \quad (27)$$

where

$$n_o = \text{constant.}$$

$$q_m = \text{constant.}$$

Substitution of Eqs. (26) and (27) into Eq. (25) and slight rearrangement yields the result

$$\theta = \int_0^{\infty} \frac{n_o e^{-q/q_m}}{1 + \frac{e^{-q/RT}}{K_o p}} dq \quad (28)$$

If the heat of adsorption  $q$  considerably exceeds the thermal energy  $RT$ , Eq. (28) can be integrated to the following result:

$$\theta = n_o q_m (K_o p)^{RT/q_m} \quad (29)$$

Eq. (29) is the Freundlich isotherm [4], which is commonly presented in the form

$$\theta = ap^{1/n} \quad (30)$$

Adsorption data are usually collected in the form of pressure vs volume adsorbed curves. In order to determine which of the three adsorption isotherms best describes the data, Eqs. (18), (20), and (30) are rearranged into forms which allow the data to give a straight line for the correct adsorption mechanism. Here, the relationship between  $\theta$  and  $v$  is given by  $\theta = v/v_m$ , where  $v_m$  is a constant.

Eq. (18), the Langmuir isotherm, may be rearranged to the form given by Eq. (31). Eq. (31) shows that if Langmuir adsorption is the type encountered, a plot of

$$\frac{p}{v} = \frac{1}{Kv_m} + \frac{p}{v_m} \quad (31)$$

$p/v$  vs  $p$  will yield a straight line of slope  $1/v_m$  and intercept  $1/Kv_m$ . Eq. (20) shows that a plot of  $v$  vs  $\ln p$  should yield a straight line if Temkin adsorption describes the data. Finally, Eq. (20) shows that if the Freundlich isotherm holds, a log-log plot of  $p$  vs  $v$  will yield a straight line. Thus, adsorption data can be checked against the three adsorption isotherms in order to determine which give the best correlation. Clark, et.al., [1] have published adsorption data for hydrogen on two different catalysts at temperatures from 64 to 190°K. One of these catalysts is reported to have been a hydrous ferric oxide catalyst similar to the type that was used in the present study. Thus, it was felt that if the adsorption data could be explained by one of the previous adsorption isotherms, this would strengthen the kinetic approach. With this in mind, Figures 21, 22, and 23 were prepared. Figure 21 shows the data plotted in Langmuir fashion at a temperature of 63.14°K. This temperature was chosen mainly because a wider pressure range was covered at this temperature than at 77°K, which is closer to the operating temperature of the present work. Figure 22 shows the data as plotted for a Temkin isotherm and Figure 23 shows the data as plotted for a Freundlich isotherm. It is obvious that the data are better correlated by a Freundlich isotherm than by either of the other two. Consequently, the data for 77°K were plotted on Freundlich coordinates in order to obtain an  $n$  for the adsorption. These data are also shown in Figure 23. The value of  $n$  which was obtained from this plot was 2.54.

One question which might arise in using total hydrogen adsorption isotherms is whether or not they remain

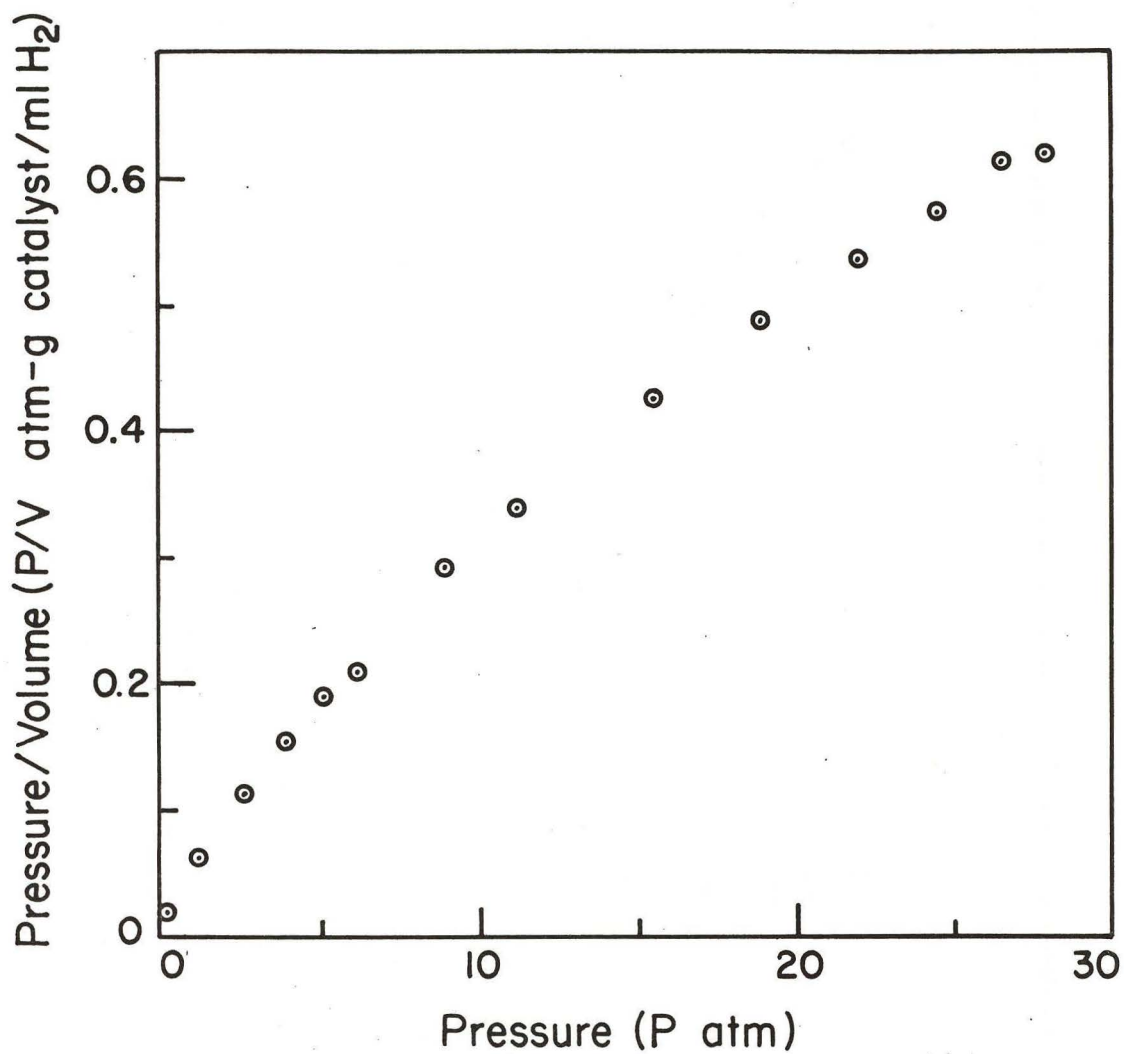


FIGURE 21. Langmuir Adsorption Plot for Data of Clark, et.al. [1].

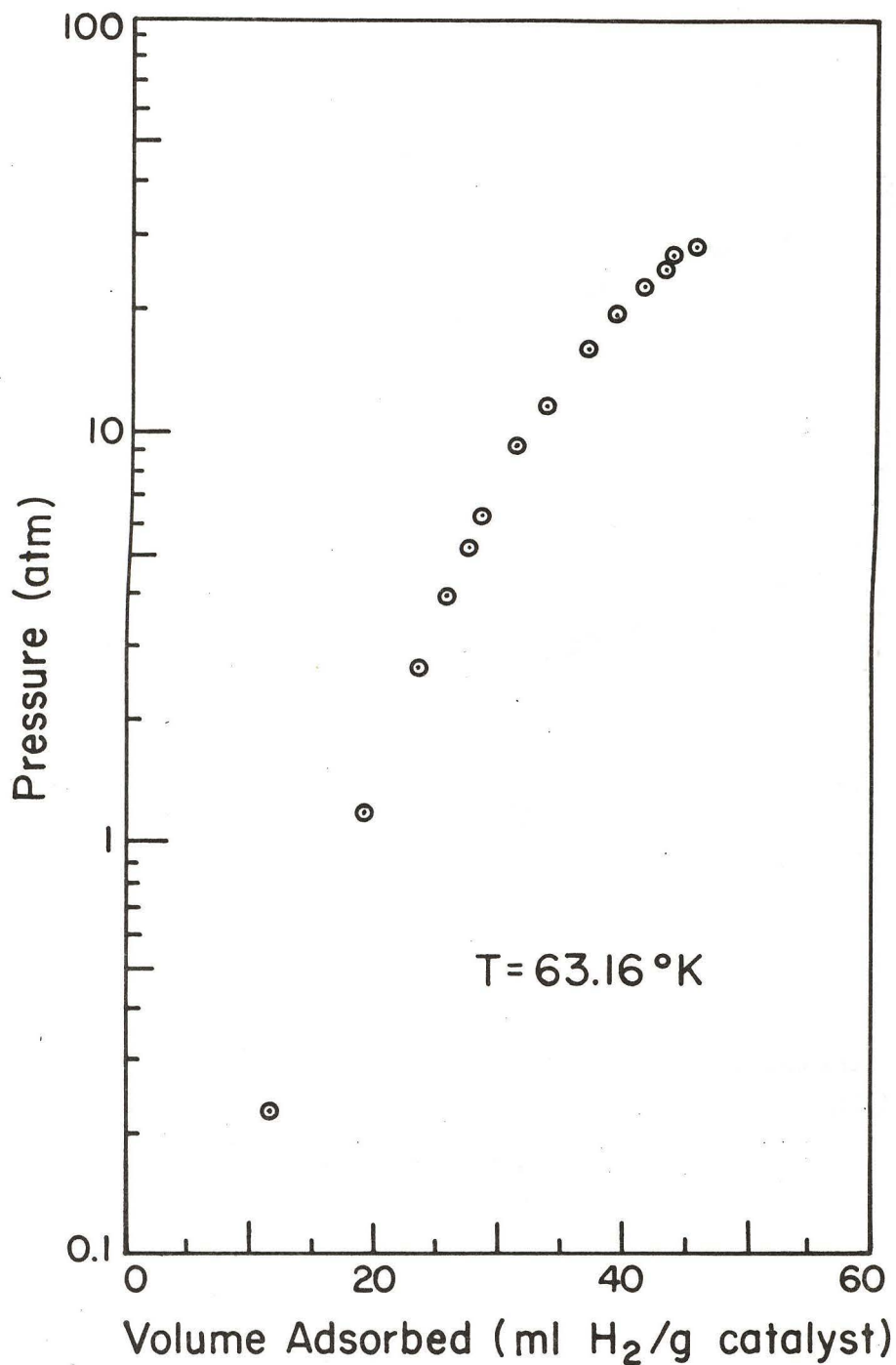


FIGURE 22. Temkin Adsorption Plot for Data of Clark, et.al. [1].

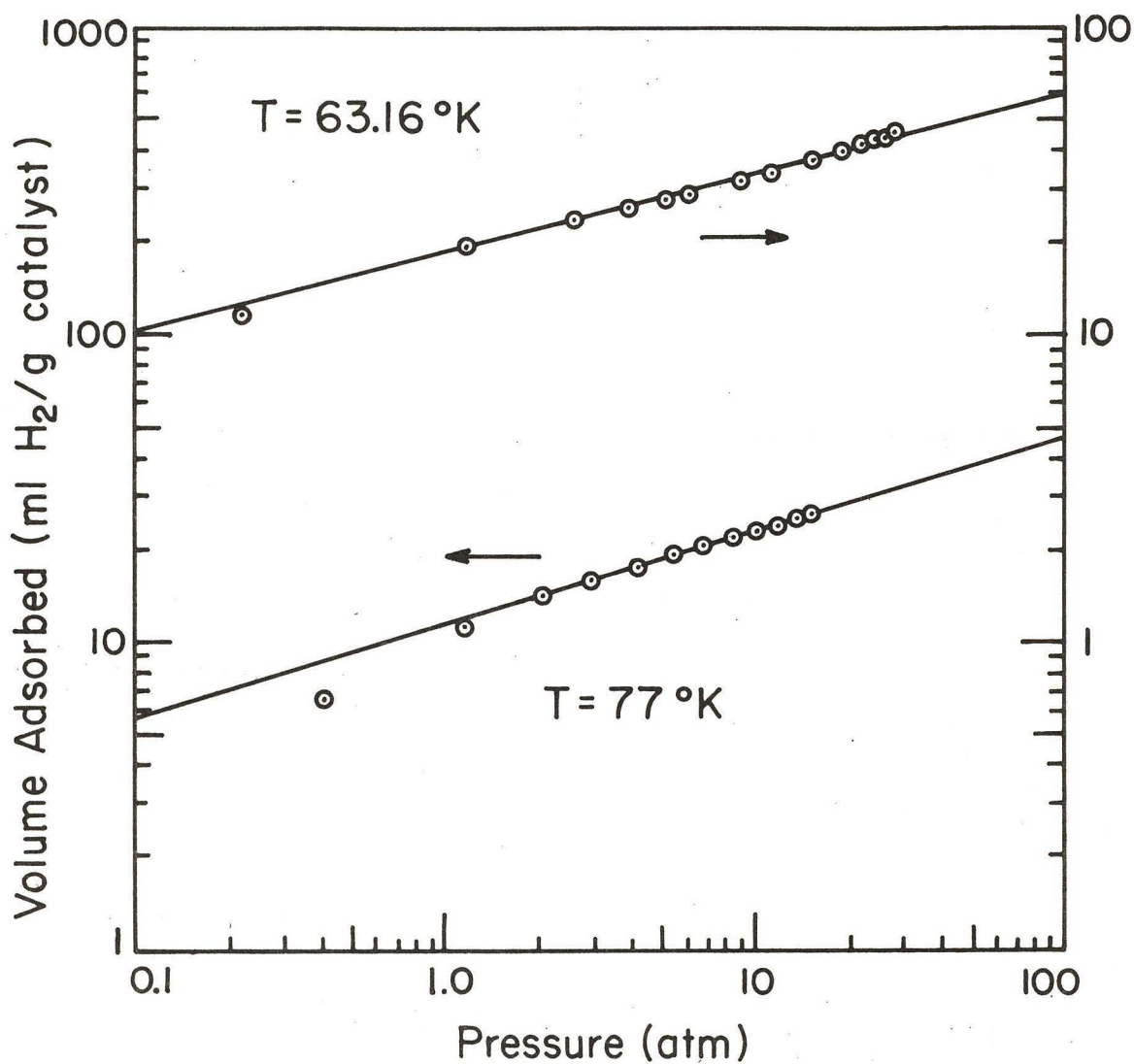


FIGURE 23. Freundlich Adsorption Plots for Data of Clark, et.al. [1].

valid for the separate ortho and para species. That this is so may be demonstrated by the following development.

A. Langmuir Adsorption. The case is when both ortho- and parahydrogen obey the Langmuir isotherm. Two basic relations which will be used in all three cases are

$$v_H = v_o + v_p \quad (32)$$

$$c_H = c_o + c_p \quad (33)$$

where

$v_H$  = volume of hydrogen adsorbed,  $\text{cm}^3$ .

$v_o, v_p$  = volumes of ortho- and parahydrogen, respectively, adsorbed,  $\text{cm}^3$ .

$c_o, c_p$  = gas phase concentration of ortho- and parahydrogen, respectively, g-moles  $\text{cm}^{-3}$ .

The separate isotherms are given by Eqs. (34) and (35).

$$v_p = \frac{K_p c_p}{1 + K_p c_p + K_o c_o} \quad (34)$$

$$v_o = \frac{K_o c_o}{1 + K_o c_o + K_p c_p} \quad (35)$$

where

$K_o, K_p$  = adsorption equilibrium constants for ortho- and parahydrogen, respectively.

Addition of Eqs. (34) and (35) and substitution of Eqs. (32) and (33) yields

$$\begin{aligned} v_H &= \frac{K_o [1 + (s-1)x] c_H}{1 + K_o [1 + (s-1)x] c_H} \\ &= \frac{K'(x, s) c_H}{1 + K'(x, s) c_H} \end{aligned} \quad (36)$$

where

$$s = K_o/K_p = \text{separation factor.}$$

$$x = \text{mole fraction parahydrogen.}$$

Eq. (36) is a Langmuir isotherm since  $K'$  is not a function of total hydrogen pressure.

B. Freundlich Adsorption. The separate isotherms are given by

$$v_p = a_p c_p^{1/n} \quad (37)$$

$$v_o = a_o c_o^{1/n} \quad (38)$$

where

$$a_o, a_p, n = \text{constants.}$$

Addition of Eqs. (37) and (38) and substitution of Eqs. (32) and (33) yields

$$\begin{aligned} v_H &= a_p [x^{1/n} + \frac{a_o}{a_p} (1-x)^{1/n}] c_H^{1/n} \\ &= a_H (x) c_H^{1/n} \end{aligned} \quad (39)$$

Eq. (39) is a Freundlich isotherm for  $c_H$  since  $a_H$  is not a function of  $c_H$ . However, if the exponent  $n$  is not the same for both ortho- and parahydrogen, then a Freundlich isotherm may or may not be observed, as shown below.

$$v_p = a_p c_p^{1/n} \quad (37a)$$

$$v_o = a_o c_o^{1/n} \quad (38a)$$

Combination of Eqs. (37a) and (38a) yields

(39a)

$$v_H = a_p [x^{1/n_p} + \frac{a_o}{a_p} c_H^{\frac{(n_p - n_o)}{n_o n_p}} (1-x)^{1/n_o}] c_H^{1/n_p}$$

Eq. (39a) shows that a Freundlich isotherm may or may not be obtained, depending upon the relative values of the two terms which are contained in the brackets.

C. Temkin Adsorption. The separate isotherms are given by Eqs. (40) and (41).

$$v_o = K'_o \ln A_o c_o \quad (40)$$

$$v_p = K'_p \ln A_p c_p \quad (41)$$

Addition of Eqs. (40) and (41) and substitution of Eqs. (32) and (33) yields

$$v_H = K'_p [\ln A_o A_p + \ln x(1-x)] + 2K'_o \ln c_H \quad (42)$$

#### 4. Adsorption of Mixtures

As the preceding development showed, complications arise in the treatment of adsorption when more than one specie is present. Perhaps the case of ortho- and parahydrogen furnishes a better example of the problems that arise than most other systems because, unless one uses the adsorption of parahydrogen at 20°K as his system, it is impossible (under equilibrium conditions) to discuss adsorption of orthohydrogen without also discussing parahydrogen adsorption. Of course, if one is considering only

high temperature ( $> 300^\circ\text{K}$ ) adsorption of hydrogen, he can effectively discuss hydrogen adsorption since the ratio of ortho- to parahydrogen remains fixed. However, in the case of the present experiments, the ratio of ortho- to parahydrogen changes drastically and therefore, since the presence of one will affect the adsorption characteristics of the other, these effects must somehow be accounted for.

Unfortunately, a great amount of work has not been done in the area of adsorption of mixtures [13]. Data concerning multicomponent adsorption are not readily available and of these, few rigorous theoretical treatments have been devised to account for gas interactions, other than the modification of the Langmuir isotherm to the form

$$\theta_A = \frac{K_A p_A}{1 + K_A p_A + \sum_i K_i p_i} \quad (43)$$

where

$i$  = species other than A which are present and adsorbed.

This modification of the Langmuir isotherm seems to have worked fairly well [11] as far as adsorption isotherms are concerned, but no predictions concerning the effects of a second gas on the rate of adsorption have been advanced. Thus, what the forms of Eqs. (3) and (10) would be in the presence of a second component is not settled at this time. Hence, the forms of the relations that are developed from Eqs. (3) and (10) can only suggest certain ways in which the interactions might possibly be taken into account.

A general equation for the rate of adsorption of component A in the presence of B might be written in the

form,

$$u_A = \frac{\sigma p_A}{\sqrt{2\pi m_A k_B T}} (1 - \theta_A - \theta_B) e^{-(E_{oA} + \alpha_A \theta_A + \alpha_B \theta_B)/RT} \quad (44)$$

and a similar relation for the rate of desorption of A

$$u'_A = K_{dA} \theta_A e^{-(E'_{oA} - \beta_A \theta_A - \beta_B \theta_B)/RT} \quad (45)$$

It is apparent that if  $\alpha_A, \alpha_B, \beta_A,$  and  $\beta_B$  are all zero, Eqs. (44) and (45) will lead to the modified Langmuir isotherm (Eq. 43). However, if the  $\alpha$ 's and  $\beta$ 's are not equal to zero, then other assumptions must be made concerning them and, at the present time, there are few guidelines to indicate just what assumptions may be valid. There is the further complication in forming a rate model that the  $\alpha$ 's and  $\beta$ 's for the adsorption and desorption of A may be different from the  $\alpha$ 's and  $\beta$ 's in the adsorption and desorption of B. More research into this area is definitely needed at this time in order to clarify what forms Eqs. (44) and (45) may take.

It is apparent from Eqs. (44) and (45) that some perhaps questionable assumptions would have to be made in order to bring them to the forms which lead to the Elovich equation for rate of adsorption and the Temkin adsorption isotherm for equilibrium adsorption. This presents a paradox to the researcher, for it was found by the present investigator (See Section VI.B.) that the rate expression which was derived from the Elovich equation assuming surface reaction to be controlling, gave a fairly good representation of the data for the ortho-parahydrogen conversion at high pressures. As Low [13] remarks, the derivation of

the Elovich equation is not unique, and it has consequently been widely attacked in this ground [cf., 6,10,14]. However it does explain adsorption rate data in a large number of cases [13]. On the other hand, as was shown in Section VI.C., the rate expression which was derived from the more exact forms (Eqs.44 and 45) did not particularly correlate the present data as well as did the Langmuir and Elovich expressions. It therefore becomes apparent that much more knowledge of the adsorption process is needed before one can proceed with the development of a true reaction model.

The above development, besides pointing out the difficulty of developing a good representative reaction model, may also serve to show why the adsorption isotherms of Clark, et.al., [1] were not particularly well correlated by any of the three commonly used isotherms.

## References for Appendix A

1. Clark, R.G., J. F. Kucirka, A. Jambhekar, G. E. Schmauch, "Investigation of the Para-Ortho Shift of Hydrogen," Air Products and Chemicals, Inc., Summary Technical Report ASD-TDR 62-833, Part II, October, 1963.
2. Denbigh, K.G., "Chemical Equilibrium," Cambridge, 158 (1961).
3. Elovich, S. Yu., G. M. Zhabrova, Zh. fiz. Khim., 13, 1761 (1939).
4. Freundlich, H., "Colloid and Capillary Chemistry," Methuen, London (1926).
5. Frumkin, A., A. Slygin, Acta. Physicochim. USSR, 3, 791 (1935).
6. Gray, T. J., in Garner, W.E., ed., "Chemistry of the Solid State," Butterworths, London, 190 (1955).
7. Hayward, D.O., B.M.W. Trapnell, "Chemisorption," 2nd ed., Butterworths, Washington, Ch. 3 (1964).
8. Ibid., Ch. 4.
9. Ibid., Ch. 5.
10. Laidler, K. J., in Emmett, P. H., ed., "Catalysis," I, Reinhold Publishing Corp., New York, 151 (1954).
11. Ibid., p. 189.
12. Langmuir, I., J. Am. Chem. Soc., 66, 1361 (1918).
13. Low, M. J.D., Chem. Rev., 60, 267 (1960).
14. Parravano, G., M. Boudart, in "Advances in Catalysis," VIII, Academic Press, New York, 50 (1955).
15. Roginsky, S., Ya. Zeldovich, Acta Physicochim., 1, 554 (1934).
16. Ibid., p. 595.

17. Tamman, G., W. Koster, Z. anorg. Chem., 123, 196 (1922).
18. Young, D. M., A. D. Crowell, "Physical Adsorption of Gases," Butterworths, Washington, Ch. 4 (1962).

APPENDIX B  
The Separation Factor

The separation factor was first defined by Sandler [11] as

$$s \equiv \frac{(N_p/N_o)_g}{(N_p/N_o)_{ad}} \quad (1)$$

where

$s$  = separation factor.

$N_o, N_p$  = number of molecules of ortho- and parahydrogen respectively.

$g$  = gas phase.

$ad$  = adsorbed phase.

The separation factor can be predicted a priori from a statistical mechanical knowledge of the partition functions of the gaseous and adsorbed molecules. A partition function is defined as

$$q = \sum_i e^{-\epsilon_i/RT} \quad (2)$$

where

$q$  = partition function

$\epsilon_i$  = energy of  $i^{\text{th}}$  molecular condition. May be associated with electron, translational, rotational, etc. energy levels.

$R$  = gas constant.

$T$  = temperature.

In general, if interaction between molecules is assumed, the resulting partition functions are not easy to handle. However, if the simplifying assumption of no molecular interactions, either in the gas or on the surface, is made, the forms of  $q$  are easy to deal with and certain qualitative

properties can be deduced.

It has been shown several places [cf., 3,4,8] that the chemical equilibrium constant for a reaction may be calculated from the partition functions of the participating species. For example, for the reaction



where

A,B,R,S = chemical species.

a,b,r,s = stoichiometric coefficients.

the equilibrium constant is given by

$$\frac{(R)^r (S)^s}{(A)^a (B)^b} = K_{eq}(T) = \frac{(q_R/V)^r (q_S/V)^s}{(q_A/V)^a (q_B/V)^b} \quad (4)$$

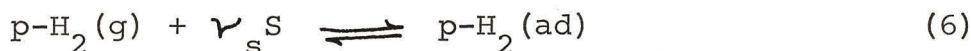
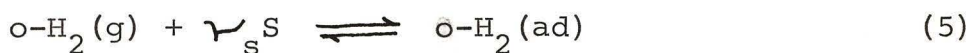
where

$K_{eq}(T)$  = equilibrium constant, a function of temperature.

$V$  = volume of system.

(A), (B), (R), (S) = concentrations of species, A,B,R,S, respectively.

If the adsorption of ortho- and parahydrogen are written in the form of chemical reactions, as shown by Eqs. (5) and (6)



where

S = surface site

$\gamma_s$  = amount of surface site that is occupied by a molecule.

Then the adsorption equilibrium constants are given by

$$\frac{(N_o)_{ad}}{(N_o/V)_g (N_s)_{\gamma_s}} = \frac{(q_o)_{ad}}{(q_o/V)_g (q_s)_{\gamma_s}} = K_o(T) \quad (7)$$

$$\frac{(N_p)_{ad}}{(N_p/V)_g (N_s)_{\gamma_s}} = \frac{(q_p)_{ad}}{(q_p/V)_g (q_s)_{\gamma_s}} = K_p(T) \quad (8)$$

If Eq. (7) is divided by Eq. (8), the result is

$$\frac{K_o(T)}{K_p(T)} = \frac{\frac{(q_o)_{ad}}{(q_p)_{ad}}}{\frac{(q_o/V)_g}{(q_p/V)_g}} = \frac{\frac{(N_o)_{ad}}{(N_p)_{ad}}}{\frac{(N_o/V)_g}{(N_p/V)_g}} = s \quad (9)$$

Thus,  $s$  can be calculated entirely from a knowledge of the partition functions of adsorbed and gaseous ortho- and parahydrogen. It is independent of any particular mechanism of adsorption (assuming both ortho- and parahydrogen occupy the same part of a site-- $\gamma_s$  is the same for both species).

The problems begin arising when one desires to calculate  $s$ . The partition functions are in general known only for the cases of no molecular interactions in the gas or on the surface. This restricts the validity of the following development somewhat.

If no interactions are assumed, then the partition functions can be separated into rotational, translation, electronic, nuclear, and whatever other kinds of partition functions are required [cf., 5,10]. If the assumption is

made that all the energy levels except the nuclear rotational ones are the same for both species, then one need be concerned only with the nuclear rotational partition functions in the gaseous and adsorbed phases. These functions are given by Eqs. (10), (11), (12), and (13)

$$(q_o)_g = 3 \sum_{j=1,3,\dots} (2j+1) e^{-j(j+1)\theta_r/T} \quad (10)$$

$$(q_p)_g = \sum_{j=2,4,\dots} (2j+1) e^{-j(j+1)\theta_r/T} \quad (11)$$

$$(q_o)_{ad} = 6 \sum_{j=1,3,\dots} e^{-j^2\theta_r/2T} \quad (12)$$

$$(q_p)_{ad} = 1 + 2 \sum_{j=2,4,\dots} e^{-j^2\theta_r/2T} \quad (13)$$

where

$j$  = quantum number.

$\theta_r$  = characteristic rotational temperature  
= 85.4°K [6].

The separation factor can now be calculated. Eqs. (10) through (13) are substituted into Eq. (9) and the results are given by Eq. (14).

$$s = \frac{2(e^{-42.7/T} + e^{-384/T})(1 + 5e^{-513/T})}{9e^{-170.8/T}(1 + 2e^{-170.8/T})} \quad (14)$$

In a previous work, Barrick, et.al., [1], calculated separation factors from the data for Hutchinson [8] on the reverse reaction. These calculations were performed with

with the assumption that the reaction followed Langmuir kinetics with surface reaction controlling. Although this assumption has been shown in the present work to be incorrect, fairly good results (as far as separation factor is concerned) were obtained by these investigators. Table VII compares the results that were obtained experimentally with two theoretically predicted values--those predicted by Eq. (14) and those predicted by Sandler [11]. The difference between Eq. (14) and Sandler's prediction is that Sandler considered only the first terms in Eqs. (1) through (13), whereas the second terms are included in Eq. (14). Sandler's formula for the separation factor is given by Eq. (15).

$$s = 2/3 e^{\epsilon_r/T} \quad (15)$$

As far as other assumptions are concerned, if interactions occur, the partition functions may not be able to be separated into translational, etc., parts and so Eq. (14) is no longer valid. However, it is qualitatively valid. It does show that orthohydrogen is more strongly adsorbed than parahydrogen. This has been verified by Cunningham, Chapin, and Johnston [2], who effected a separation of ortho- from parahydrogen at 20°K by means of repeated adsorption and desorption of hydrogen from alumina. van Itterbeek, Hellemans, and van Dael [12] also reported a preferential adsorption of orthohydrogen on glass at 21°K. These experiments demonstrated that the separation factor does indeed exist and that orthohydrogen in almost pure form [2] can be obtained by using this fact.

Table VII. Separation Factors

<u>Temperature</u>	<u>s (Eq. 14)</u>	<u>s (Eq. 15)</u>	<u>s* (expt'l)</u>
40°K	5.32	5.55	9.61
50	2.97	3.68	7.03
60	1.69	2.75	5.99
70	1.23	2.21	5.27
80	1.082	1.93	5.00

\* From data of Hutchinson [8].

An interesting sidelight may be developed at this point. According to Eq. (14),  $s$  is independent of pressure.  $s$  may be expressed as

$$s = \frac{(N_p/N_o)_{ad}}{(N_p/N_o)_{ad}} = \frac{\frac{c_p}{c_o}}{\frac{\theta_p}{\theta_o}} = \frac{c_p \theta_o}{c_o \theta_p} \quad (16)$$

If Freundlich adsorption is assumed,  $\theta_o$  and  $\theta_p$  are given by

$$\theta_o = a_o c_o^{1/n_o} \quad (17a)$$

$$\theta_p = a_p c_p^{1/n_p} \quad (17b)$$

where

$$a_o, a_p, n_o, n_p = \text{constants.}$$

Therefore

$$s = \frac{\frac{c_p c_o^{1/n_o}}{c_o c_p^{1/n_p}} \frac{a_o}{a_p}}{c_o c_p^{1/n_p}} \quad (18)$$

or

$$s = \frac{a_o}{a_p} \frac{\frac{n_p - 1}{n_p} \frac{n_p - n_o}{n_o n_p}}{\frac{n_o - 1}{n_o} (1 - x)^{n_o}} c_H \quad (18)$$

If  $n_p \neq n_o$ ,  $s$  will be dependent upon total pressure and also upon composition. (If Langmuir kinetics were followed the separation factor would be independent of pressure and composition, as the following development shows.)

$$s = \frac{c_p \theta_o}{c_o \theta_p} \quad (16)$$

$$\theta_o = \frac{K_o c_o}{1 + K_o c_o + K_p c_p} \quad (19)$$

$$\theta_p = \frac{K_p c_p}{1 + K_o c_o + K_p c_p} \quad (20)$$

Therefore

$$s = \frac{c_p}{c_o} \frac{\frac{K_o c_o}{1 + K_o c_o + K_p c_p}}{\frac{K_p c_p}{1 + K_o c_o + K_p c_p}}$$

$$= \frac{K_o}{K_p} \quad (21)$$

Here,  $K_o$  and  $K_p$  are independent of pressure and composition. This is because the development of the Langmuir adsorption isotherm assumes them so. Hence,  $s$  is a function only of temperature for Langmuir adsorption. The same assumptions that led to Eq. (14) can be used to derive the Langmuir isotherm from statistical mechanics [cf., 7]. Hence, Eq. (14) and the Langmuir approach are consistent with each other.

For Temkin kinetics, the separation factor is given by

$$s = \frac{c_p}{c_o} \frac{k_o \ln A_o c_o}{k_p \ln A_p c_p}$$

$$= \frac{k_o}{k_p} \frac{x}{1-x} \frac{\ln[A_o c_H (1-x)]}{\ln[A_p c_H x]} \quad (22)$$

Again,  $s$  is seen to be dependent upon composition and pressure (through the logarithmic terms). However, the assumptions which led to the Temkin isotherm (Appendix A) are different from those which led to the Langmuir isotherm and, consequently, the assumptions which led to Eq. (14) will no longer be valid for Temkin adsorption.

## References for Appendix B

1. Barrick, P. L., L. F. Brown, H. L. Hutchinson, "Kinetics and Diffusion Study of the Para-Ortho Shift of Hydrogen," Technical Documentary Report APL-TDR-64-77, September, 1964.
2. Cunningham, C. M., D.S. Chapin, H. L. Johnston, J. Am. Chem. Soc., 80, 2382 (1958).
3. Denbigh, K. G., "Principles of Chemical Equilibrium," Cambridge U. Press, Cambridge, 379 (1961).
4. Hill, T. L., "An Introduction to Statistical Thermodynamics," Addison-Wesley, Reading, Mass., (1960).
5. Ibid., p.147.
6. Ibid., p.470.
7. Ibid., p. 128.
8. Hutchinson, H.L., M.S. Thesis, University of Colorado, (1964).
9. Mayer, J.E., M.G. Mayer, "Statistical Mechanics," John Wiley and Sons, New York, 200 (1940).
10. Ibid., p. 68.
11. Sandler, Y.L., J. Phys. Chem., 58, 58 (1954).
12. van Itterbeek, A., R. Hellermans, W. van Dael, Physica, 30, 324 (1964).

## APPENDIX C

### Diffusion

It has been shown that a catalytic reaction takes place via a series of individual steps. These have been listed previously as:

1. Diffusion of reactants from the bulk phase to the pore mouths.
2. Diffusion of reactants through the pores into the interior of the catalyst pellet.
3. Adsorption of reactants onto the surface.
4. Reaction on the surface to form products.
5. Desorption of products from the surface.
6. Diffusion of products through the pores to the pore mouths.
7. Diffusion of products from the pore mouths to the bulk phase.

The assumptions were made in Sections III, V and VI that only steps 3, 4, and 5 were important under the present conditions. This assumption was based upon the findings of previous investigators [7,11] who had shown that diffusion effects were relatively unimportant. A look at the methods which were used to attack the diffusion problems is instructive and enables the verification that diffusion effects are indeed negligible for the present series of experiments.

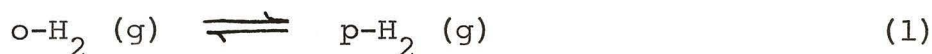
#### 1. Bulk Diffusion

Steps (1) and (7) deal solely with ordinary interparticle mass transfer and can thus be grouped together for study. Similarly, steps (2) and (6) deal with intraparticle mass transfer and will be grouped together for study

in Part 2 of this appendix.

Wakao, et.al. [11] have made use of an effective method for studying the effects of diffusion on the ortho-parahydrogen reaction (although there is no reason why the method could not be extended to other catalytic systems, provided that the reaction can be represented reasonably well by a simple first-order rate expression).

Briefly, the method is outlined as follows: The overall reaction, (Eq. (1)), is represented as being governed by a first-order reaction rate expression, Eq. (2).



$$r = k_{\text{ov}} (c_{\text{o}} - c_{\text{oe}}) \quad (2)$$

where

$$\begin{aligned} r &= \text{reaction rate, g-moles cm}^{-3} \text{ min}^{-1}. \\ k_{\text{ov}} &= \text{overall reaction rate constant, min}^{-1}. \\ c_{\text{o}} &= \text{ortho-hydrogen concentration, g-moles cm}^{-3}. \\ c_{\text{oe}} &= \text{equilibrium ortho-hydrogen concentration,} \\ &\quad \text{g-moles cm}^{-3}. \end{aligned}$$

The reaction is then separated into two steps: the external mass transfer step, and the reaction step, whose rates are represented by Eqs. (3) and (4), respectively.

$$r_{\text{diff}} = k_{\text{G}} (c_{\text{og}} - c_{\text{os}}) \quad (3)$$

$$r_{\text{react}} = k_{\text{r}} (c_{\text{os}} - c_{\text{oe}}) \quad (4)$$

where

$$\begin{aligned} k_{\text{G}} &= \text{mass transfer coefficient, min}^{-1}. \\ c_{\text{og}} &= \text{gas phase concentration ortho-hydrogen,} \\ &\quad \text{g-moles cm}^{-3}. \end{aligned}$$

$c_{os}$  = equivalent surface concentration orthohydrogen,  
g-moles  $\text{cm}^{-3}$ .

$k_r$  = surface reaction rate constant,  $\text{min}^{-1}$ .

The surface reaction step is here taken to include steps (2) through (6).  $c_{os}$  is not a directly measurable variable and hence, it would be desirable to eliminate it from the rate expressions. This can be done as follows: first, it is noted that  $r_{\text{diff}} = r_{\text{react}}$ .

Then  $r = k_G(c_{og} - c_{os}) = k_r(c_{os} - c_{oe})$

This may be rearranged into the forms

$$c_{og} - c_{os} = r/k_G$$

$$c_{os} - c_{oe} = r/k_r$$

If the latter two equations are added, the results is given by Eq. (5).

$$c_{og} - c_{oe} = r\left(\frac{1}{k_G} + \frac{1}{k_r}\right) \quad (5)$$

This is identical with Eq. (2) with the following equivalence:

$$\frac{1}{k_{ov}} = \frac{1}{k_G} + \frac{1}{k_r} \quad (6)$$

Thus, the relative importance of external mass transfer to the reaction can now be assessed. If the reaction, Eq. (1), is represented by a first-order rate expression, Eq. (2), then a value of  $k_{ov}$  can be obtained from the data. Values of  $k_G$  may be obtained independently by one of several mass transfer correlations available [e.g., 2,3,4,

10,13]. From these two numbers, Eq. (6) allows the calculation of  $k_r$ . Thus  $k_r$  and  $k_G$  can be directly compared in order to determine the relative importance of mass transfer. If  $k_G$  is much larger than  $k_r$ , the mass transfer driving force,  $(c_{og} - c_{os})$  will be very small and mass transfer will not exhibit much resistance to reaction rate compared to the kinetics step. The reverse holds if  $k_r$  is much greater than  $k_G$ .

Hutchinson [6] calculated mass transfer coefficients and pseudo first-order rate constants in his study of the para-to-ortho conversion. He found that, for a given Reynolds number (gas flow rate), mass transfer was most likely to be a rate-influencing factor under conditions of high temperature and low pressure. He calculated a first-order rate constant of  $3.1 \times 10^2 \text{ min}^{-1}$  at  $80^\circ\text{K}$  and 42 psia. The mass transfer coefficient under similar conditions for a Reynolds number corresponding to a point at which diffusion was expected was about  $10^5 \text{ min}^{-1}$ . It is noteworthy that all the above correlations for mass transfer in packed beds [2,3,4,10,13] gave approximately the same value for the mass transfer coefficient [cf. 1]. There are three orders of magnitude difference between these values and hence, it is clear from the previous development, that mass transfer is not a factor in influencing the reaction rate.

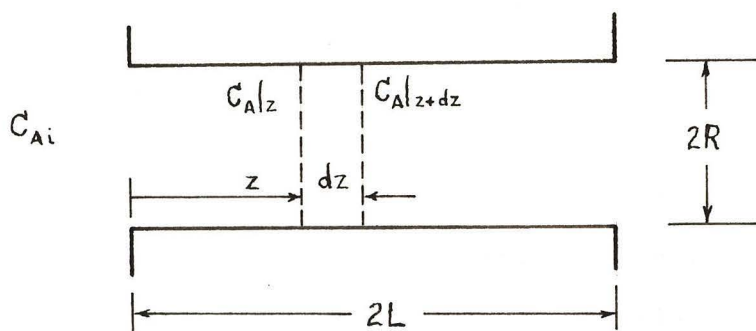
## 2. Pore Diffusion

The next problem is that of diffusion in pores. As was pointed out above, steps (2) and (6), pore diffusion of reactants and products, can be treated in the same fashion. Thiele [9] and Zeldowitsch [14] were the first

to successfully attack the problem of pore diffusion and the following development is due principally to their work, as reported by Wheeler [12].

As in Part 1, for simplicity it will be assumed that the reaction can be represented by a first-order reaction rate law. Other assumptions which will be used are (1) the catalyst particle is a slab of thickness  $2L$  with (2) uniform diameter pores passing through it at right angles to the surface, and (3) the diffusion process in the pores can be represented by a form of Fick's Law of Diffusion. With these assumptions, the following development can now be made.

Consider a pore as shown in the sketch which represents a typical pore of circular cross-section.



If a material balance about the element  $dz$  is written, the terms which arise are the following:

$$\begin{aligned} \text{In by diffusion:} & \quad -\mathcal{D}_{\text{eff}} \pi R^2 \left. \frac{dc_A}{dz} \right|_z \\ \text{Out by diffusion:} & \quad -\mathcal{D}_{\text{eff}} \pi R^2 \left. \frac{dc_A}{dz} \right|_{z + dz} \\ \text{Out by reaction:} & \quad -2 \pi R dz r_A \end{aligned}$$

where

$\mathcal{D}_{\text{eff}}$  = effective diffusivity,  $\text{cm}^2 \text{sec}^{-1}$ .

$R$  = pore radius, cm.

$c_A$  = reactant concentration, g-mole  $\text{cm}^{-3}$ .

$z$  = distance down pore, cm.

$r_A$  = rate of reaction, g-mole  $\text{cm}^{-2} \text{sec}^{-1}$ .

If the above terms are combined into the material balance equation (in - out = accumulation), Eq. (7) is the result.

$$\frac{d^2 c_A}{dz^2} - \frac{2}{R \mathcal{D}_{\text{eff}}} r_A = 0 \quad (7)$$

Up to this point, no assumption has been explicitly made concerning the nature of the surface rate expression. However, unless the rate can be represented by a first-order, or at worst by an  $n^{\text{th}}$  order expression (of the type  $r = k c_A^n$ ), the differential equation (7) is extremely difficult to solve by analytical methods. For demonstration purposes, it will be assumed, therefore, that the reaction, which includes steps 3, 4, and 5, can at least be represented by a first-order rate law. Thus

$$r_A = k_s c_A \quad (8)$$

where

$k_s$  = surface rate constant,  $\text{cm min}^{-1}$ .

Eq. (7) then becomes, upon substitution of Eq. (8) into it

$$\frac{d^2 c_A}{dz^2} - \frac{2k_s}{R \mathcal{D}_{\text{eff}}} c_A = 0 \quad (9)$$

The general solution of Eq. (9) may be written in the form

$$c_A = A \sinh\left(\sqrt{\frac{2k_s}{R\mathcal{D}_{\text{eff}}}} z\right) + B \cosh\left(\sqrt{\frac{2k_s}{R\mathcal{D}_{\text{eff}}}} z\right) \quad (10)$$

The constants A and B may be evaluated from the boundary conditions of the problem. For the present situation the boundary conditions are (1)  $c_A = c_{Ai}$  at  $z = 0$ , and (2)  $dc_A/dz = 0$  at  $z = L$ . The application of these boundary conditions to Eq. (10) yields the result

$$\frac{c_A}{c_{Ai}} = \frac{\cosh\left[h\left(1 - \frac{z}{L}\right)\right]}{\cosh h} \quad (11)$$

where

$$h = L \sqrt{(2k_s/R\mathcal{D}_{\text{eff}})}.$$

The quantity  $h$  is known as the "Thiele modulus." While Eq. (11) does describe the concentration profile along the length of the pore, it itself is not the most useful result of the foregoing development. What is desired is how this concentration profile affects the rate of the reaction.

The actual rate of reaction, per pore, is equal to the amount of reactant that diffuses into the pore, i.e.,

$$\begin{aligned} r_{\text{act}} &= -2\pi R^2 \mathcal{D}_{\text{eff}} \left. \frac{dc_A}{dz} \right|_{z=0} \\ &= -2\pi R^2 \mathcal{D}_{\text{eff}} \frac{hc_{Ai}}{L} \tanh h \end{aligned} \quad (12)$$

The factor 2 is necessary to account for the fact that reactant diffuses into both ends of the pore. If the total pore area were available to the reactant, the rate

of reaction would be

$$r_{\text{poss}} = 2\pi R(2L)k_s c_{\text{Ai}} \quad (13)$$

Thus, the fraction of area available to the reactant is obtained by dividing Eq. (12) by Eq. (13).

$$\frac{r_{\text{act}}}{r_{\text{poss}}} = \frac{1}{h} \tanh h = \mathcal{E} \quad (14)$$

The quantity  $\mathcal{E}$  is known as the "effectiveness factor."

From Eq. (14) it is apparent that

$$r_{\text{act}} = \mathcal{E} r_{\text{poss}} \quad (15)$$

and since  $r_{\text{poss}} = k_s c_{\text{Ai}}$ , it follows that

$$r_{\text{act}} = \mathcal{E} k_s c_{\text{Ai}} \quad (16)$$

Eq. (16) shows that a first-order surface reaction will still appear as a first-order reaction under conditions where pore diffusion affects the rate. The change is that the first-order rate constant is not as great as it would be under conditions where pore diffusion is not a rate-influencing factor.

For reactions other than first order, Thiele [9] showed that the approach is identical to the above, with somewhat different results. He showed that, for a rate expression of the type

$$r = k_s c_{\text{Ai}}^n \quad (17)$$

the Thiele modulus and effectiveness factor are given respectively by

$$h = L \sqrt{\frac{2k_s c_{Ai}^{n-1}}{R_{eff}}} \quad (18)$$

$$\mathcal{E} = \frac{1}{2^{n/2} h} \quad (19)$$

Thus, for reactions of order higher than unity, pore diffusion will have an influence on the reaction order such that the observed order will be less than the true order. This is seen explicitly upon substitution of Eqs. (18) and (19) into Eq. (15):

$$\begin{aligned} r_{act} &= \frac{1}{2^{n/2} L} \sqrt{\frac{R_{eff} \mathcal{D}}{2k_s}} k_s c_{Ai}^{n-1} \frac{n-1}{2} \\ &= k_{eff} c_{Ai}^{\frac{n+1}{2}} \end{aligned} \quad (20)$$

where

$$k_{eff} = (1/2^{n/2} L) k_s \sqrt{(R_{eff} \mathcal{D} / 2k_s)},$$

$\frac{n+3}{2}$                        $\frac{n-1}{2}$   
 cm                      g-mole                      sec<sup>-1</sup>.

Experimentally, the reaction may be carried out over catalysts of different particle sizes in order to determine whether or not intraparticle diffusion influences the reaction. This follows from the fact that  $\mathcal{E}$  is a function of  $h$  and that  $h$  is directly proportional to  $L$ , the pore half length, which is proportional to the size of the catalyst pellet.

As  $L$  becomes smaller,  $h$  becomes smaller and  $\mathcal{E}$  becomes larger. Consequently, as one goes down in particle size, a pellet size should eventually be reached at which there is no change in the rate of reaction. This is the size at which one assumes that intraparticle diffusion is no longer playing a significant role in influencing the reaction rate. Keeler, et.al., [7] performed this work for a study of the forward reaction. They found that the reaction rate was no longer affected by particle size below 30-50 mesh. 30-50 mesh particles were used in the present investigation.

In a later publication, Roberts and Satterfield [8] explored in detail the solution to Eq. (4) when  $r_H$  is given by a Langmuir-Hinshelwood rate expression of the type shown in Eq. (21).

$$r_A = \frac{k K_A c_A}{1 + K_A c_A + K_Q c_Q} \quad (21)$$

where

$K_A, K_Q$  = adsorption equilibrium constants for species A and Q, respectively.

Q = reaction product for reaction  $A \rightarrow Q$ .

Solution of the equation which results when Eq. (21) is substituted into Eq. (7) was carried out numerically by Roberts and Satterfield [8]. The results of their calculations are a series of plots in which effectiveness factor is plotted against a modified Thiele modulus for various values of the parameter  $K_A p_A$ . Their modified Thiele modulus is defined by Eq. (22).

$$\phi_M = L \sqrt{\frac{k'RT}{D_{\text{eff}}}} \quad (22)$$

where

$$k' = \frac{k}{1 + \sum_i K_i [p_{i,s} + (c_{A,s} \nu_i \frac{D_{\text{eff}A}}{D_{\text{eff}i}})]} \quad (23)$$

where

$i$  = any species other than A.

$\nu_i$  = stoichiometric coefficient for species  $i$ .

$D_{\text{eff},i}$  = effective diffusivity for species  $i$ .

$c_{A,s}$  = surface concentration of species  $i$ .

Roberts and Satterfield show that for a given value of  $\phi_M$ ,  $h$  is lower as the value of  $K_A p_A$  is lowered. This condition occurs at lower reactant particle pressures. Using the data of Hutchinson [6] for the reverse reaction, values of  $\phi_M$  and  $K_A p_A$  were calculated. The results of these calculations showed that under the present conditions the reaction is essentially outside the range where pore diffusion significantly influences the reaction rate [1]. Geddes [5], in his study of the structure of the iron oxide catalyst, reported the same findings, although his approach was based upon a first-order rate law. Since effectiveness factors greater than 0.9 were obtained by all of the above mentioned workers who studied, the ortho-parahydrogen reactions, it is concluded that pore diffusion is not a serious factor in influencing the reaction rate under the present set of experimental conditions.

## References for Appendix C

1. Barrick, P. L., L. F. Brown, H. L. Hutchinson, "Kinetics and Diffusion Study of the Para-Ortho Shift of Hydrogen," Technical Documentary Report HPL-TDR-64-77, September, 1964.
2. Bradshaw, R. D., C. O. Bennett, A.I.Ch.E. J., 7, 48 (1961).
3. Carberry, J. J., A.I.Ch.E. J., 6, 460 (1960).
4. DeAcetis, J., G. Thodos, Ind. Eng. Chem., 52, 1003 (1960).
5. Geddes, D. D., M.S. Thesis, U. of Colorado (1964).
6. Hutchinson, H. L., M.S. Thesis, U. of Colorado (1964).
7. Keeler, R. N., D. H. Weitzel, J. H. Blake, M. Konecink, Adv. Cryo. Eng., 5, 511 (1960).
8. Roberts, G. W., C. N. Satterfield, Ind. Eng. Chem. Fundamentals, 4, 288 (1965).
9. Thiele, E. W., Ind. Eng. Chem., 31, 916 (1939).
10. Wakao, N., T. Oshima, S. Yagi, Chem. Eng. (Japan), 22, 780 (1958).
11. Wakao, N., P. W. Selwood, J. M. Smith, A.I.Ch.E. J., 8, 478 (1962).
12. Wheeler, A., in "Advances in Catalysis," III, Academic Press, New York, 249 (1951).
13. Yeh, G. C., J. Chem. Eng. Data, 6, 526 (1961).
14. Zeldowitsch, J. B., Acta. Physicochim. USSR, 10, 583 (1939).

APPENDIX D

Space Velocity Curves from  
Langmuir Rate Equations

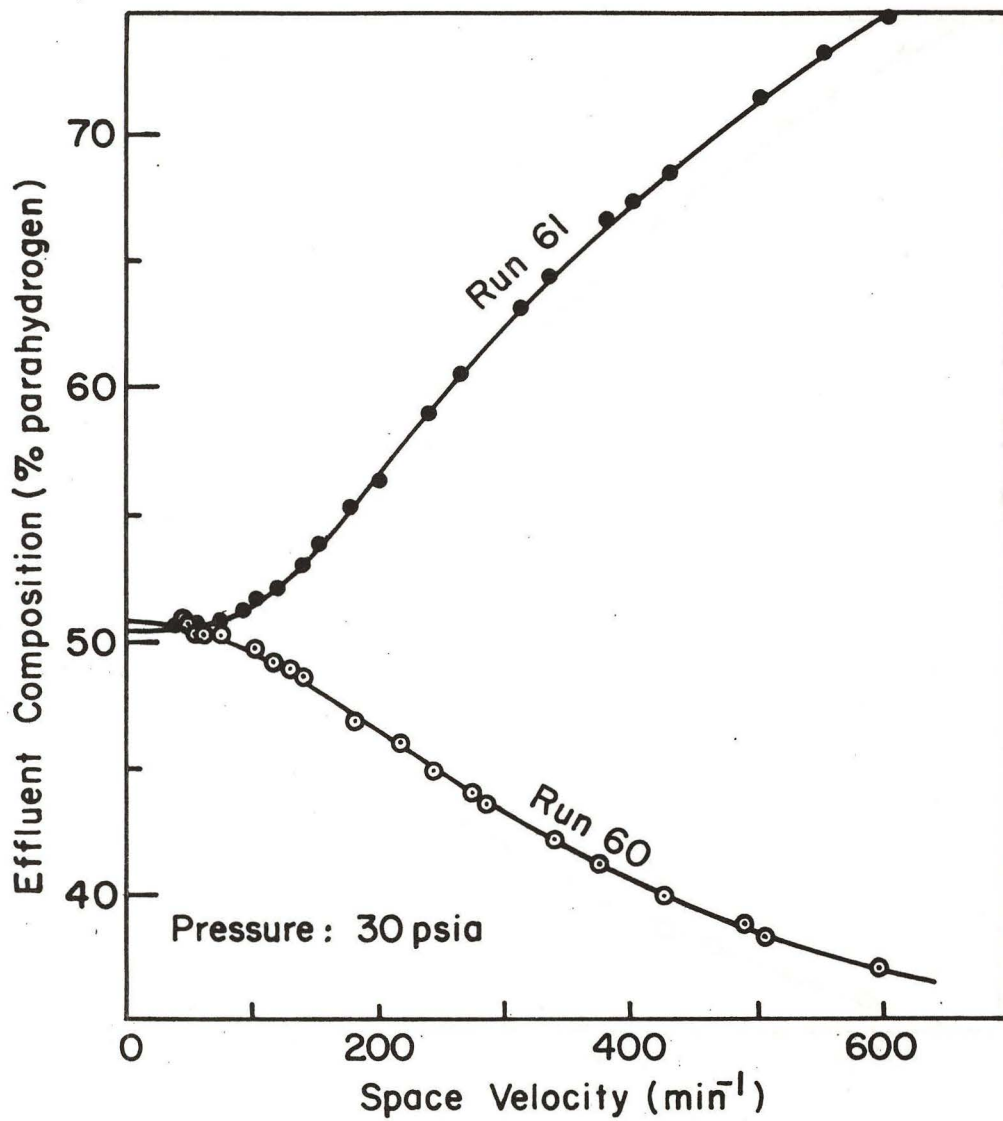


FIGURE 24. Predicted and Observed Space Velocities from Langmuir Rate Equation for Runs 60 and 61

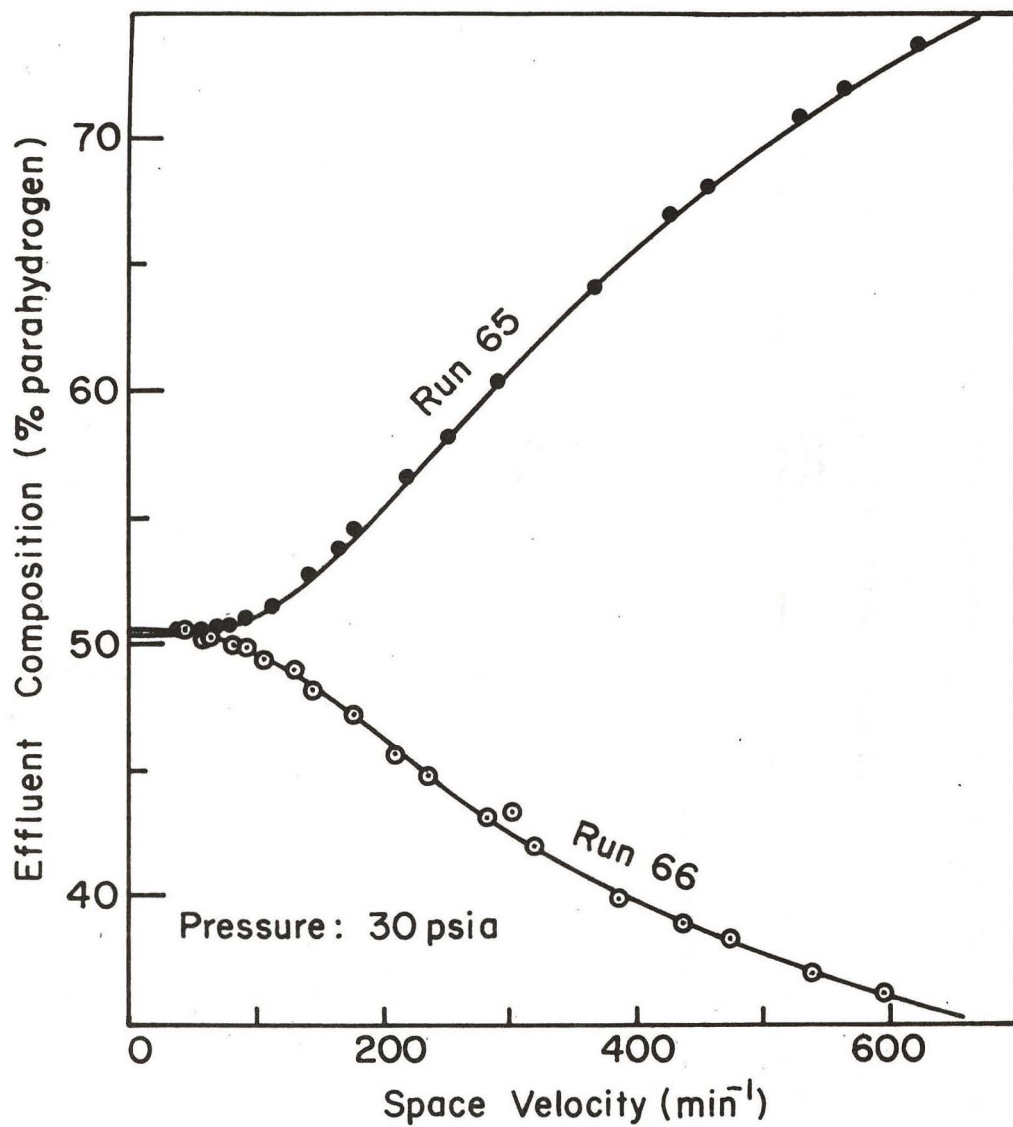


FIGURE 25. Predicted and Observed Space Velocities from Langmuir Rate Equation for Runs 65 and 66

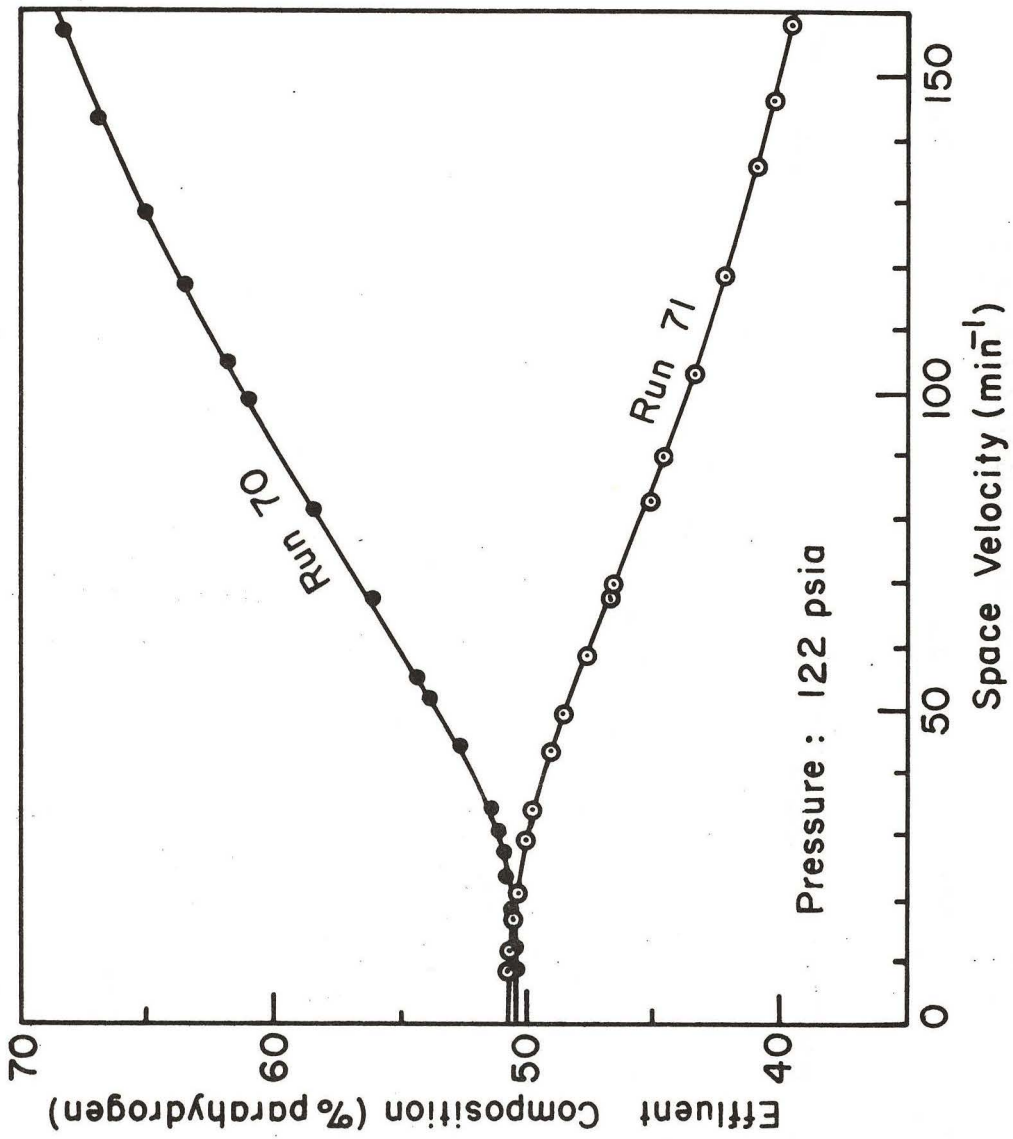


FIGURE 26. Predicted and Observed Space Velocities from Langmuir Rate Equation for Runs 70 and 71

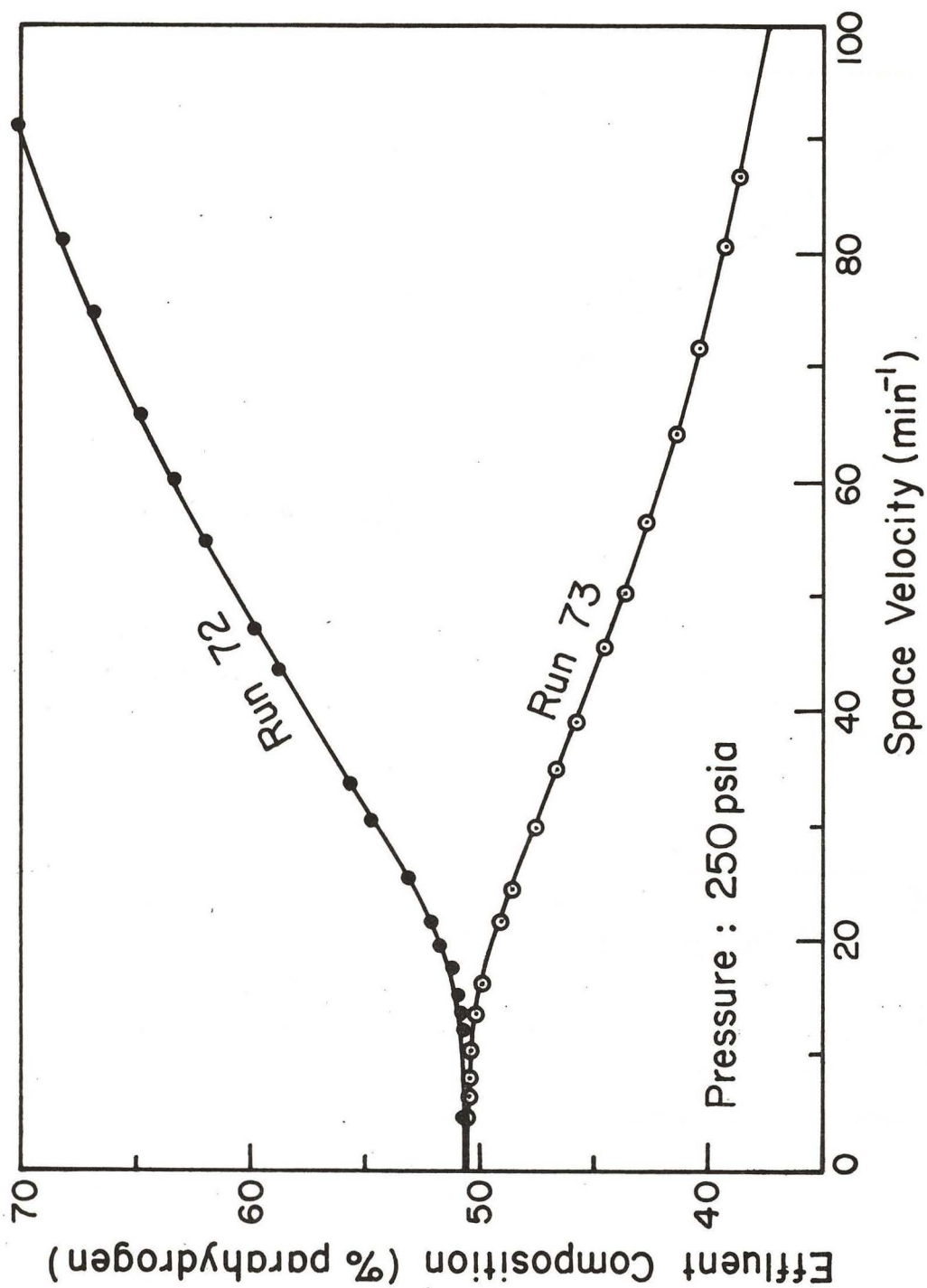


FIGURE 27. Predicted and Observed Space Velocities from Langmuir Rate Equation for Runs 72 and 73

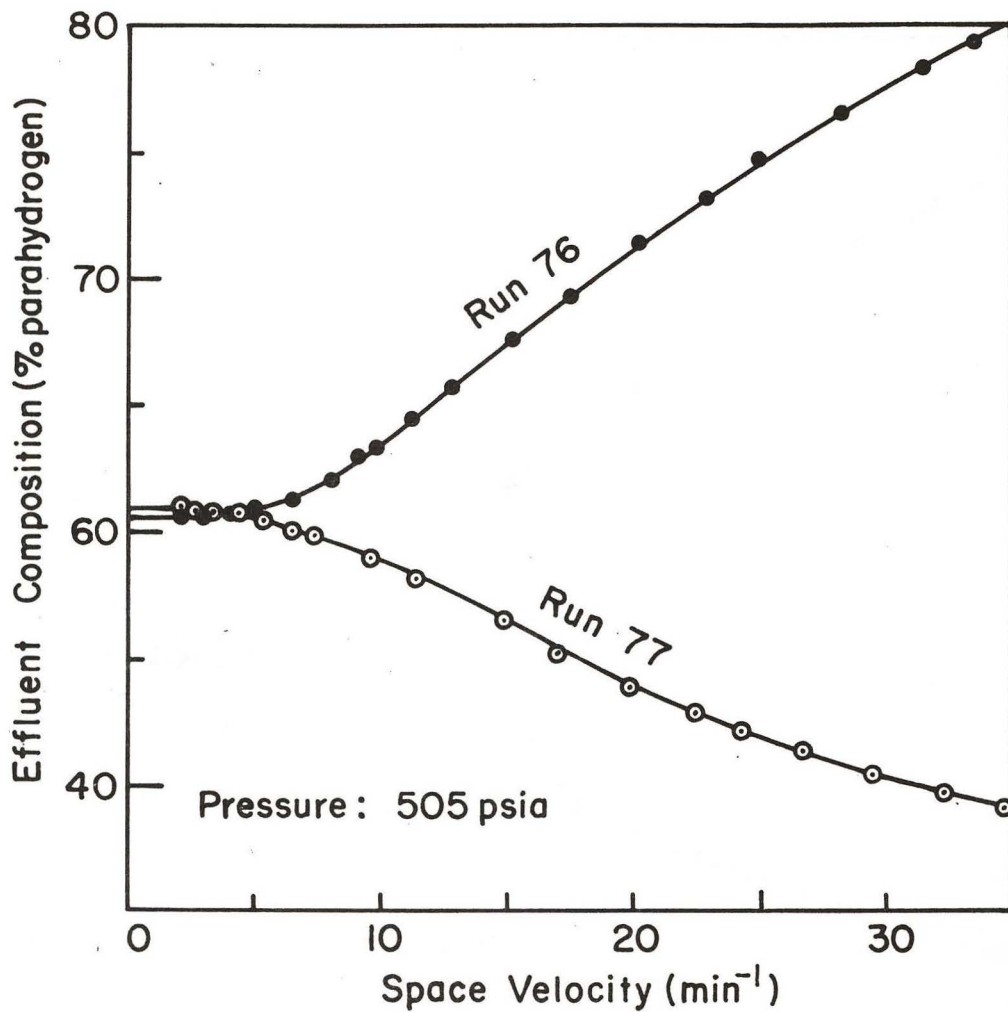


FIGURE 28. Predicted and Observed Space Velocities from Langmuir Rate Equation for Runs 76 and 77

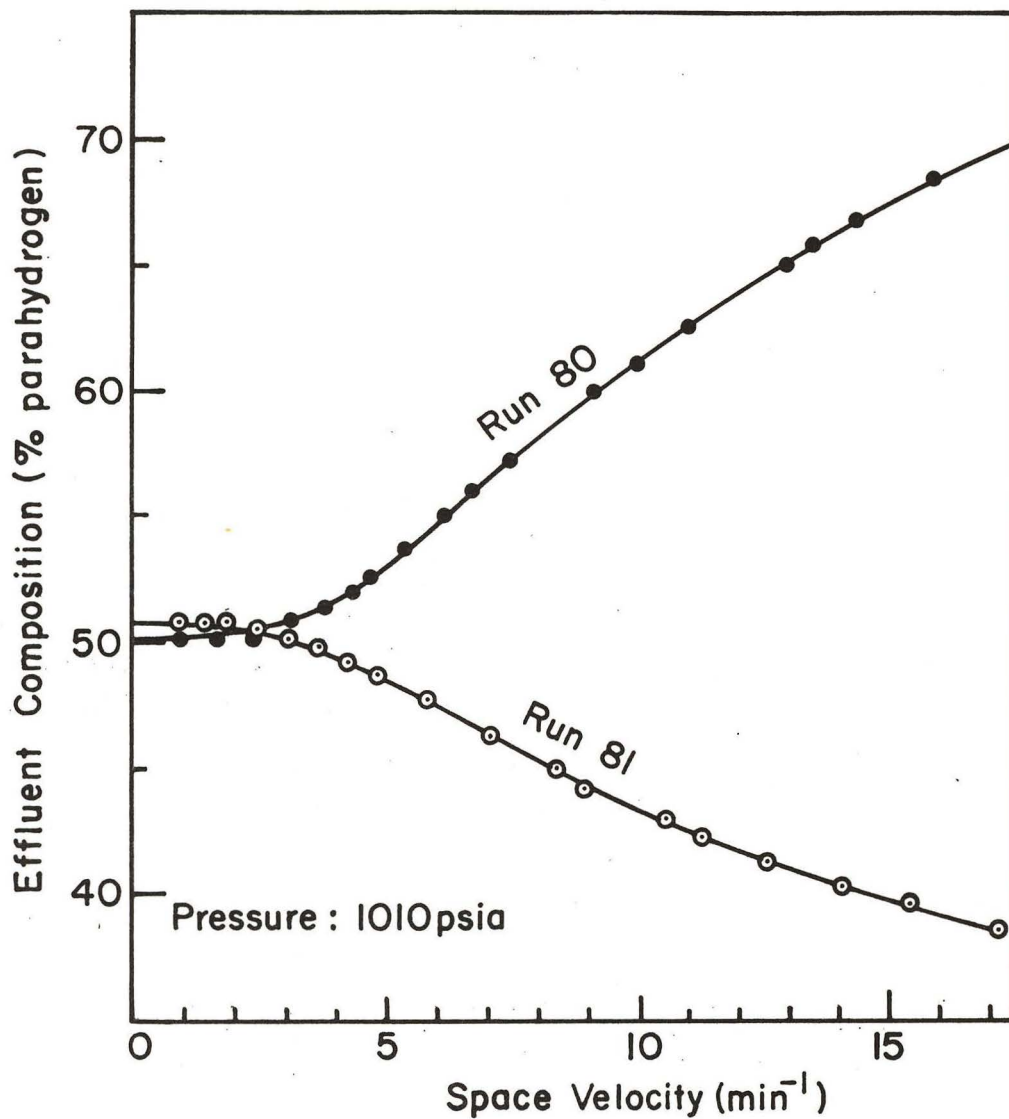


FIGURE 29. Predicted and Observed Space Velocities from Langmuir Rate Equation for Runs 80 and 81

APPENDIX E

Space Velocity Curves from  
Elovich Rate Equation

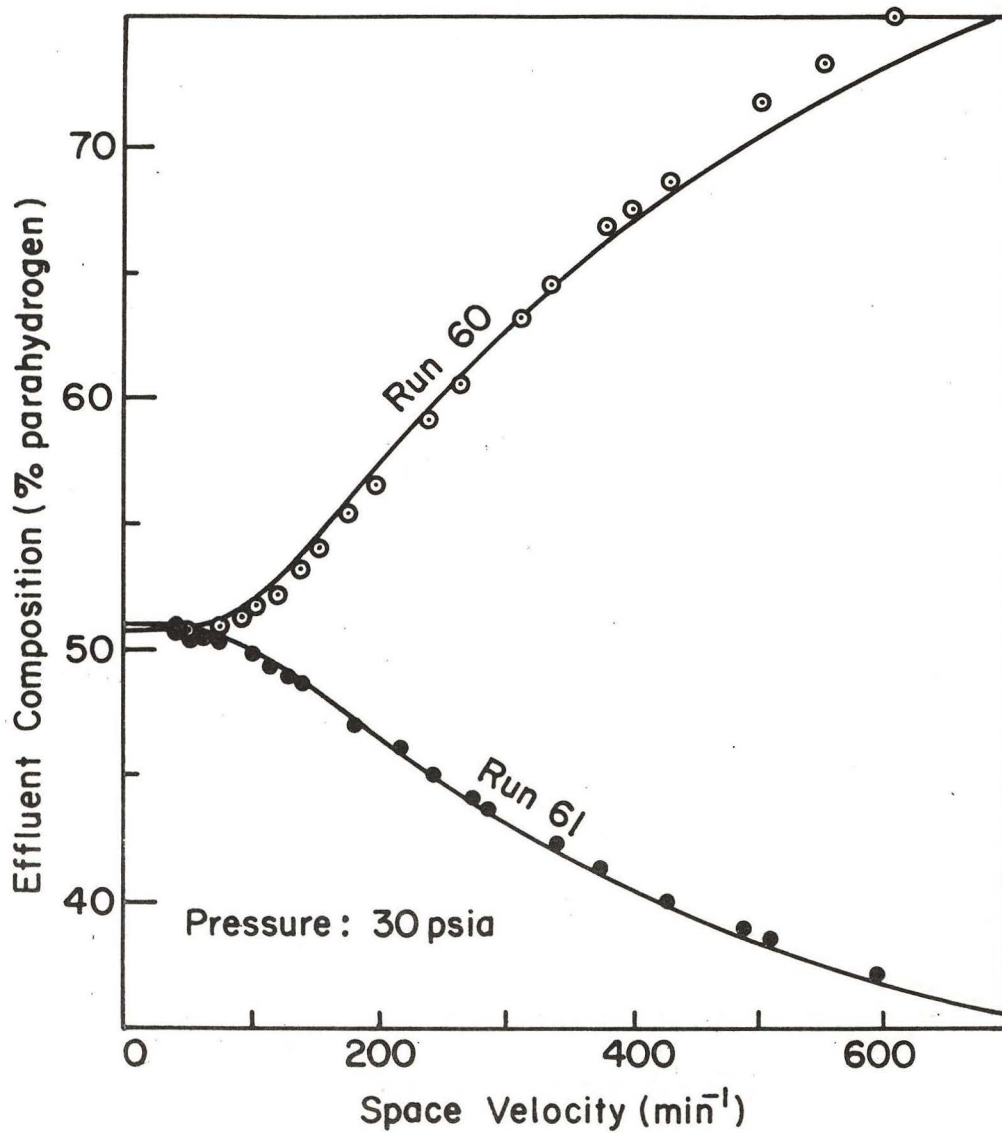


FIGURE 30. Predicted and Observed Space Velocities from Elovich Rate Equation for Runs 60 and 61

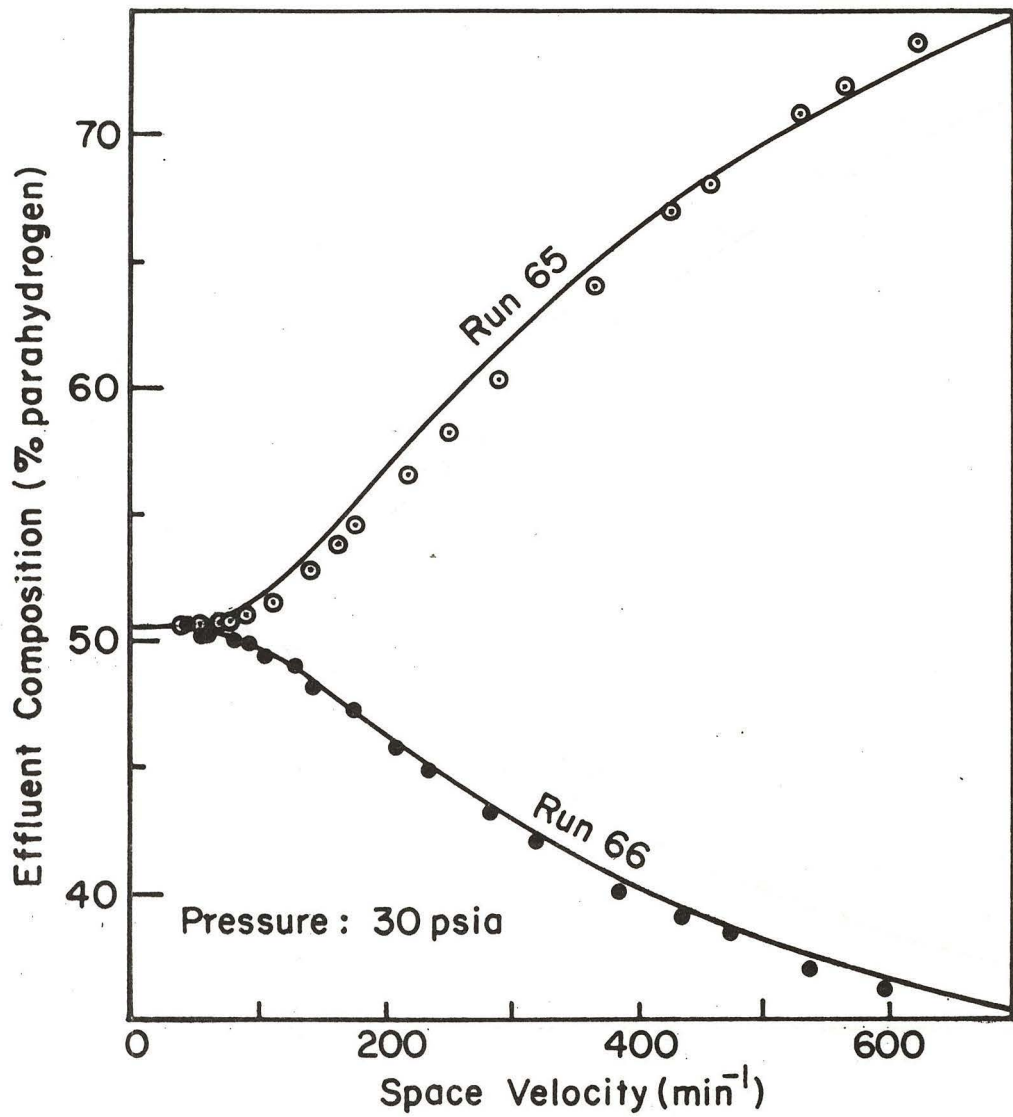


FIGURE 31. Predicted and Observed Space Velocities from Elovich Rate Equation for Runs 65 and 66 .

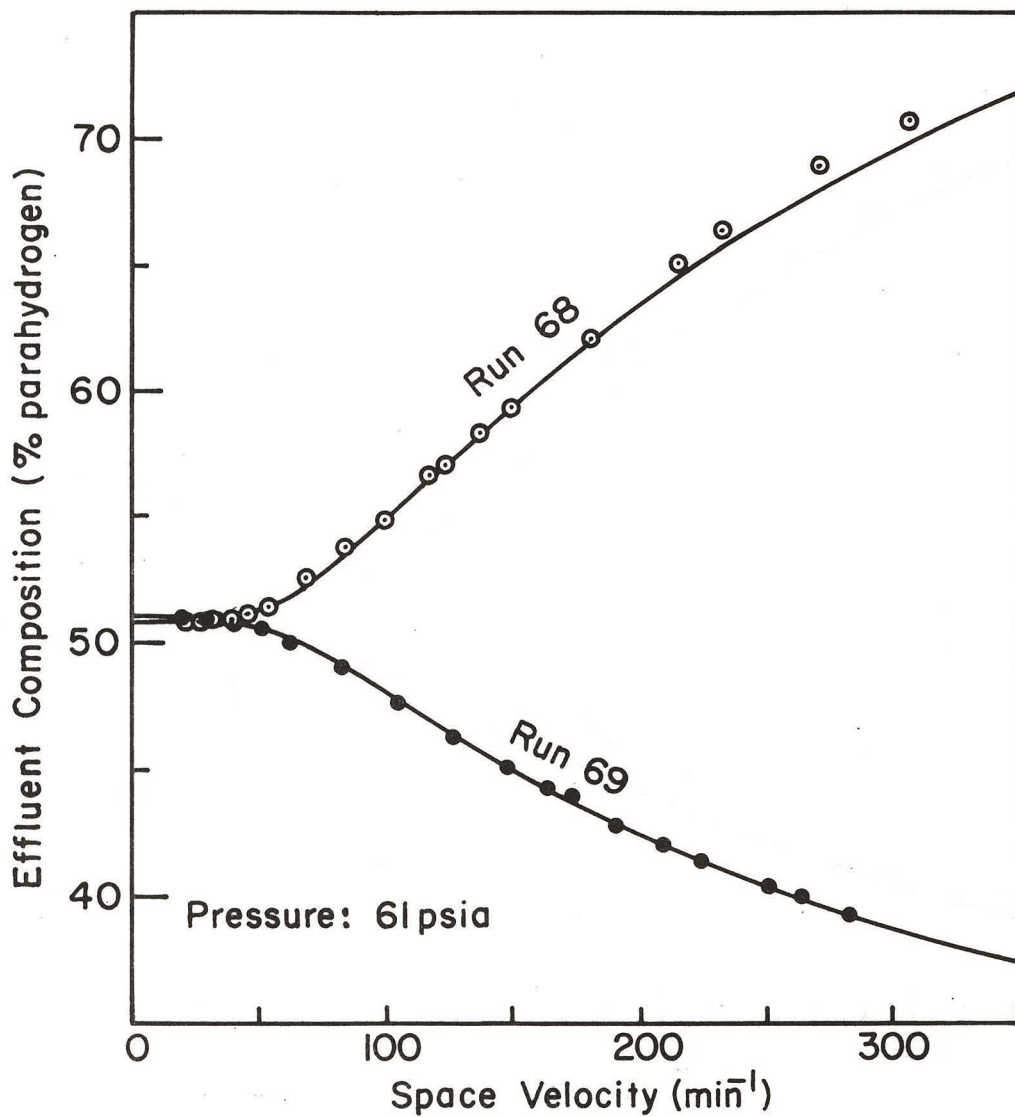


FIGURE 32. Predicted and Observed Space Velocities from Elovich Rate Equation for Runs 68 and 69

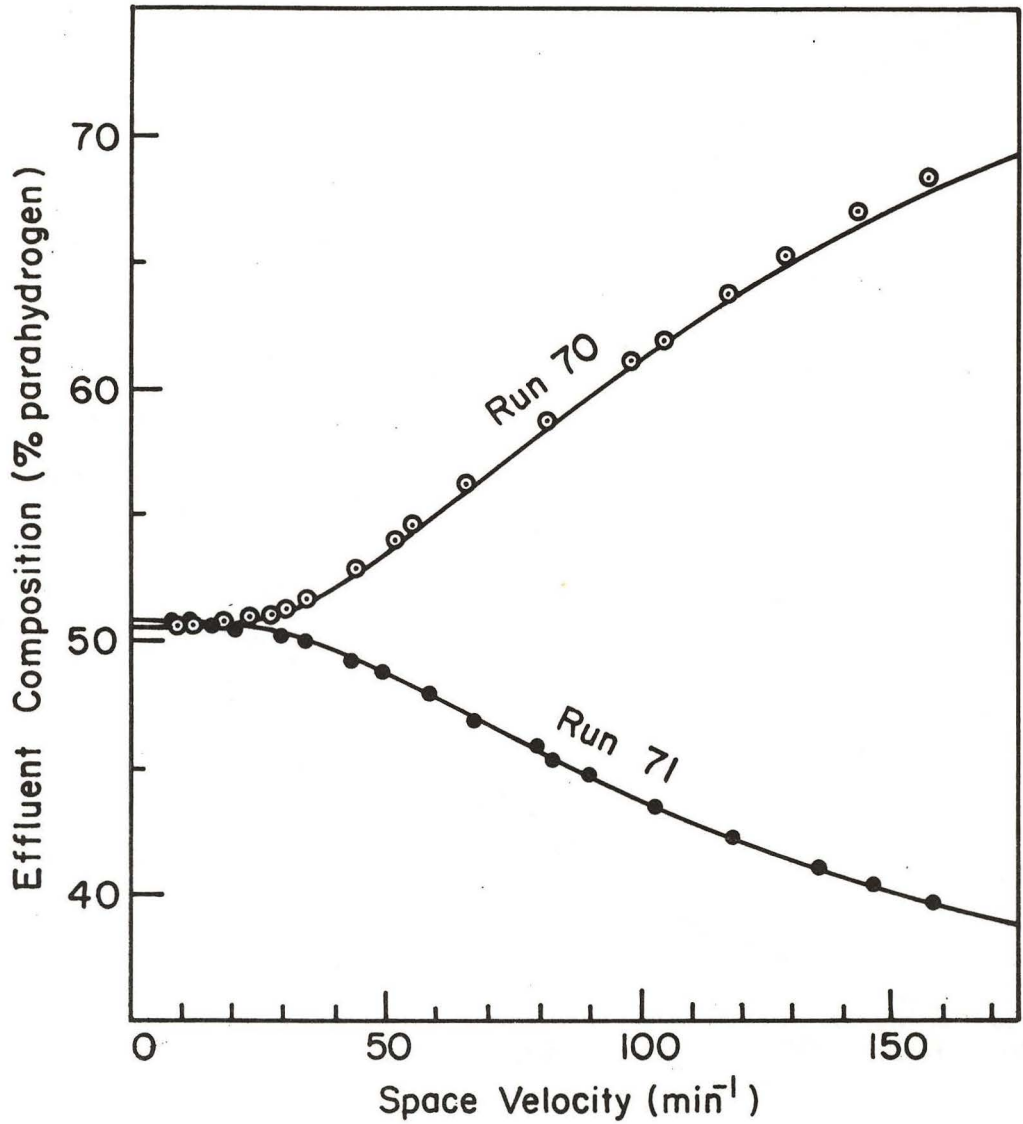


FIGURE 33. Predicted and Observed Space Velocities from Elovich Rate Equation for Runs 70 and 71 .

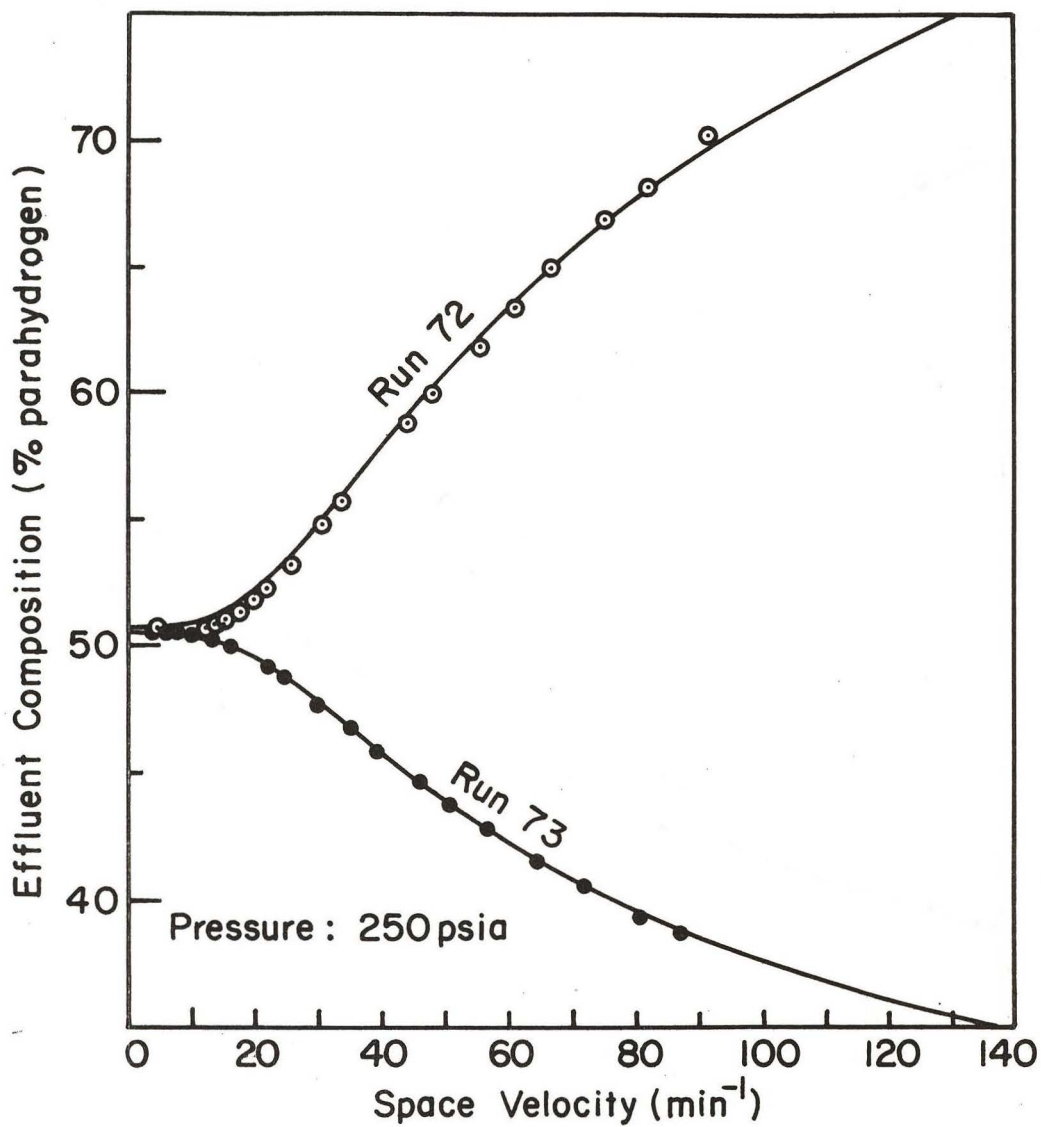


FIGURE 34. Predicted and Observed Space Velocities from Elovich Rate Equation for Runs 72 and 73

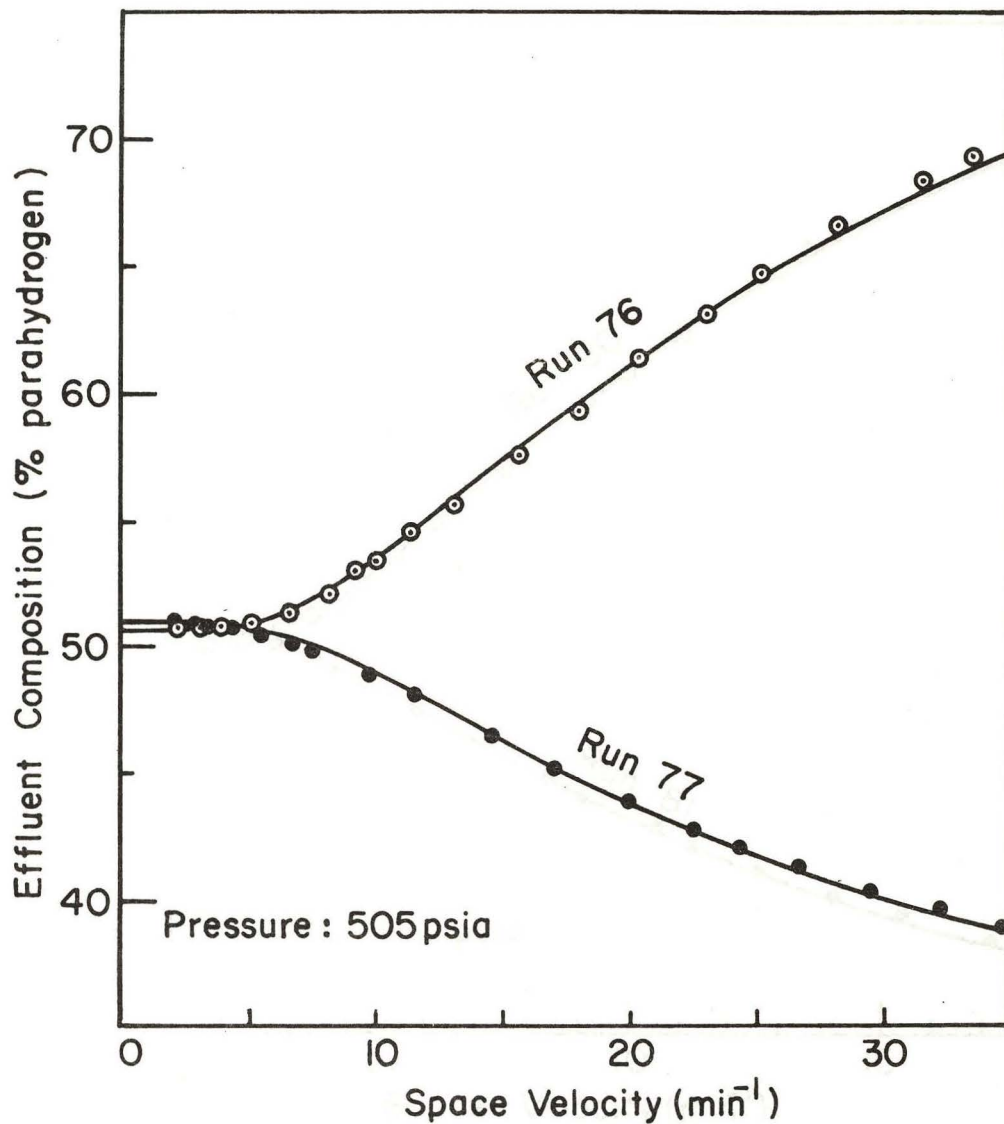


FIGURE 35. Predicted and Observed Space Velocities from Elovich Rate Equation for Runs 76 and 77

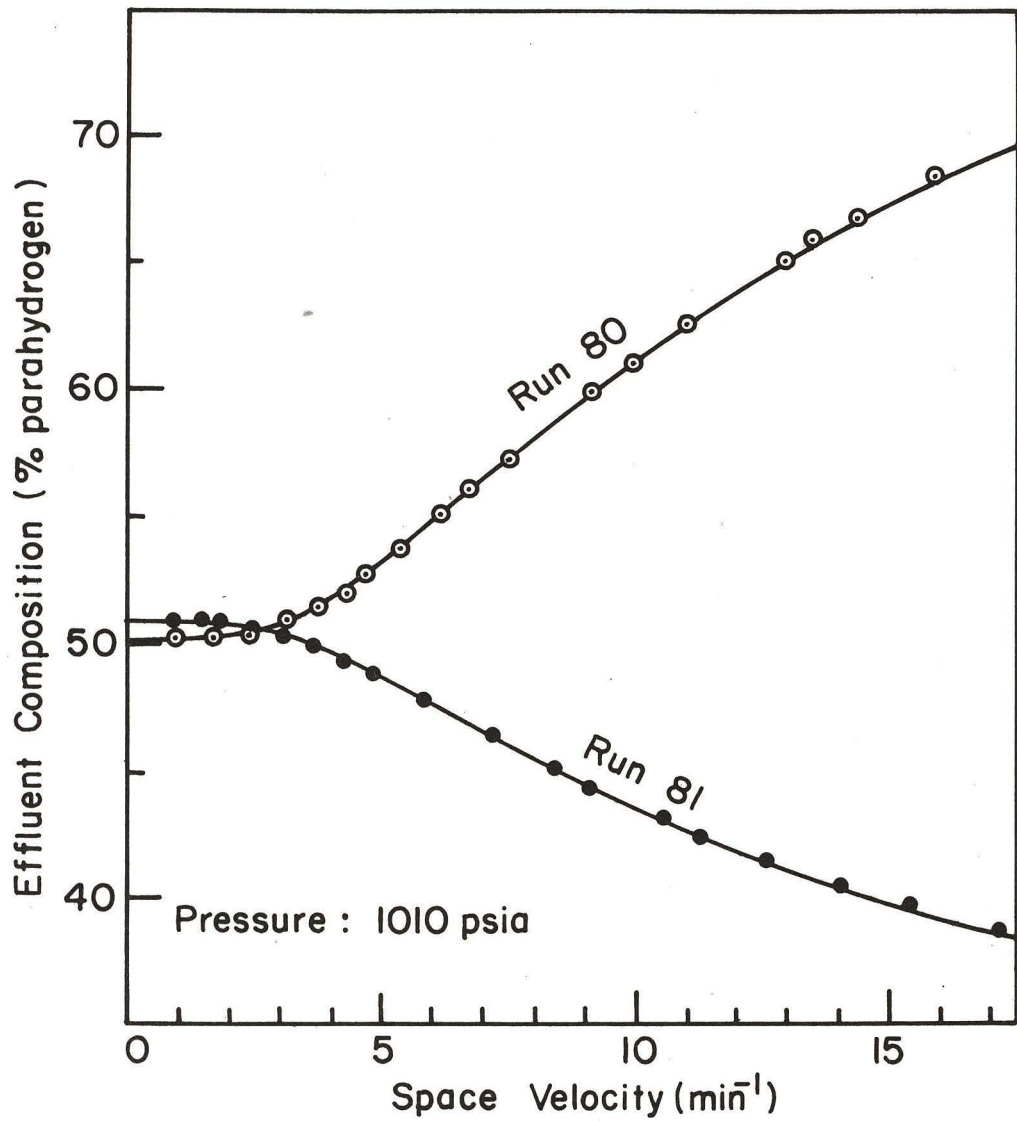


FIGURE 36. Predicted and Observed Space Velocities from Elovich Rate Equation for Runs 80 and 81

APPENDIX F

Langmuir Rate Plots

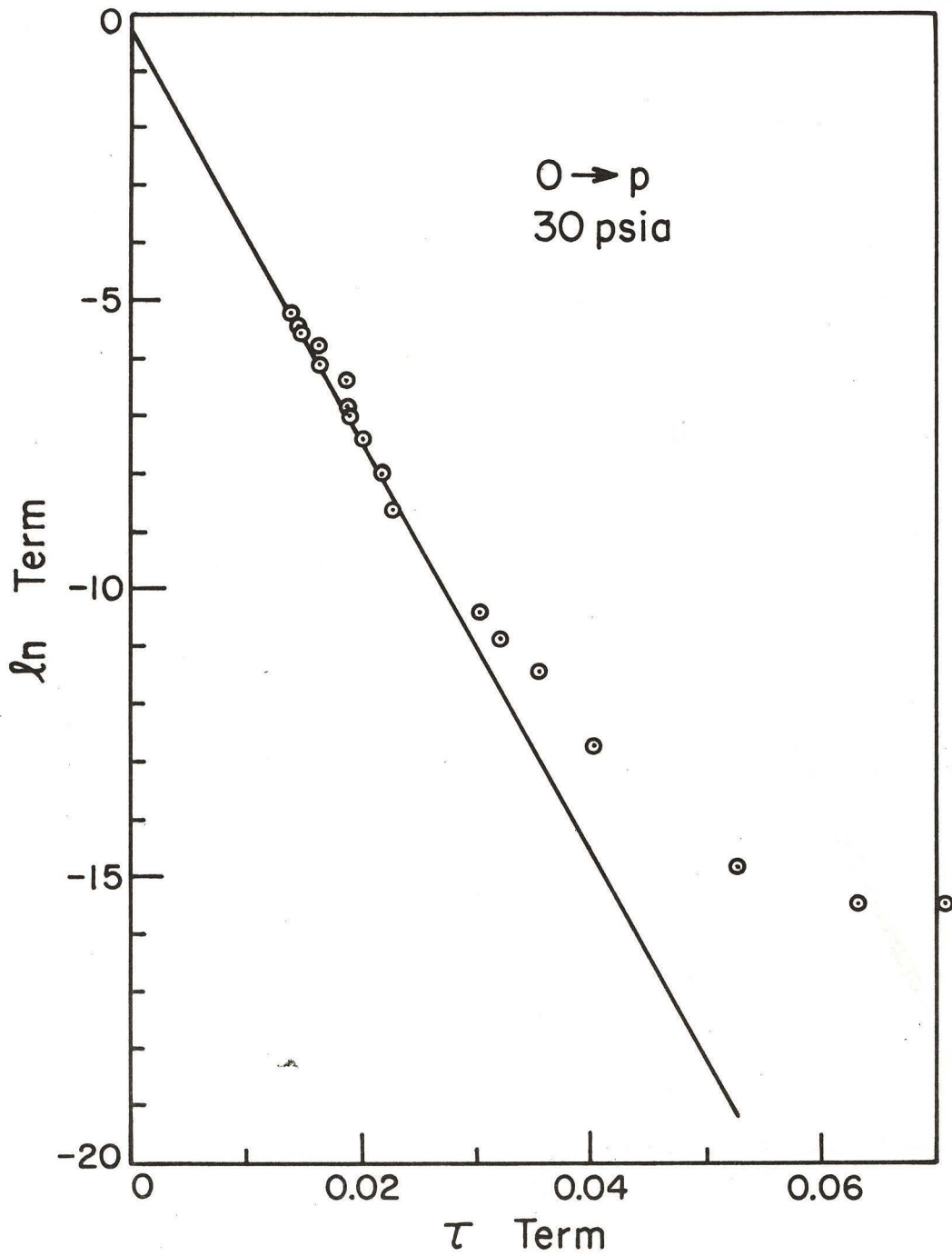


FIGURE 37. Langmuir Plot for Run 60

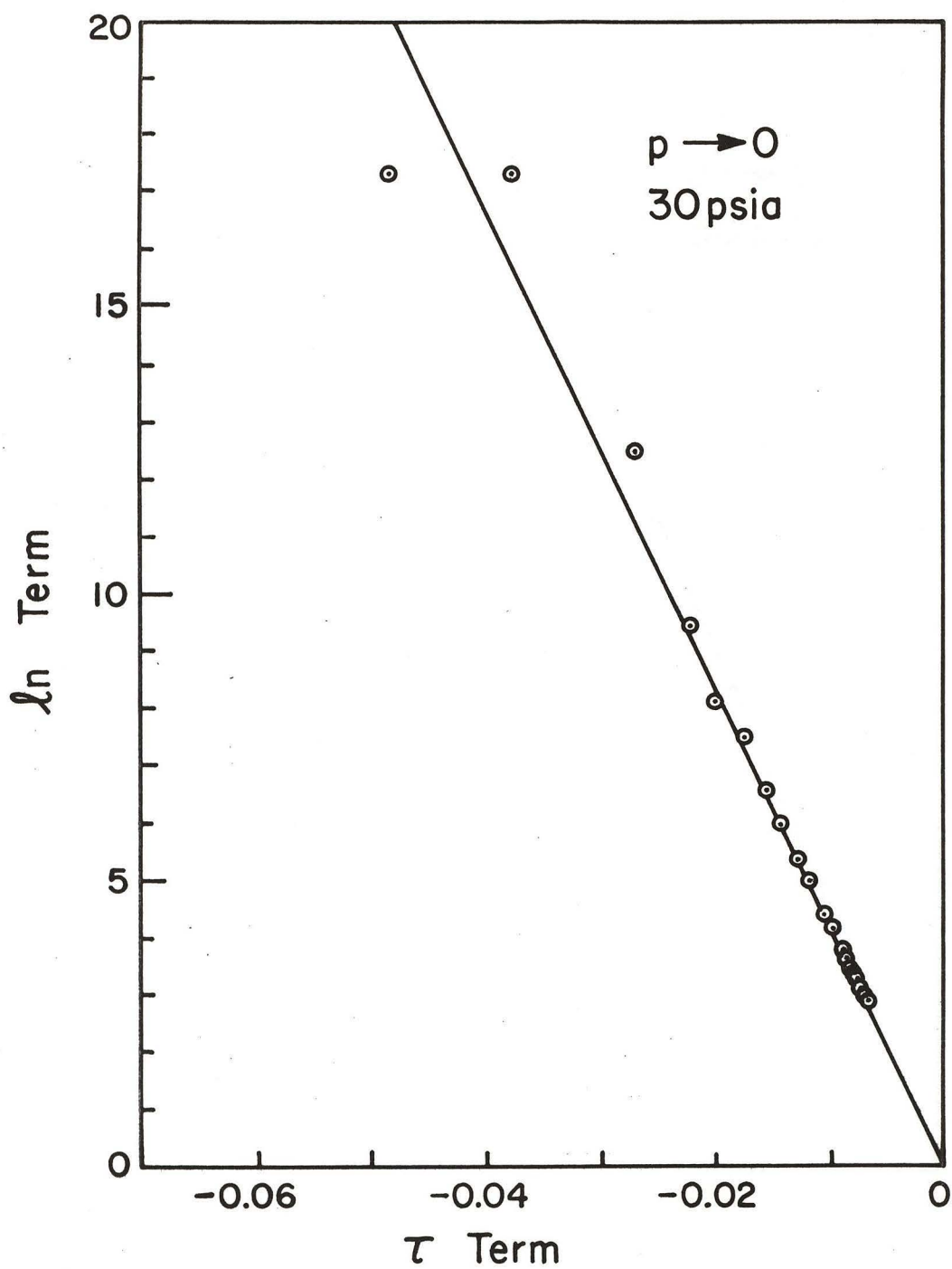


FIGURE 38. Langmuir Plot for Run 61

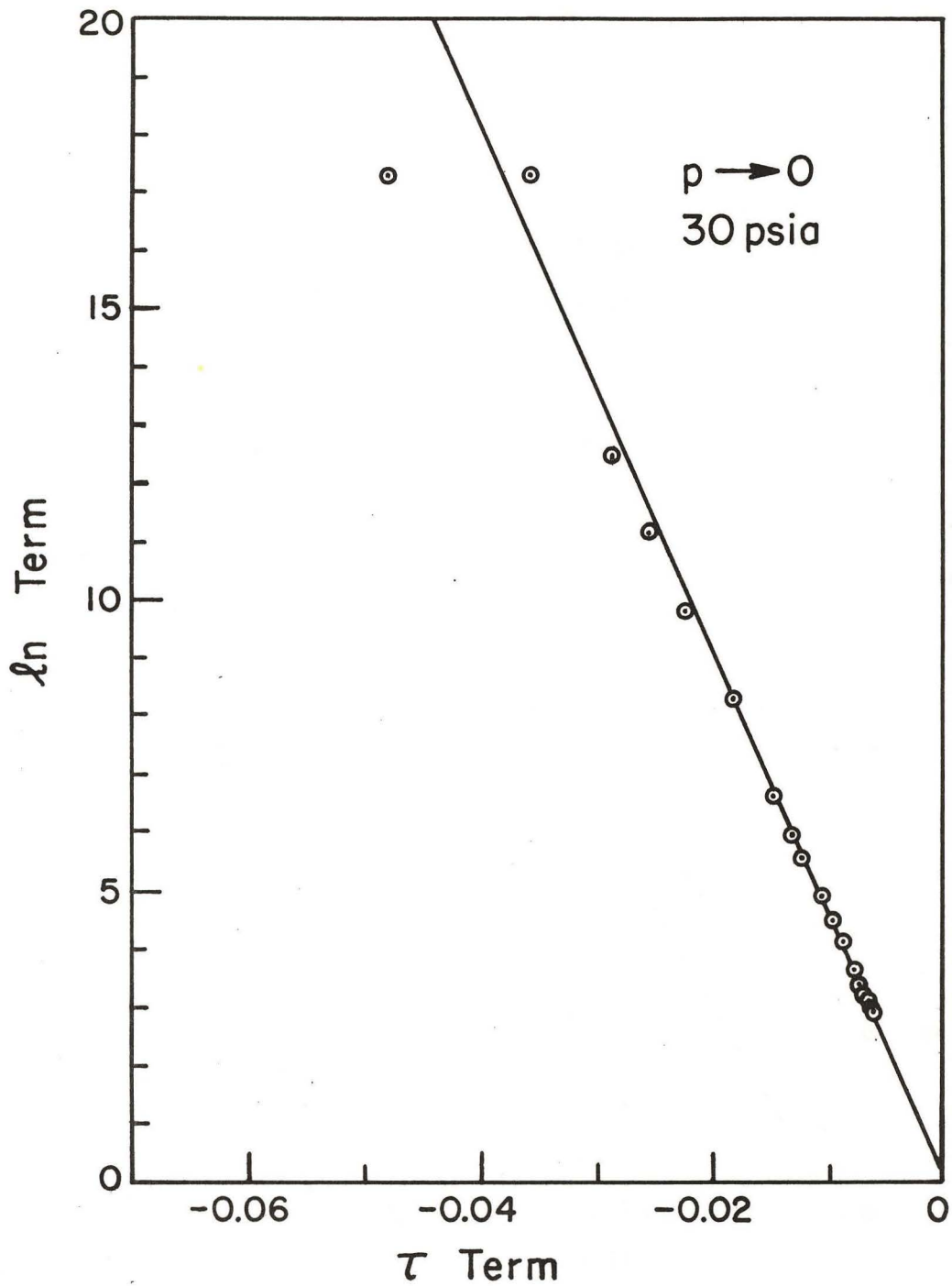


FIGURE 39. Langmuir Plot for Run 65

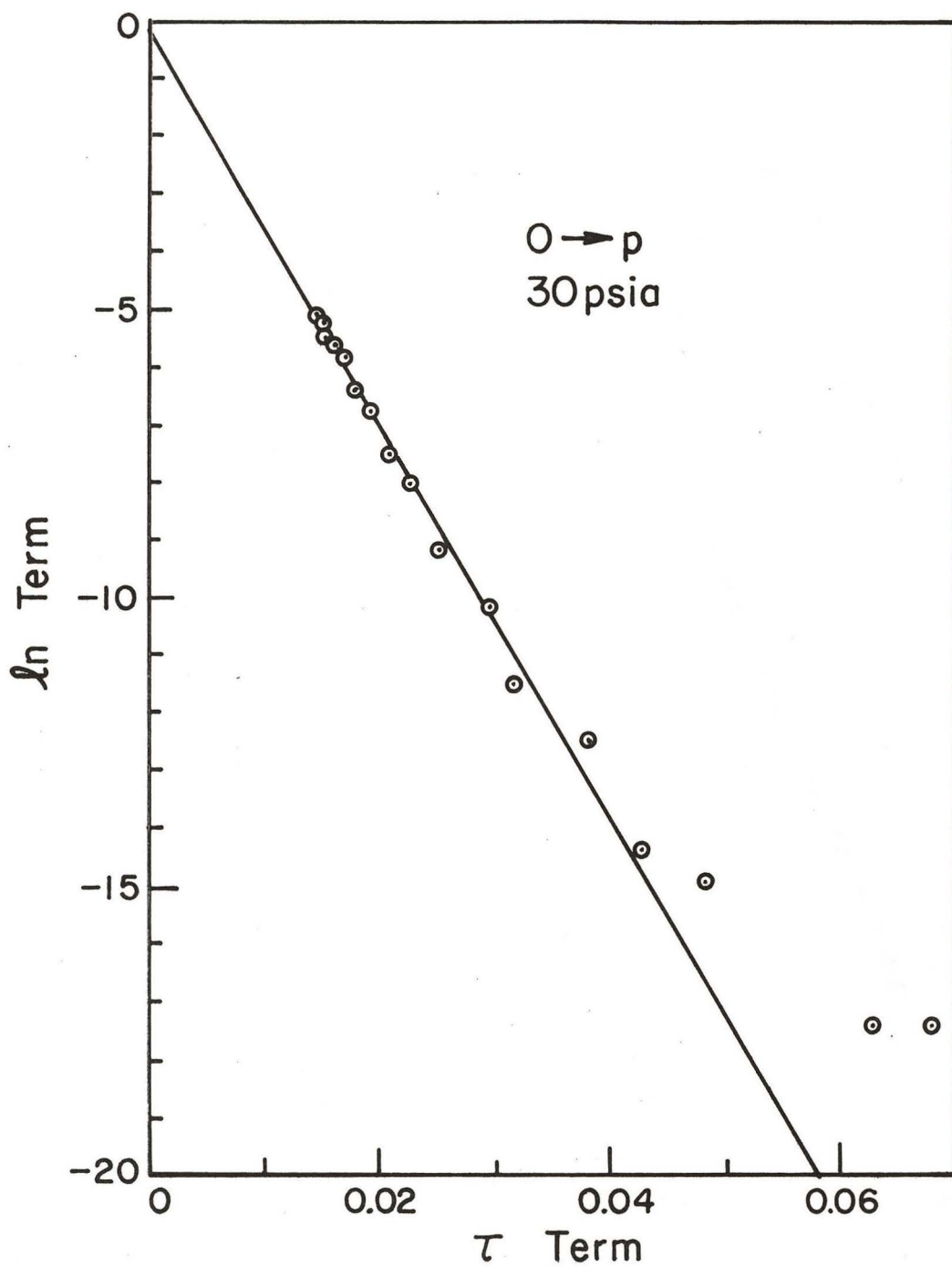


FIGURE 40. Langmuir Plot for Run 66

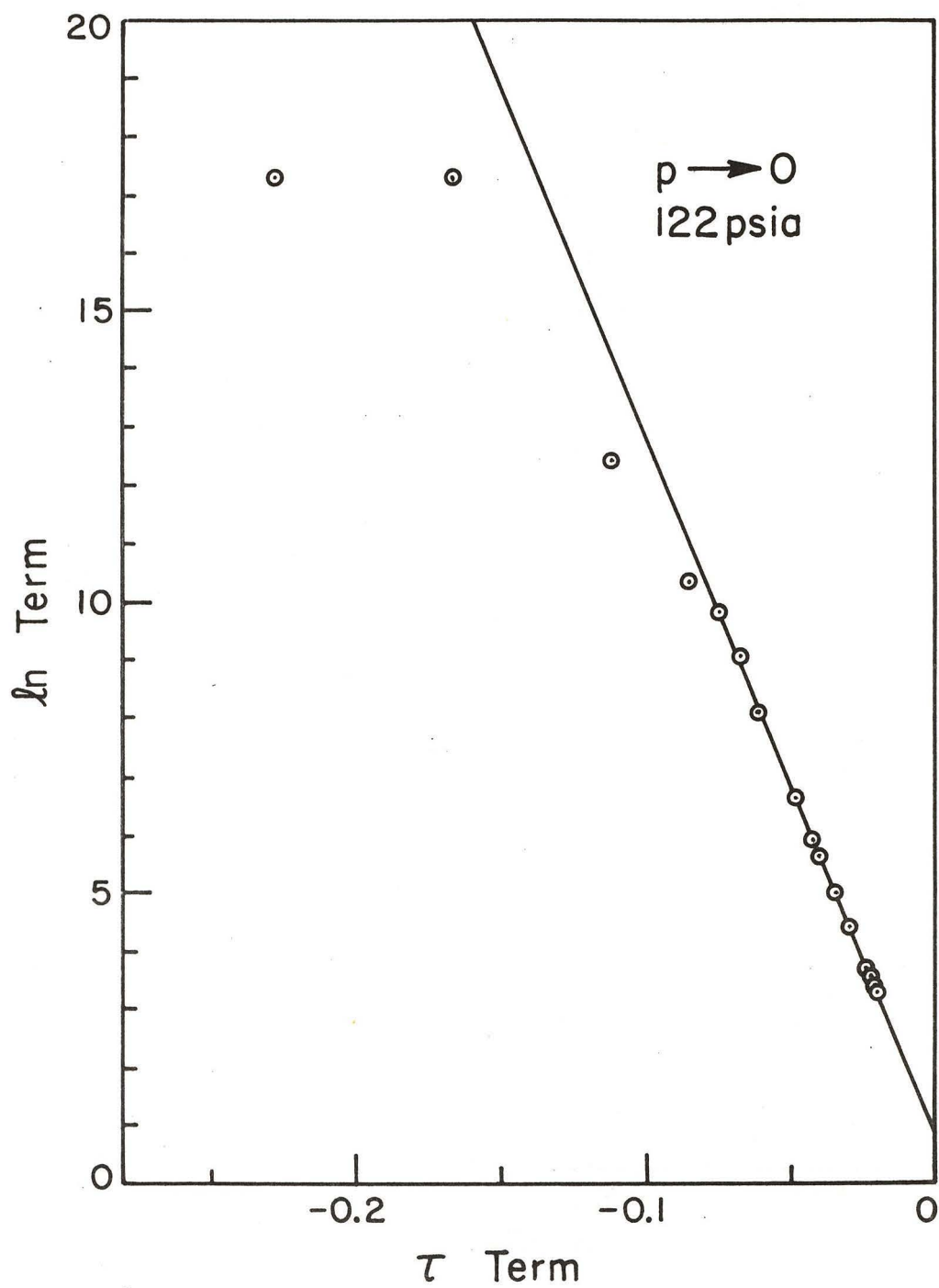


FIGURE 41. Langmuir Plot for Run 70

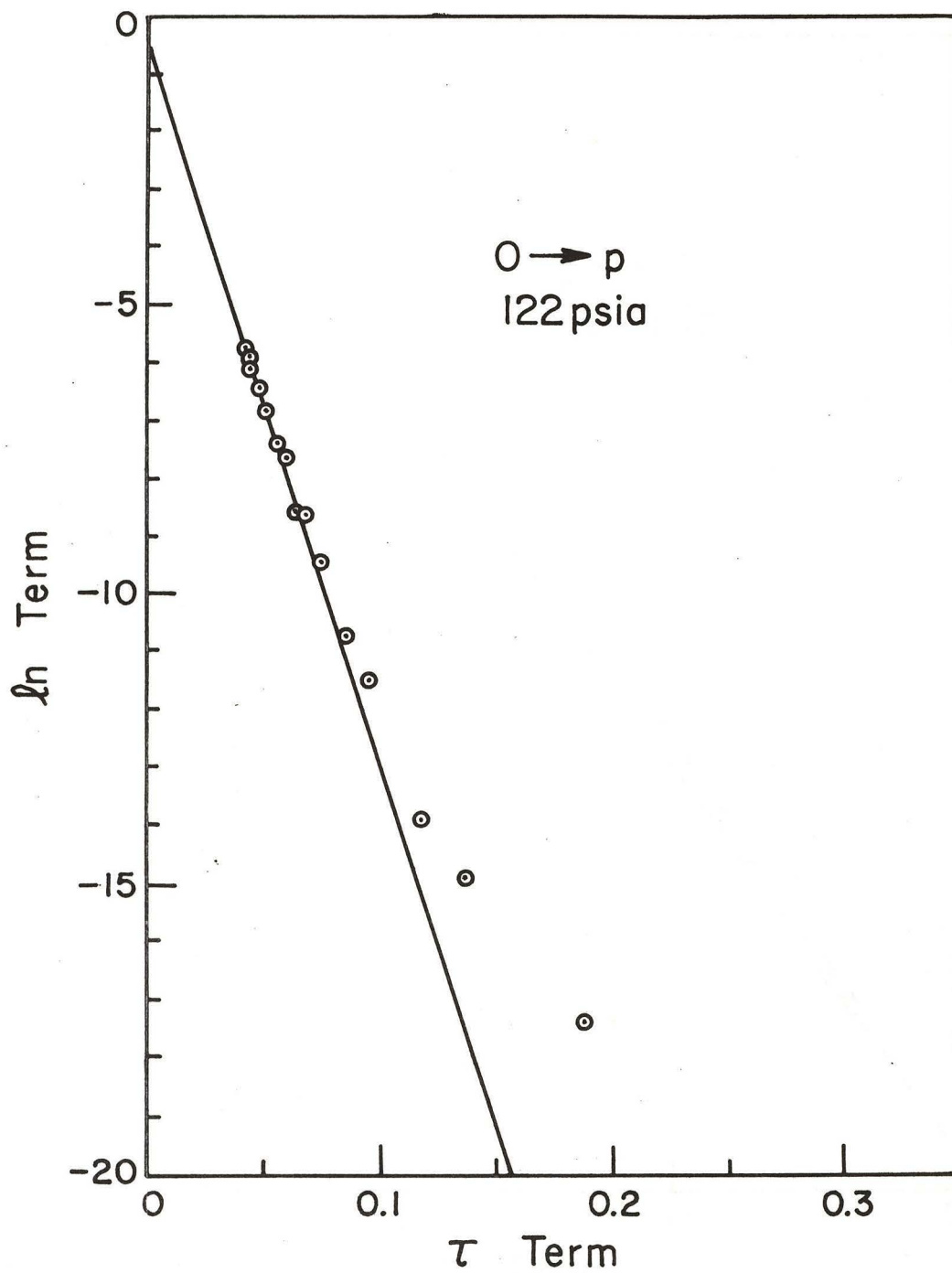


FIGURE 42. Langmuir Plot for Run 71

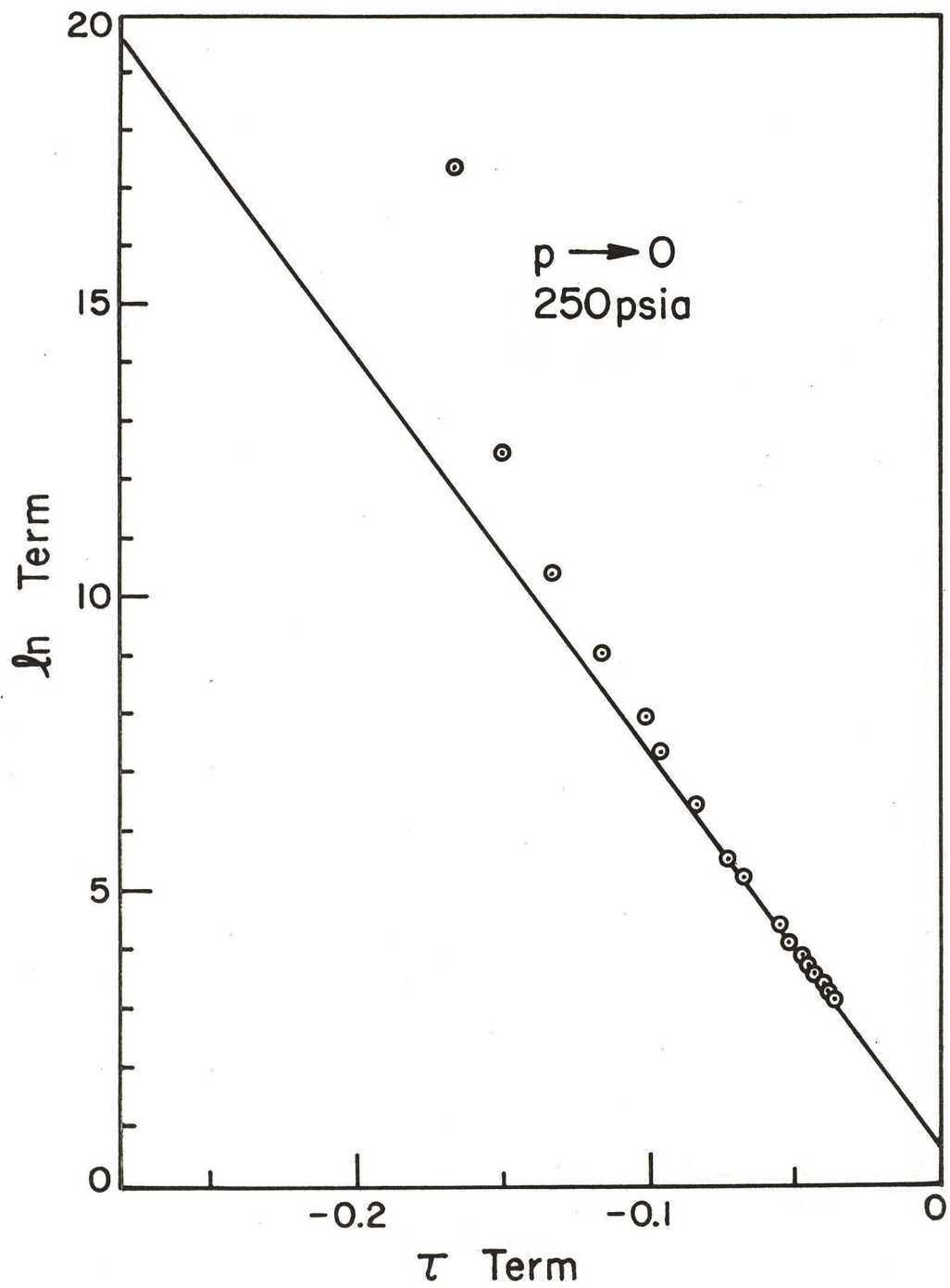


FIGURE 43. Langmuir Plot for Run 72

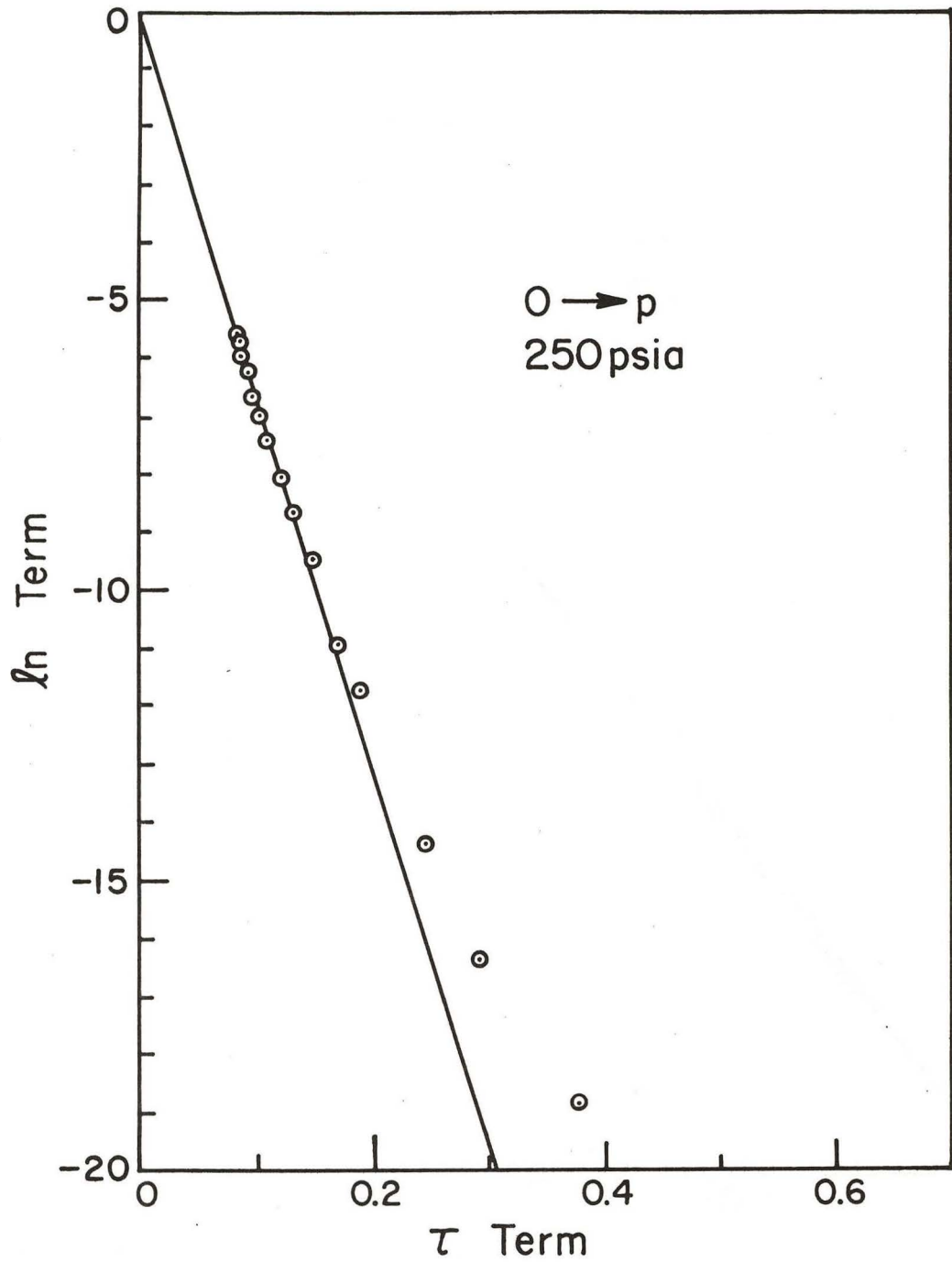


FIGURE 44. Langmuir Plot for Run 73

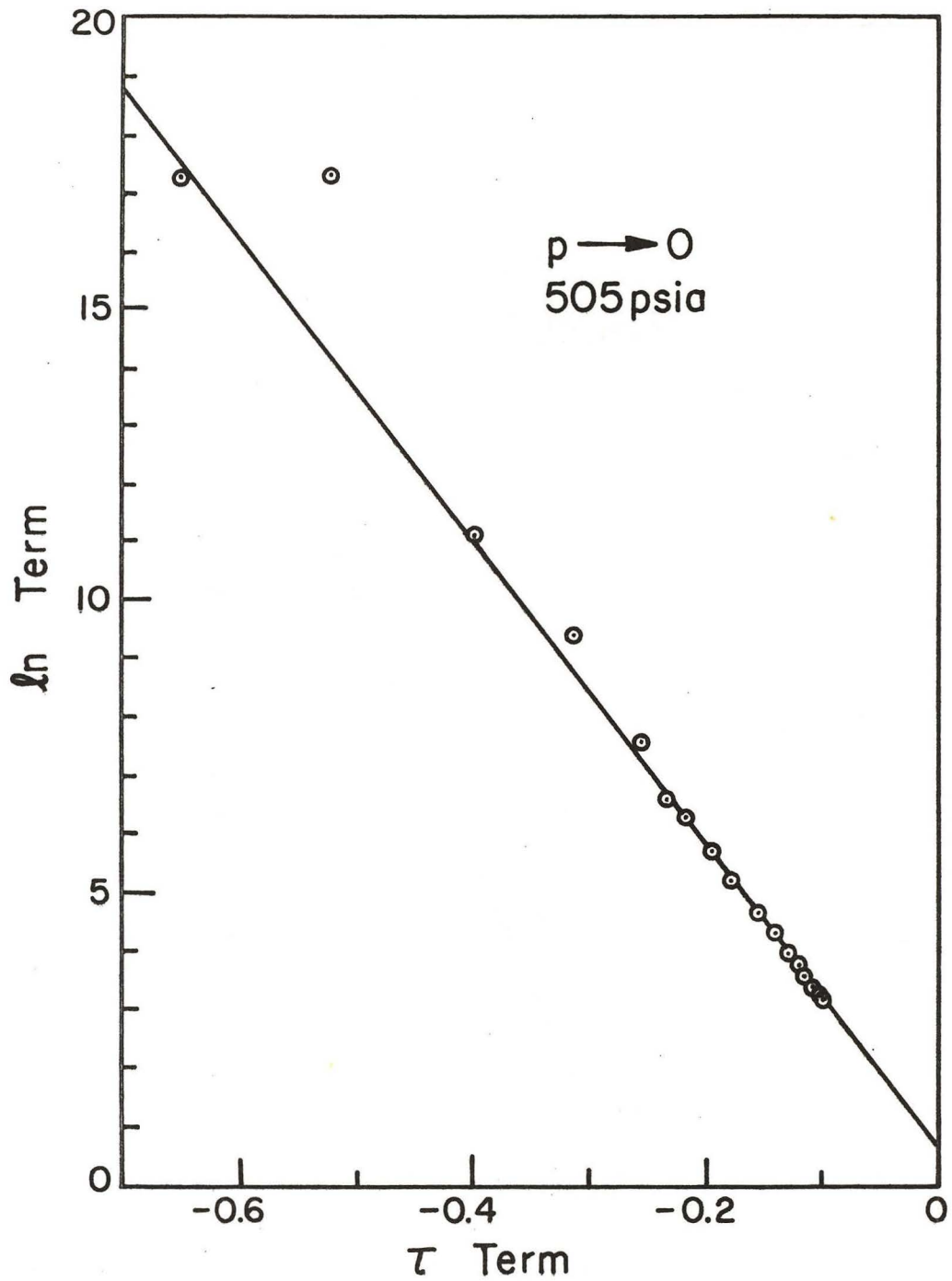


FIGURE 45. Langmuir Plot for Run 76

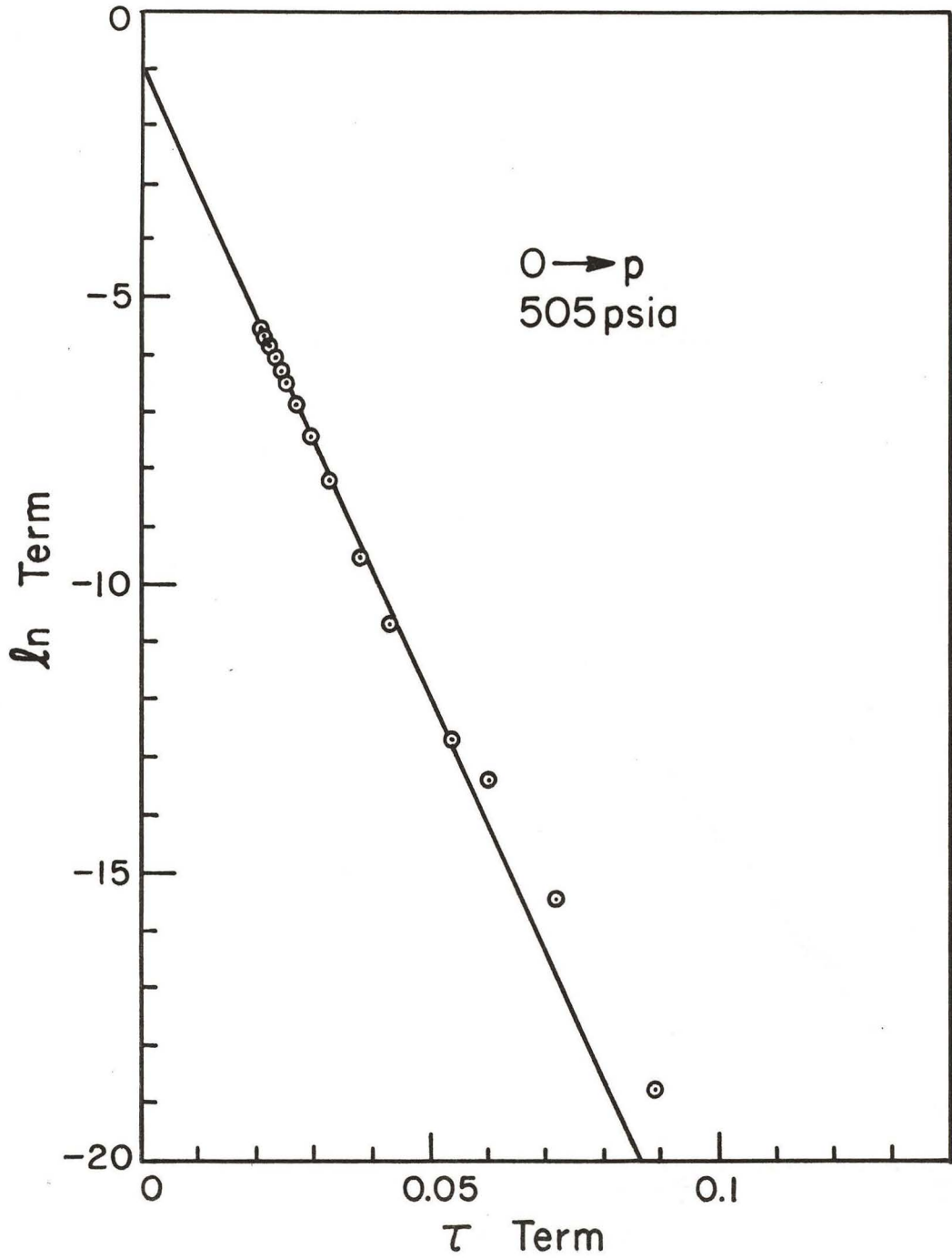


FIGURE 46. Langmuir Plot for Run 77

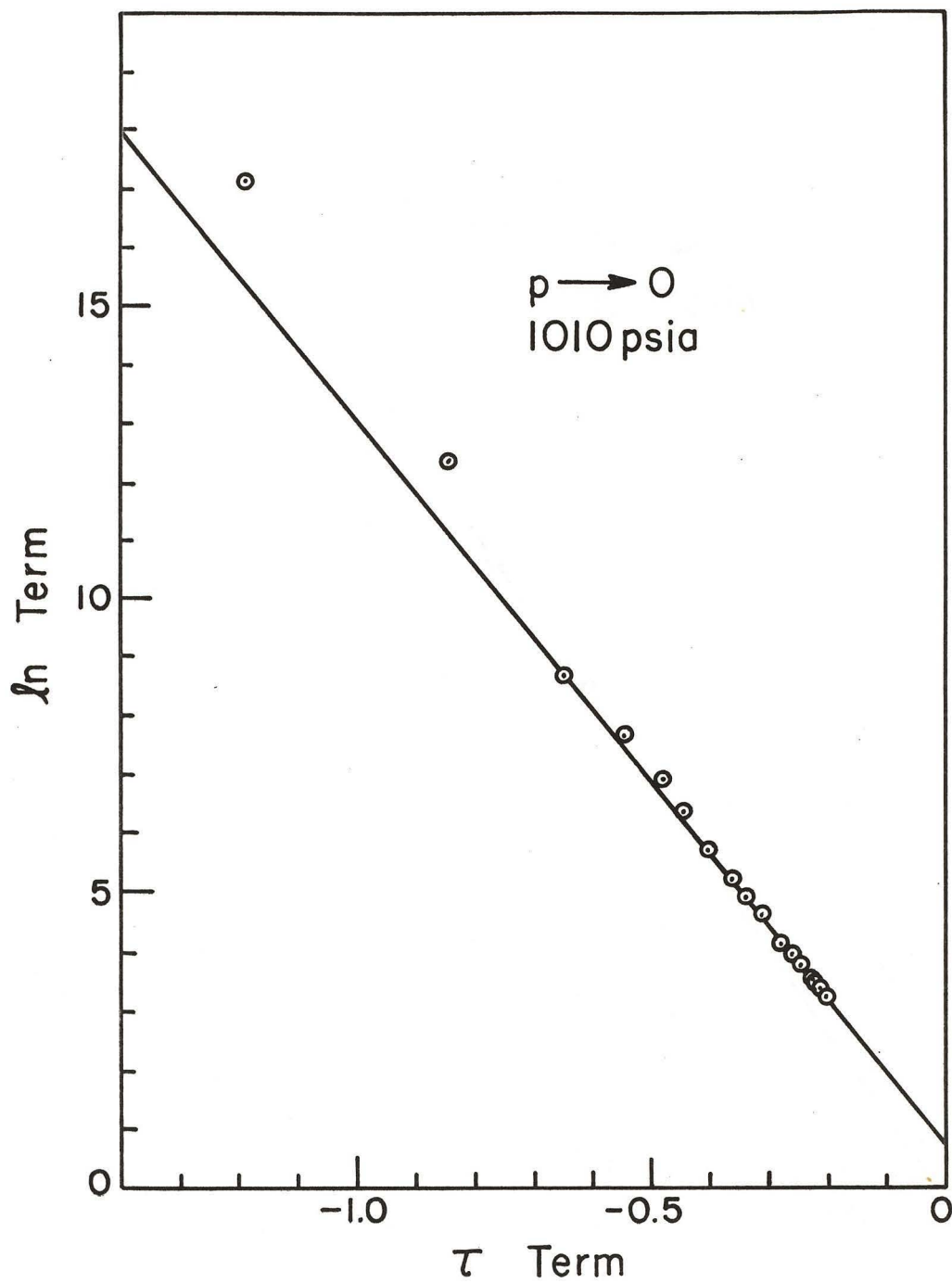


FIGURE 47. Langmuir Plot for Run 80

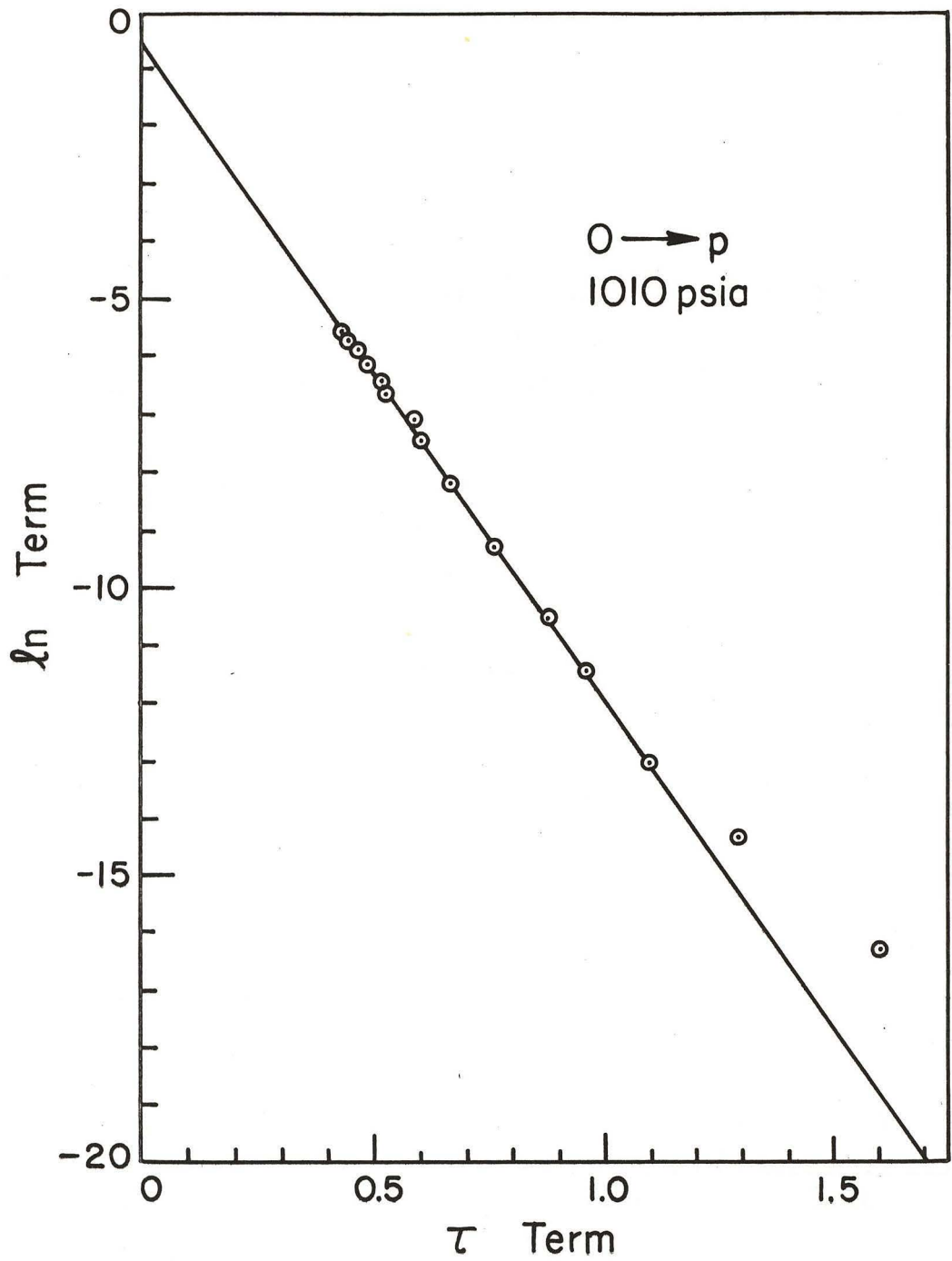


FIGURE 48. Langmuir Plot for Run 81

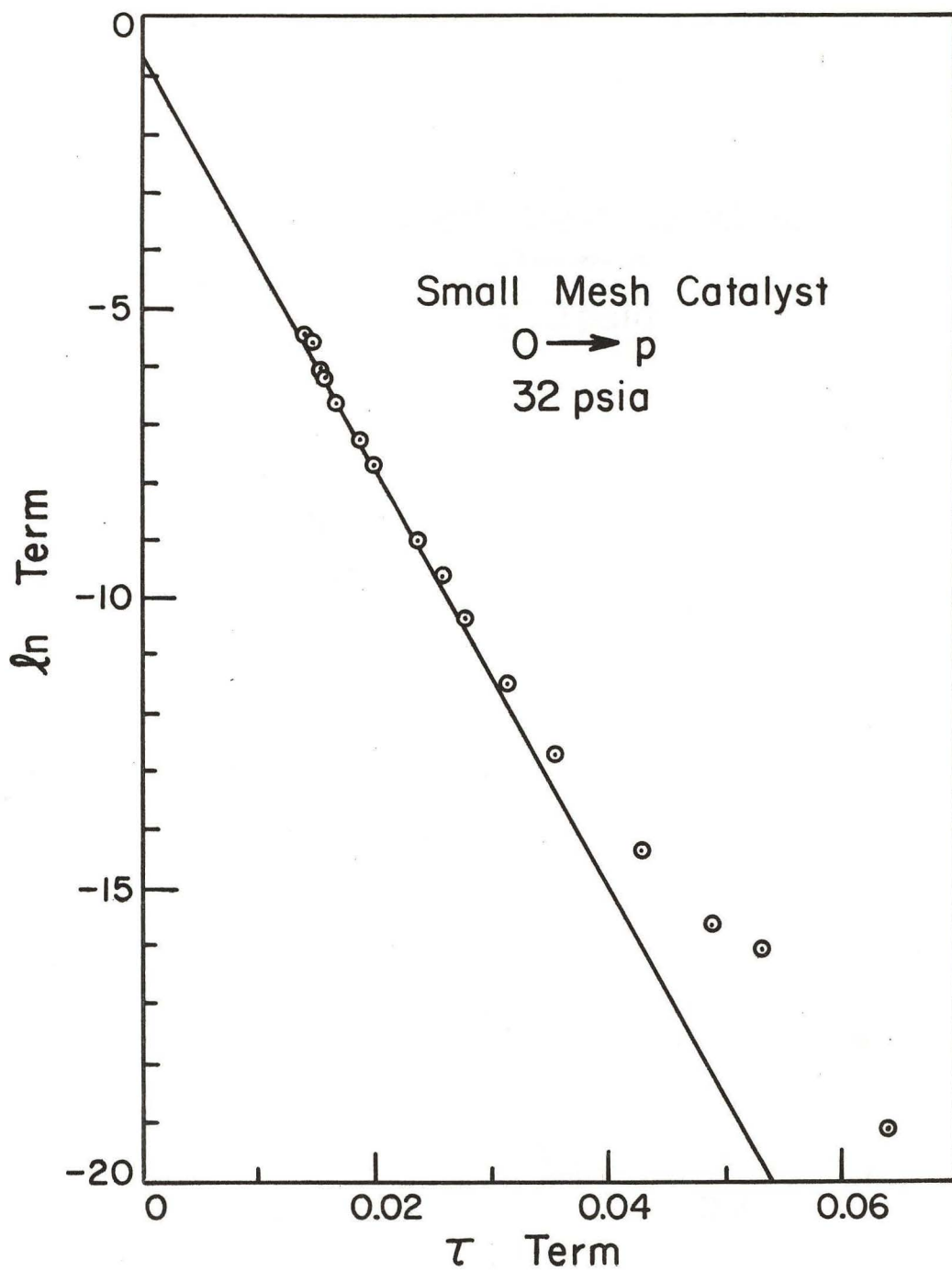


FIGURE 49. Langmuir Plot for Run 82

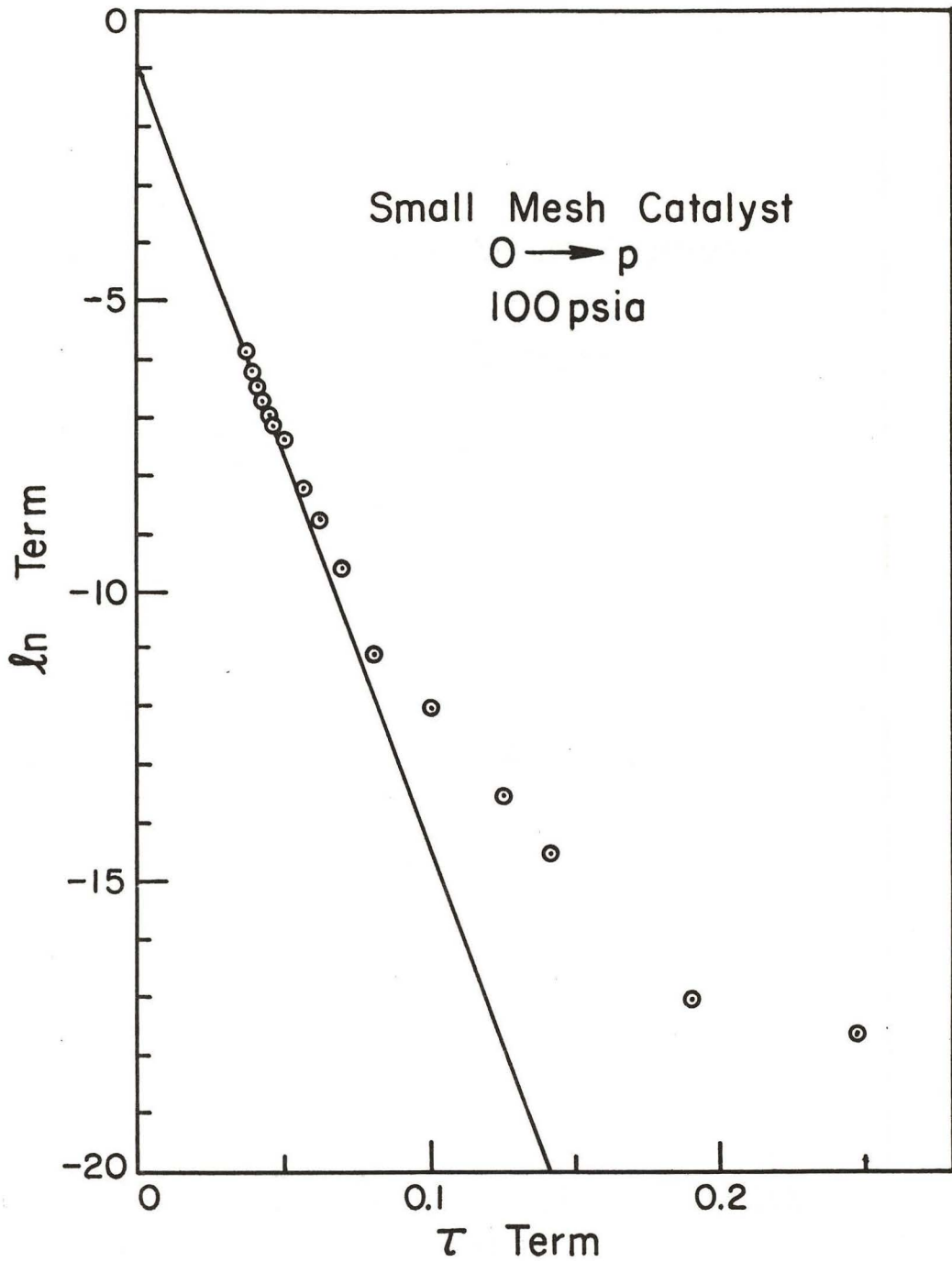


FIGURE 50. Langmuir Plot for Run 83

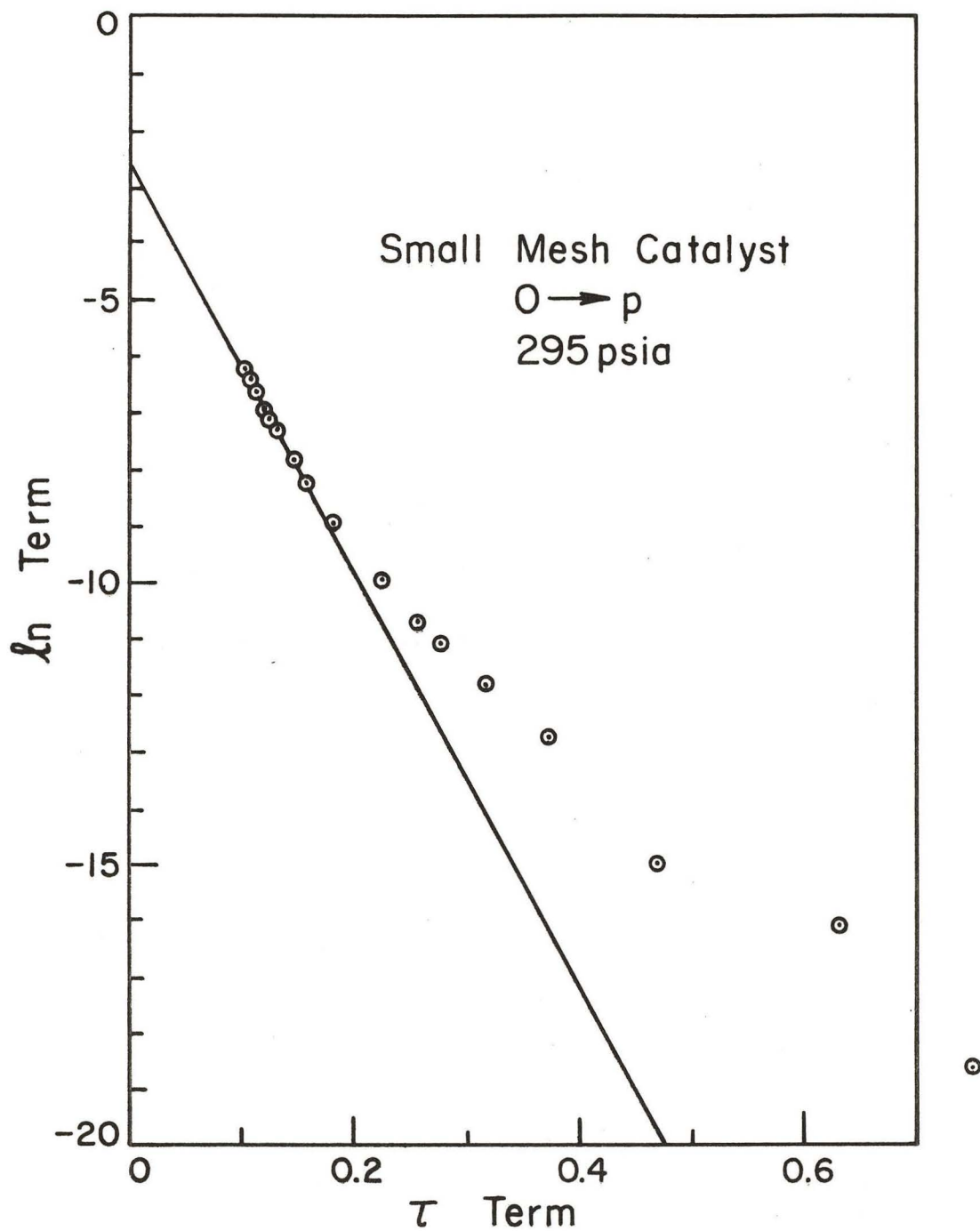


FIGURE 51. Langmuir Plot for Run 85

APPENDIX G

Elovich Rate Plots

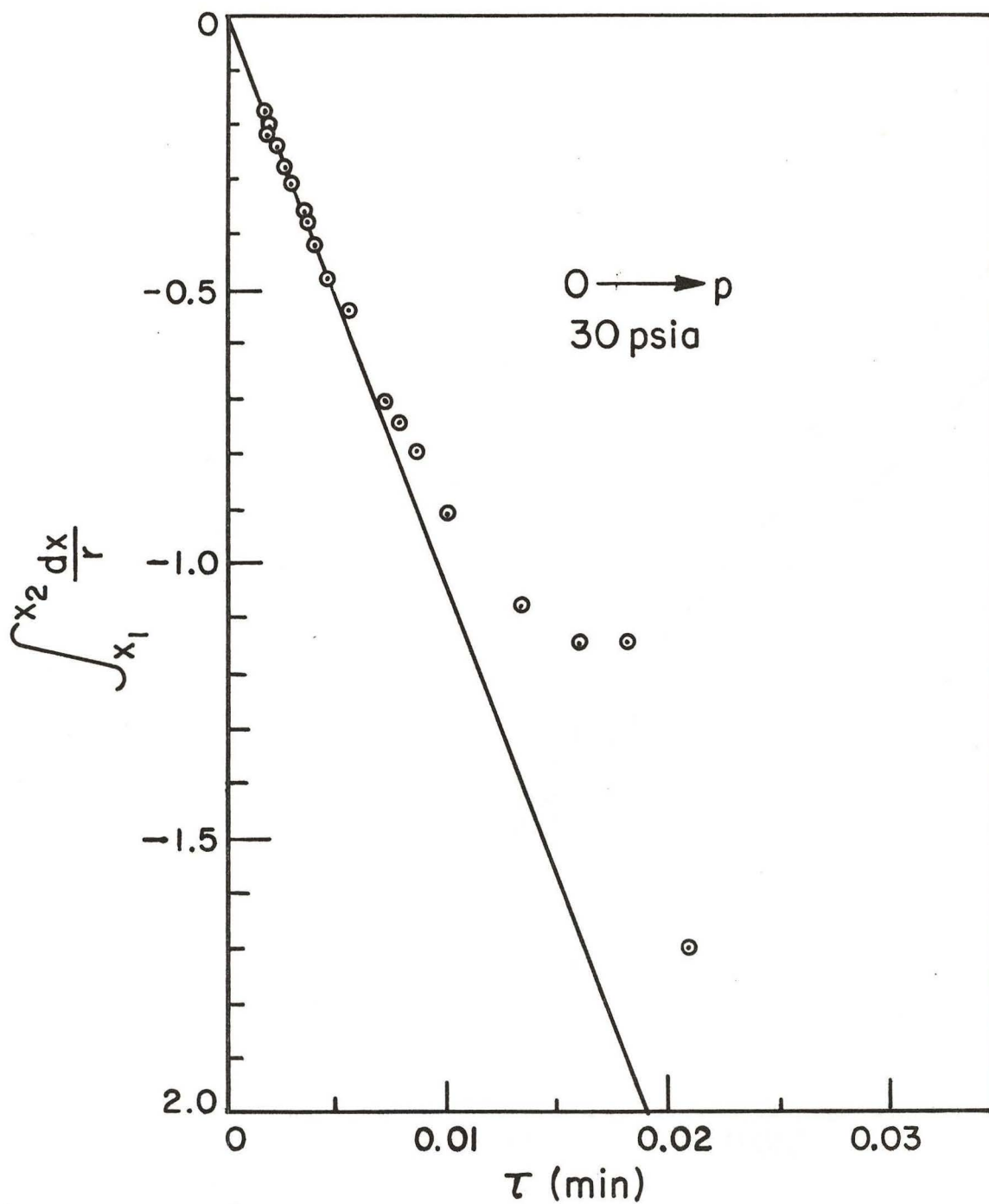


FIGURE 52. Elovich Plot for Run 60

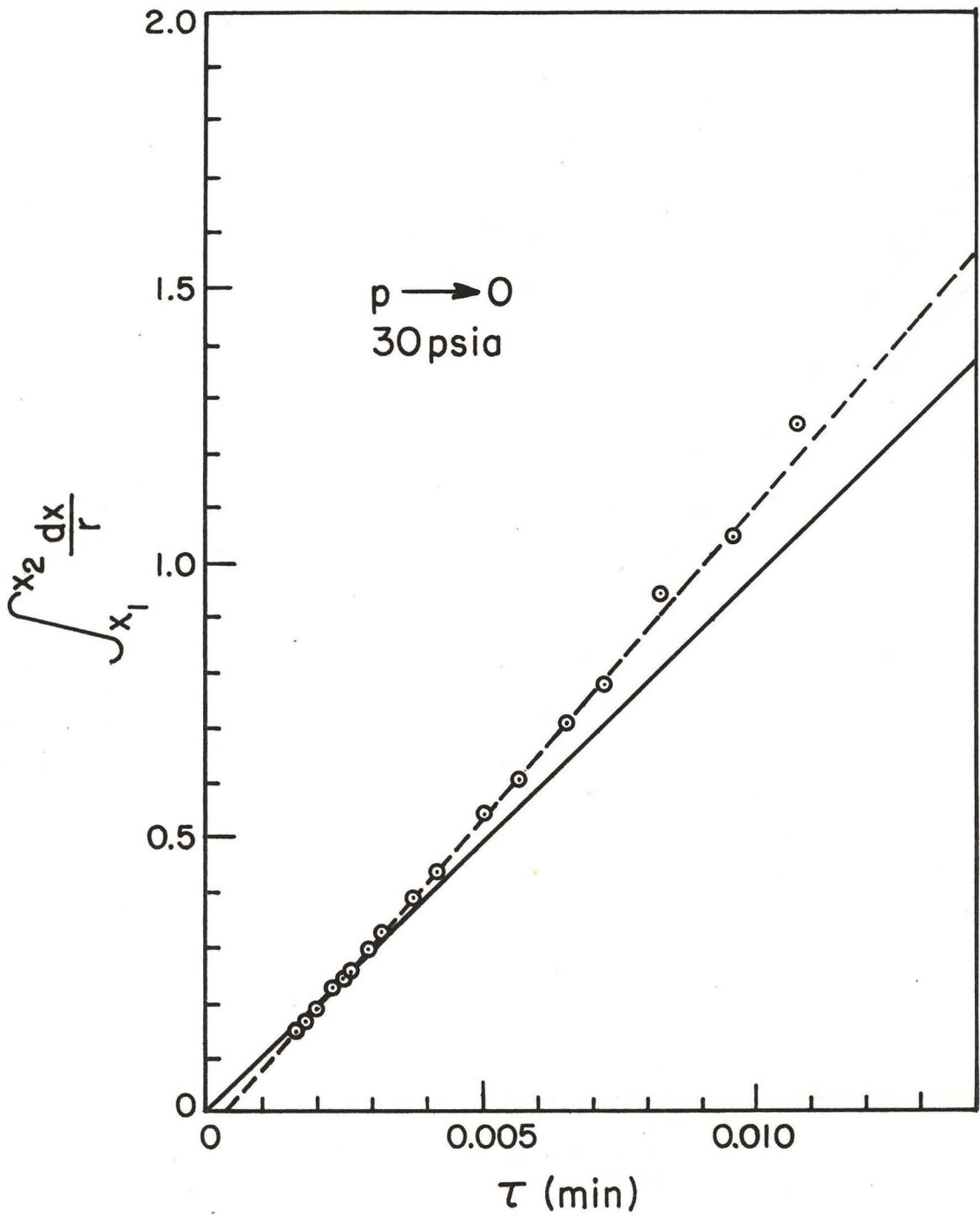


FIGURE 53. Elovich Plot for Run 61

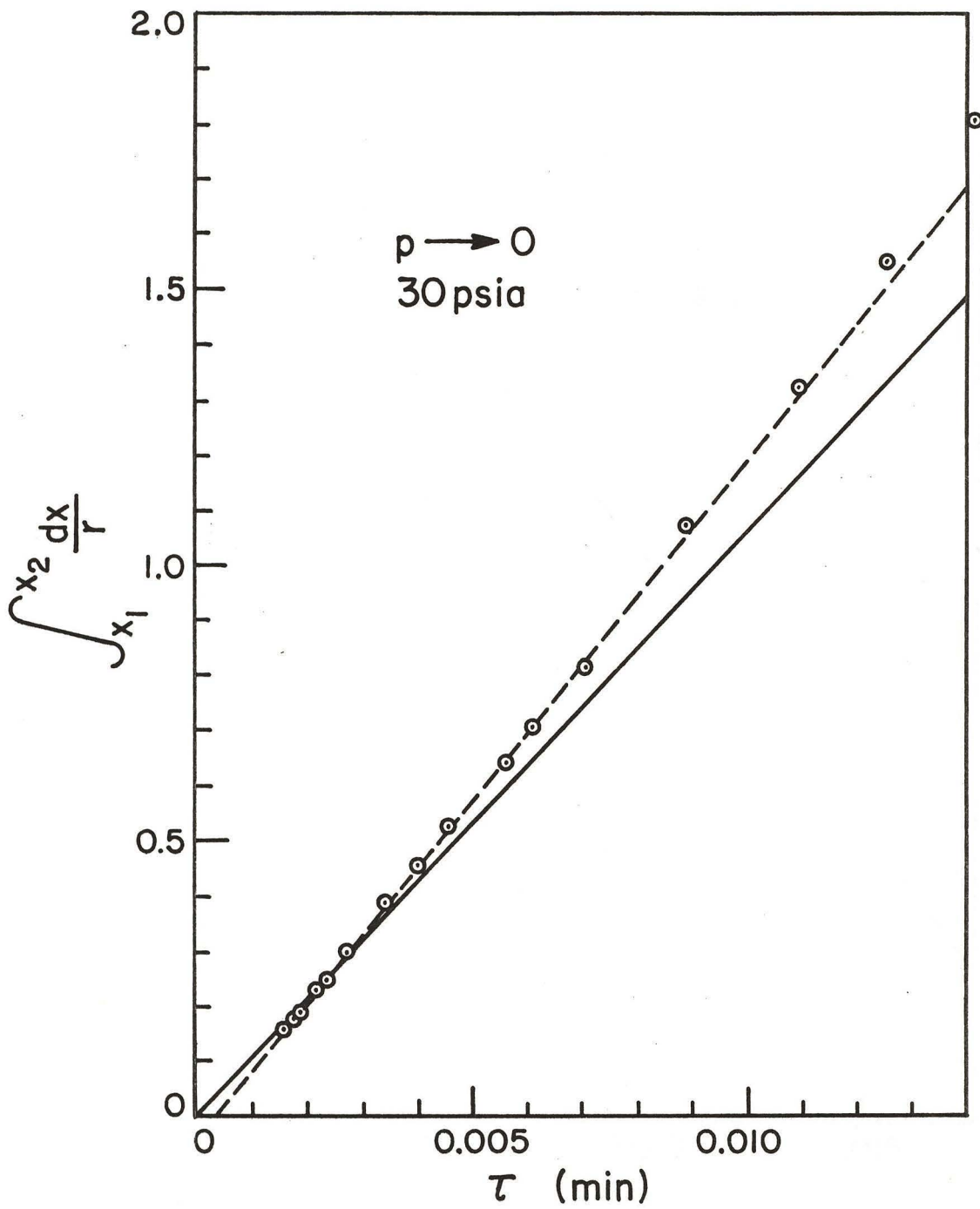


FIGURE 54. Elovich Plot for Run 65

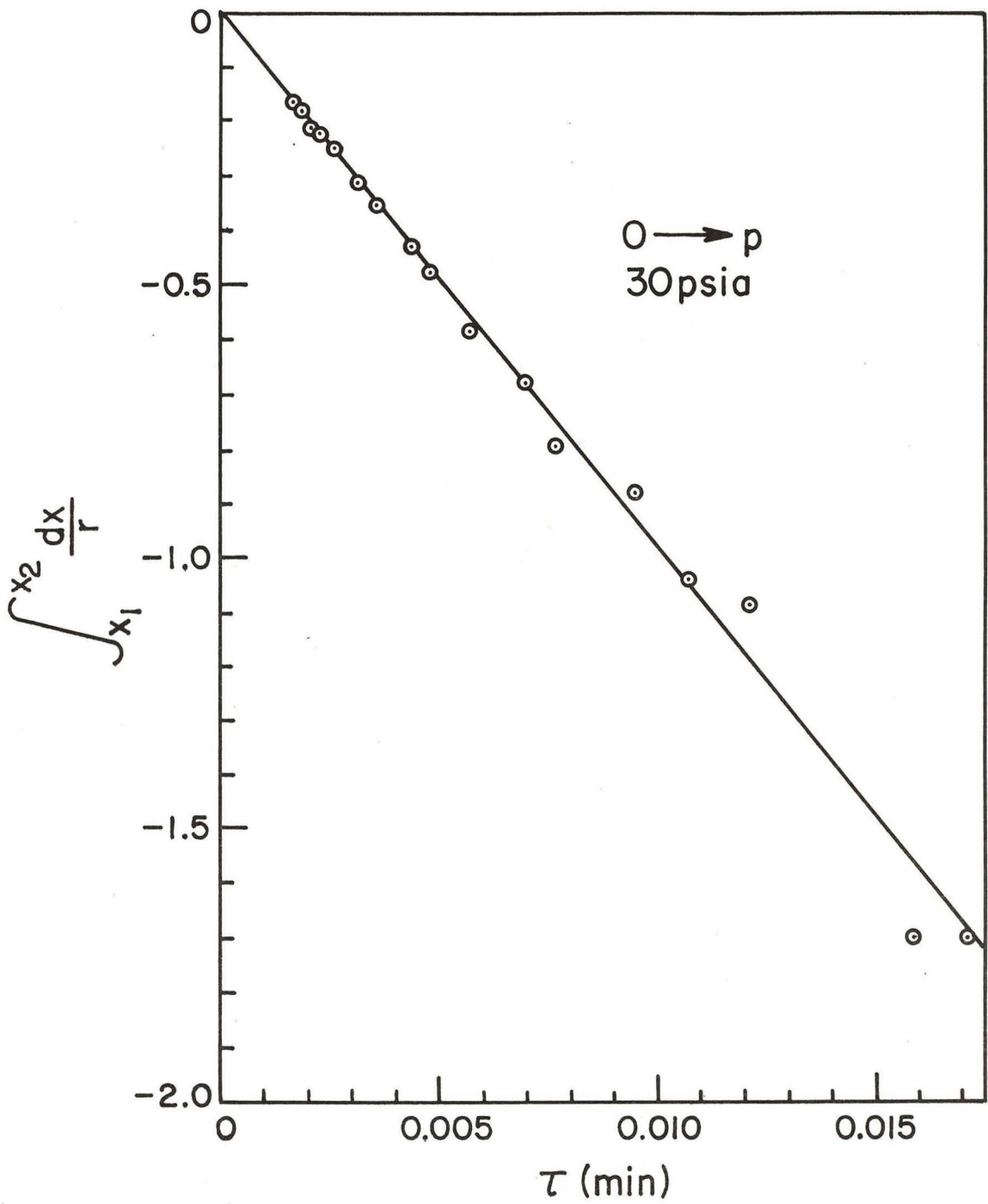


FIGURE 55. Elovich Plot for Run 66

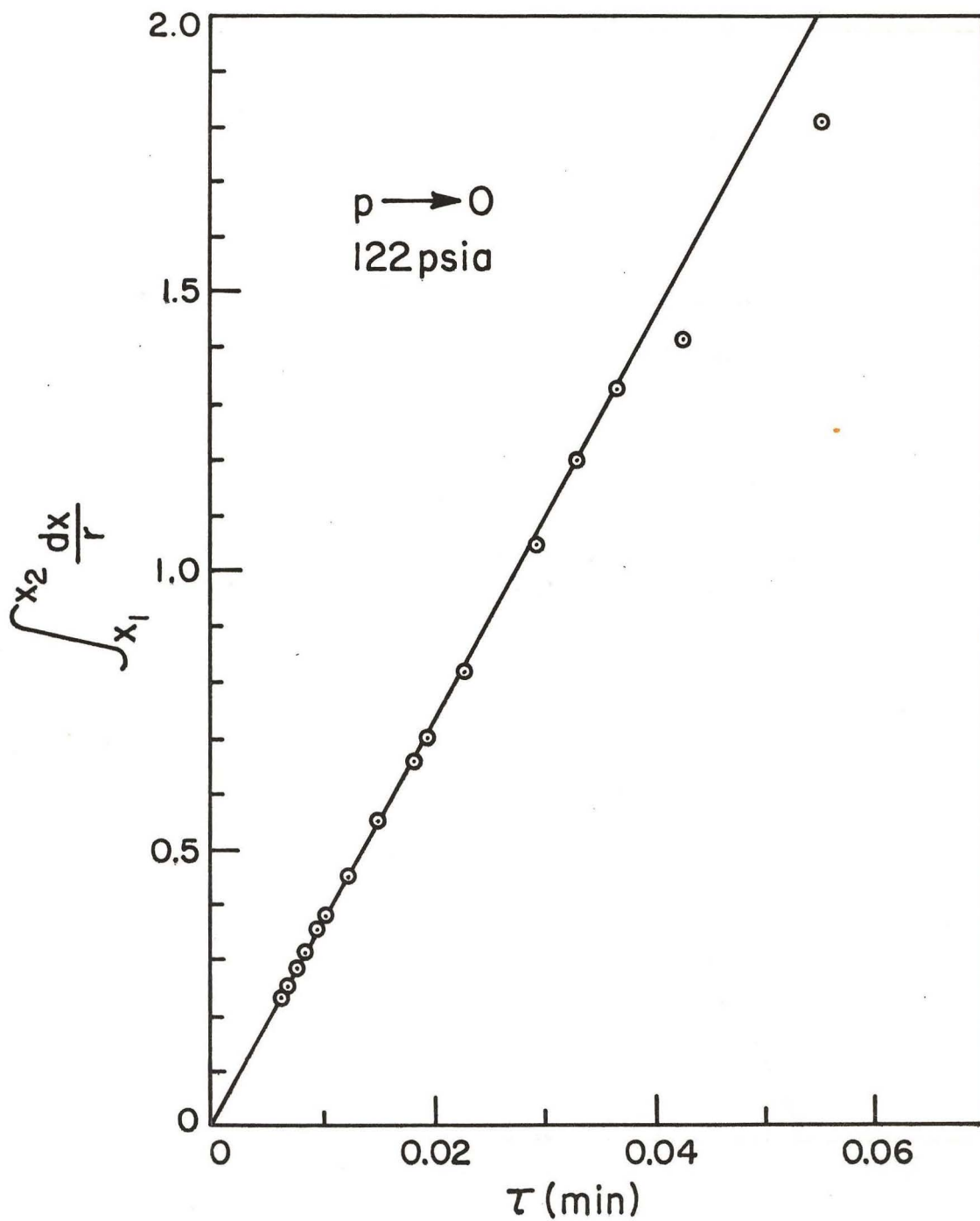


FIGURE 56. Elovich Plot for Run 70

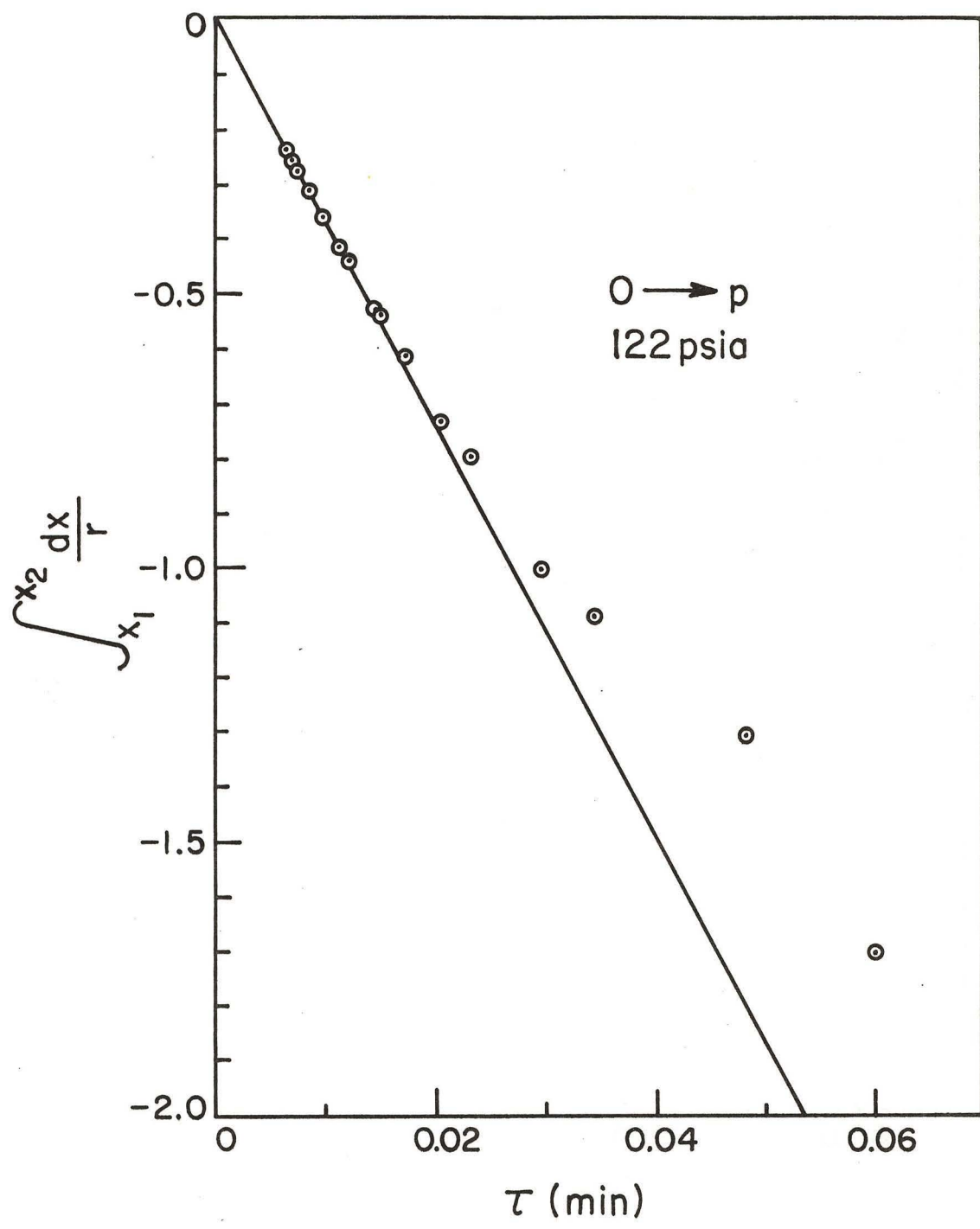


FIGURE 57. Elovich Plot for Run 71

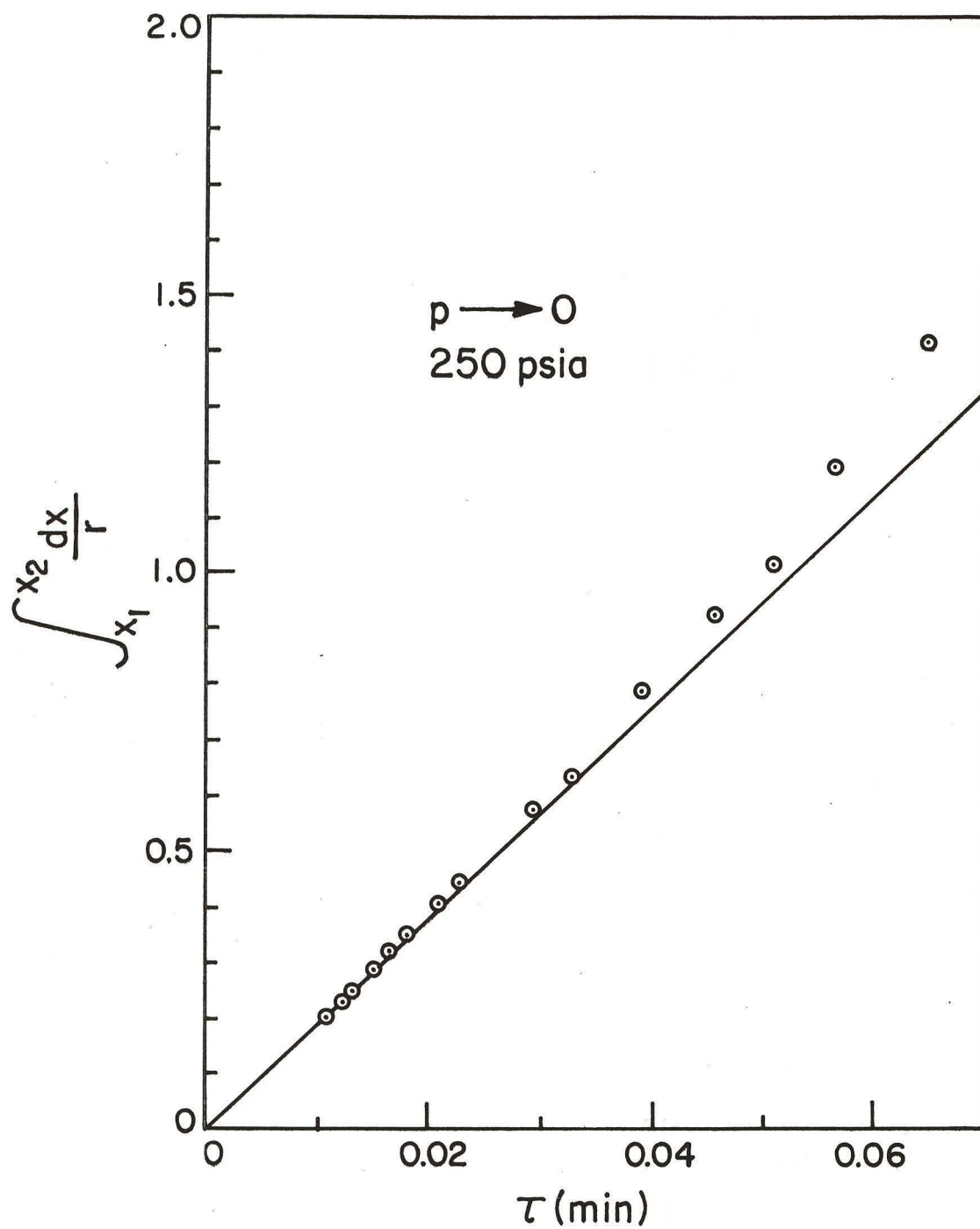


FIGURE 58. Elovich Plot for Run 72

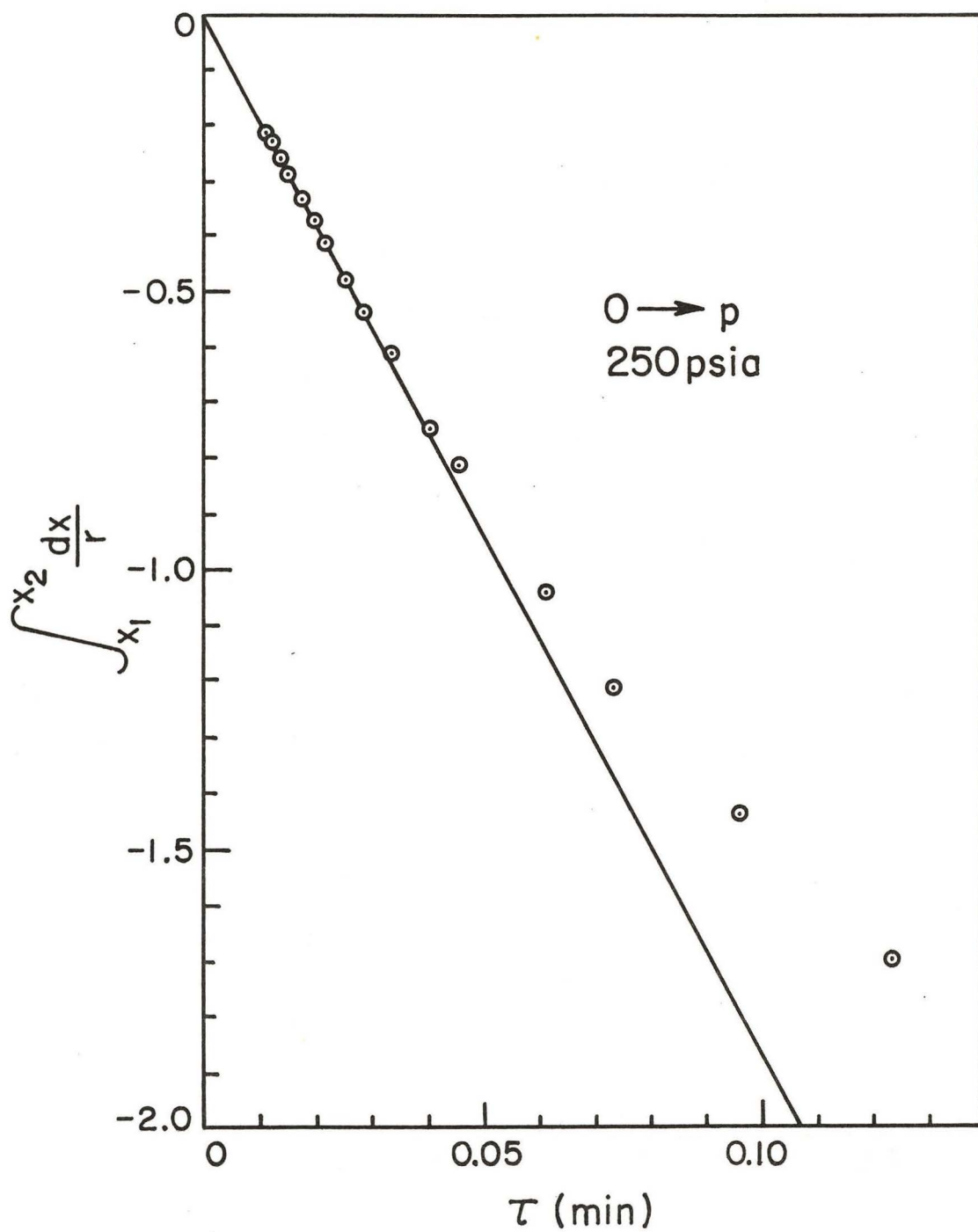


FIGURE 59. Elovich Plot for Run 73

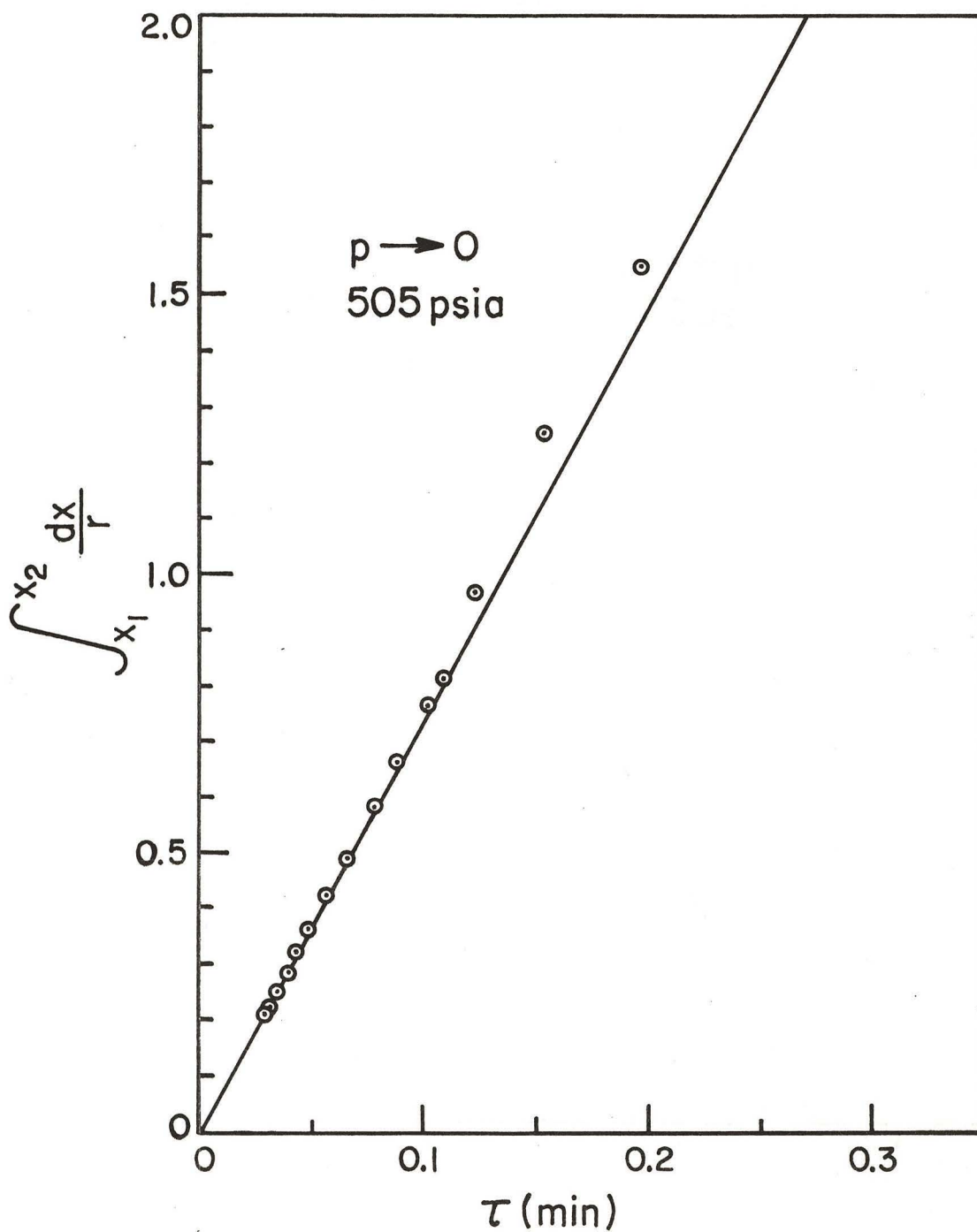


FIGURE 60. Elovich Plot for Run 76

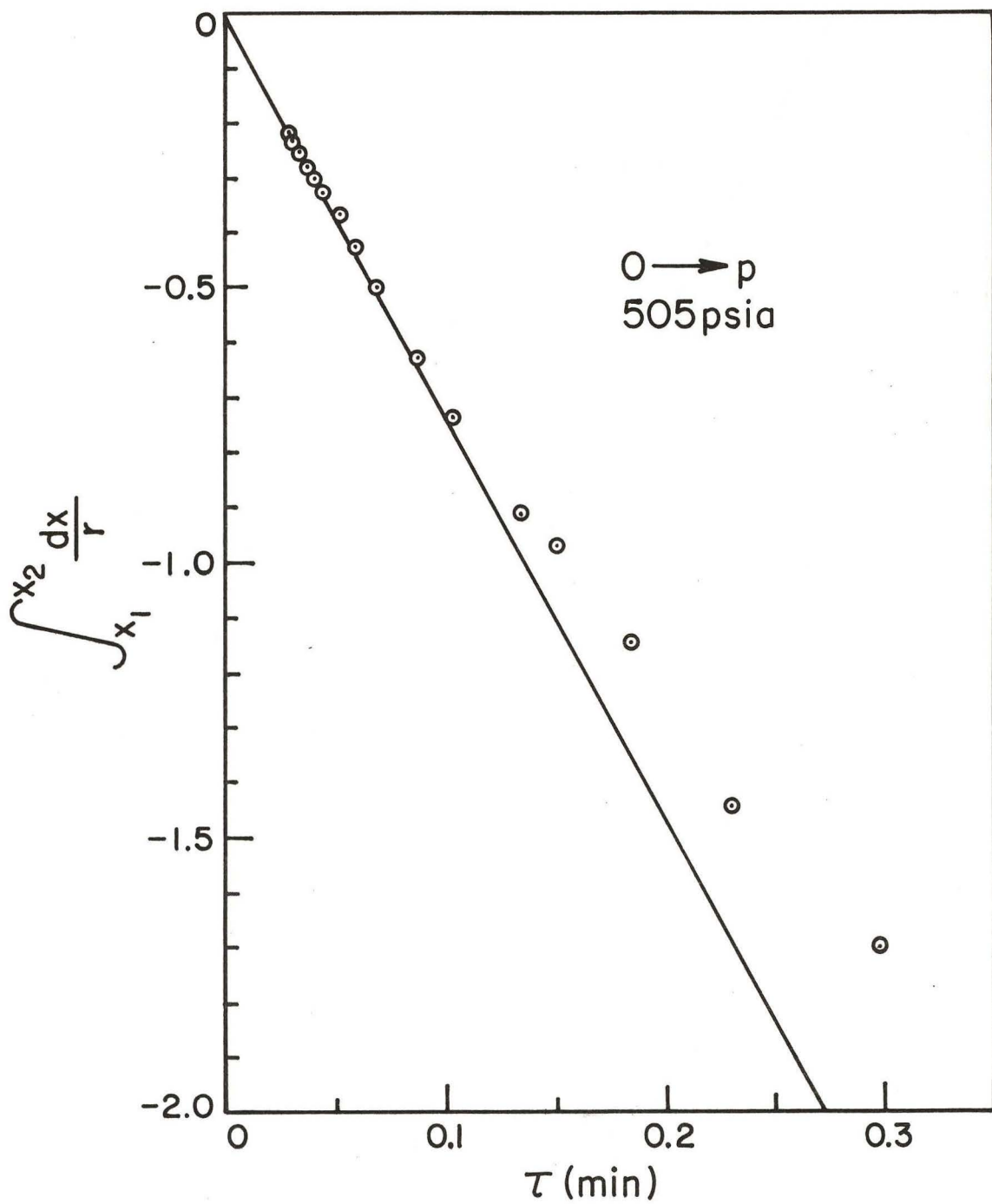


FIGURE 61. Elovich Plot for Run 77

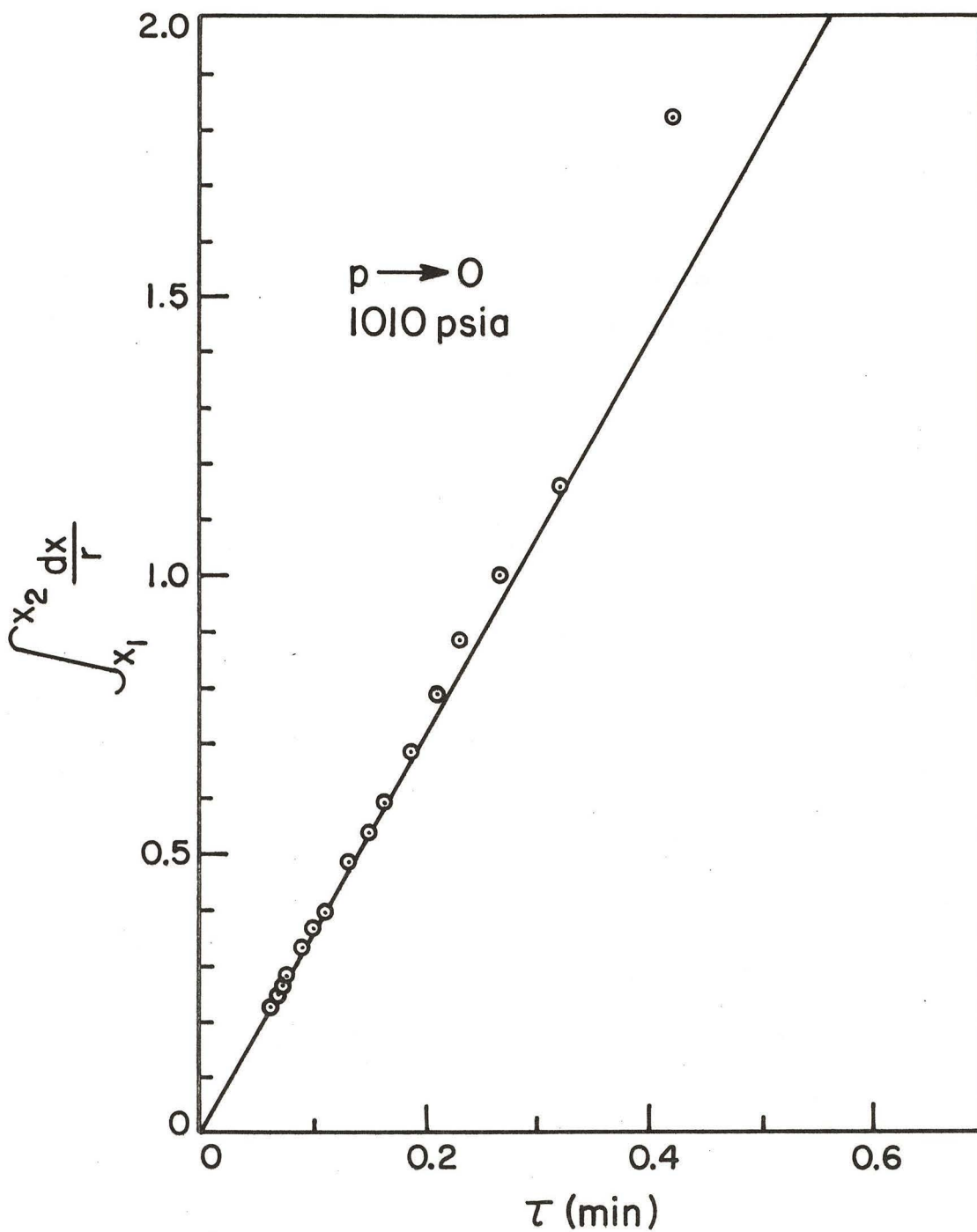


FIGURE 62. Elovich Plot for Run 80

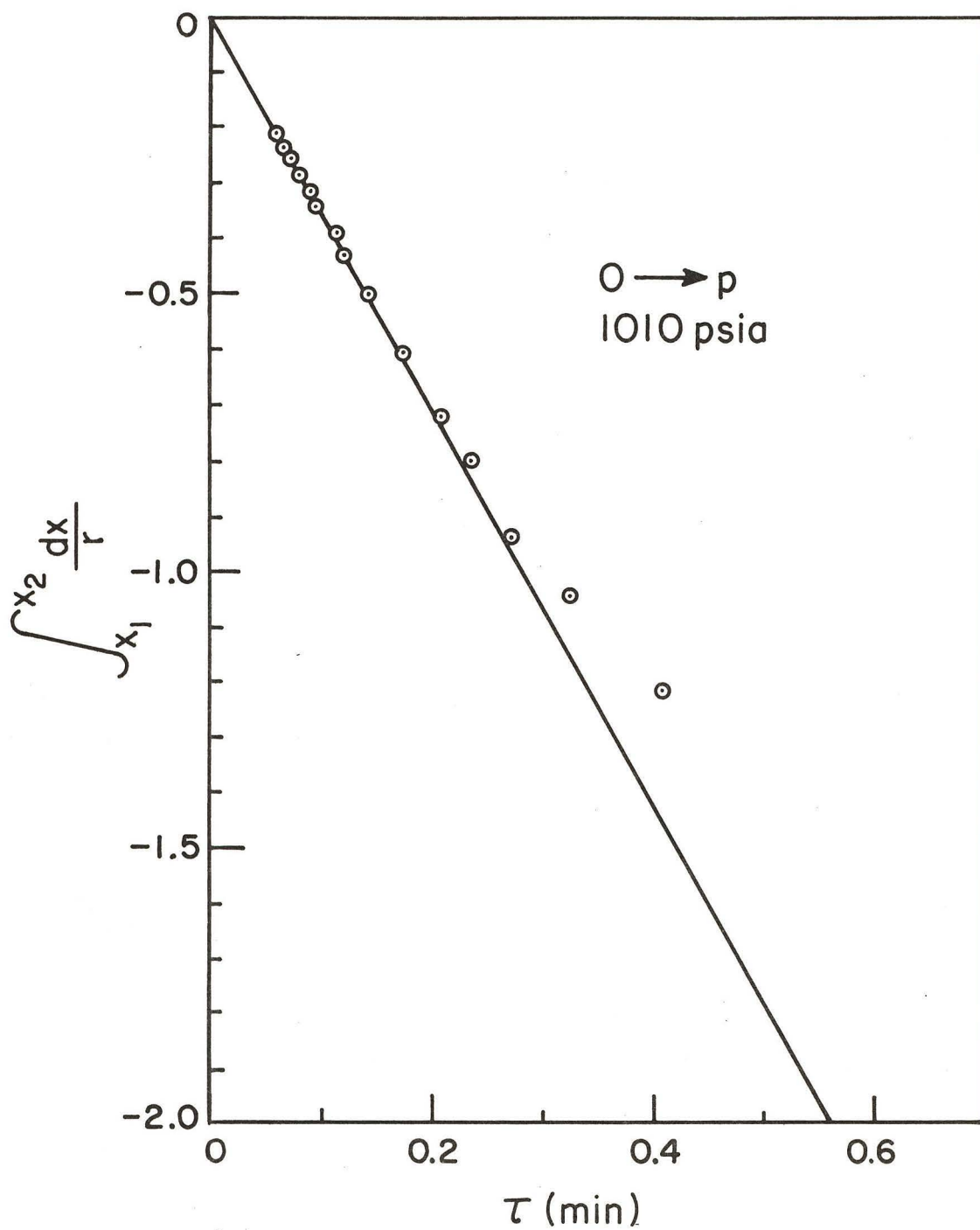


FIGURE 63. Elovich Plot for Run 81

APPENDIX H

Data

Run #60  
30 psia  
o-H<sub>2</sub> → p-H<sub>2</sub>

Space Velocity (min <sup>-1</sup> )	$\tau$ (min)	x
45.4	0.022	0.508
47.8	0.0209	0.507
55.3	0.0181	0.503
62.6	0.016	0.503
75.0	0.0133	0.502
100.7	0.00994	0.497
116.0	0.00862	0.492
130.3	0.00767	0.489
139.6	0.00716	0.486
218	0.00458	0.460
180.8	0.00553	0.469
287	0.00349	0.436
244	0.00401	0.449
275	0.00363	0.440
340	0.00294	0.422
375	0.00267	0.412
428	0.00223	0.399
510	0.00196	0.383
490	0.00204	0.388
595	0.00168	0.370

Run #61  
30 psia  
p-H<sub>2</sub> → o-H<sub>2</sub>

Space Velocity (min <sup>-1</sup> )	$\tau$ (min)	x
42.3	0.0237	0.507
59.1	0.0185	0.507
75.9	0.0132	0.508
93.0	0.01074	0.512
121.2	0.00825	0.521
104.3	0.00959	0.517
138.6	0.00721	0.530
153.2	0.00652	0.539
198.7	0.00503	0.564
176.7	0.00566	0.553
239	0.00419	0.590
313	0.00319	0.631
265	0.00377	0.605
401	0.00249	0.674
381	0.00263	0.667
336	0.00297	0.644
503	0.00199	0.716
430	0.00233	0.685
552	0.00181	0.732
608	0.00165	0.749

Run #65  
30 psia



Space Velocity ( $\text{min}^{-1}$ )	$\tau$ (min)	x
42.1	0.0237	0.506
56.9	0.0176	0.506
91.5	0.0109	0.510
79.9	0.0125	0.508
70.8	0.0141	0.507
113.1	0.00884	0.515
142.4	0.00702	0.528
164.9	0.00606	0.538
219	0.00455	0.566
178.4	0.00560	0.546
291	0.00343	0.604
251	0.00399	0.583
365	0.00274	0.641
425	0.00235	0.670
456	0.00219	0.681
528	0.00189	0.709
621	0.00161	0.737
564	0.00177	0.720

Run #66  
30 psia



Space Velocity ( $\text{min}^{-1}$ )	$\tau$ (min)	x
44.4	0.0225	0.506
58.3	0.01715	0.503
62.9	0.0159	0.503
82.7	0.0121	0.500
93.5	0.0107	0.499
106.8	0.00936	0.494
130.8	0.00764	0.490
177	0.00565	0.473
144.7	0.00691	0.482
211	0.00474	0.458
284	0.00352	0.432
237	0.00421	0.449
321	0.00311	0.421
283	0.00353	0.432
438	0.00228	0.390
387	0.00259	0.400
474	0.00211	0.384
597	0.00166	0.362
539	0.00185	0.370

Run #68  
61 psia  
 $p\text{-H}_2 \longrightarrow o\text{-H}_2$

Space Velocity ( $\text{min}^{-1}$ )	$\tau$ (min)	x
21.1	0.0474	0.508
45.3	0.0221	0.511
39.2	0.0255	0.509
31.5	0.0318	0.509
26.7	0.0361	0.508
53.4	0.0187	0.514
68.8	0.0145	0.525
84.2	0.0119	0.537
116.7	0.00857	0.566
99.7	0.01003	0.548
123.3	0.00811	0.570
137	0.0073	0.583
149	0.00671	0.593
215	0.00465	0.650
179.9	0.00556	0.620
232	0.00431	0.662
306	0.00327	0.706
270	0.0037	0.688

Run #69  
61 psia  
 $o\text{-H}_2 \longrightarrow p\text{-H}_2$

Space Velocity ( $\text{min}^{-1}$ )	$\tau$ (min)	x
20.0	0.0501	0.510
30.0	0.0333	0.509
33.3	0.0300	0.509
39.7	0.0252	0.508
51.0	0.0196	0.505
62.6	0.0160	0.500
82.7	0.0121	0.490
127.1	0.00786	0.463
105.7	0.00946	0.477
164.3	0.00609	0.442
148.3	0.00674	0.450
173.4	0.00577	0.439
210	0.00476	0.420
190.5	0.00525	0.428
251	0.00398	0.403
225	0.00444	0.413
264	0.00379	0.399
284	0.00352	0.392

Run #70  
122 psia  
p-H<sub>2</sub> → o-H<sub>2</sub>

Space Velocity (min <sup>-1</sup> )	$\tau$ (min)	x
9.06	0.112	0.506
12.2	0.082	0.506
18.2	0.055	0.507
23.5	0.0425	0.509
27.5	0.0364	0.510
30.5	0.0328	0.512
51.6	0.0194	0.539
34.1	0.0293	0.516
44.1	0.0227	0.528
55.0	0.0182	0.544
67.1	0.0149	0.562
81.4	0.0123	0.586
104.7	0.00955	0.619
97.3	0.0103	0.610
117.1	0.00854	0.636
128.6	0.00778	0.651
143.3	0.00698	0.669
157.3	0.00636	0.683

Run #71  
122 psia  
o-H<sub>2</sub> → p-H<sub>2</sub>

Space Velocity (min <sup>-1</sup> )	$\tau$ (min)	x
8.75	0.1142	0.507
11.73	0.0853	0.507
16.64	0.0601	0.506
20.8	0.0481	0.504
29.2	0.0343	0.501
33.9	0.0295	0.499
43.3	0.0231	0.491
49.1	0.0203	0.487
67.1	0.0149	0.468
58.5	0.0171	0.477
89.8	0.0111	0.447
82.7	0.0121	0.452
69.5	0.0144	0.467
118.3	0.00846	0.422
103	0.00971	0.434
135.7	0.00737	0.410
146.2	0.00684	0.403
158	0.00633	0.396

Run #72  
 240 psia  
 $p\text{-H}_2 \longrightarrow o\text{-H}_2$

Space Velocity ( $\text{min}^{-1}$ )	$\tau$ (min)	x
4.72	0.212	0.507
12.26	0.0816	0.507
15.43	0.0648	0.510
13.66	0.0733	0.508
17.76	0.0563	0.513
19.76	0.0507	0.518
21.9	0.0456	0.522
25.6	0.0391	0.531
33.8	0.0295	0.557
30.5	0.0327	0.548
43.9	0.0227	0.588
48.0	0.0208	0.599
60.6	0.0165	0.633
55.2	0.0181	0.620
66.1	0.0151	0.648
81.6	0.0123	0.681
74.9	0.0133	0.668
91.3	0.0109	0.701

Run #73  
 240 psia  
 $o\text{-H}_2 \longrightarrow p\text{-H}_2$

Space Velocity ( $\text{min}^{-1}$ )	$\tau$ (min)	x
4.64	0.215	0.506
6.55	0.1526	0.505
8.08	0.1237	0.505
10.40	0.0961	0.504
13.65	0.0733	0.502
16.34	0.0612	0.499
21.8	0.0458	0.491
24.6	0.0406	0.487
35.0	0.0286	0.467
29.9	0.0335	0.476
45.6	0.0219	0.446
39.2	0.0255	0.458
56.7	0.0176	0.427
50.4	0.0198	0.437
64.3	0.0155	0.414
71.8	0.0139	0.404
86.9	0.0115	0.386
80.8	0.0124	0.392

Run #76  
500 psia



Space Velocity ( $\text{min}^{-1}$ )	$\tau$ (min)	x
2.23	0.448	0.507
3.14	0.319	0.507
3.90	0.257	0.507
5.10	0.196	0.509
6.55	0.1526	0.512
8.15	0.1226	0.520
9.17	0.1091	0.529
11.28	0.0887	0.544
9.88	0.1012	0.533
12.81	0.0781	0.556
15.30	0.0653	0.575
17.68	0.0566	0.593
20.3	0.0492	0.614
22.9	0.0437	0.631
25.1	0.0399	0.647
28.2	0.0355	0.665
31.5	0.0317	0.684
33.5	0.0299	0.693

Run #77  
500 psia



Space Velocity ( $\text{min}^{-1}$ )	$\tau$ (min)	x
2.19	0.456	0.509
3.36	0.297	0.508
2.83	0.353	0.508
4.36	0.229	0.507
5.45	0.1834	0.504
6.65	0.1504	0.500
7.47	0.134	0.498
9.71	0.103	0.489
11.46	0.0873	0.480
14.45	0.0692	0.464
16.99	0.0568	0.451
19.92	0.0502	0.438
22.5	0.0445	0.427
26.7	0.0374	0.412
24.3	0.0411	0.420
29.5	0.0339	0.403
32.3	0.0310	0.396
34.7	0.0288	0.389

Run #80  
1010 psia  
p-H<sub>2</sub> → o-H<sub>2</sub>

Space Velocity (min <sup>-1</sup> )	$\tau$ (min)	x
0.978	1.023	0.501
1.695	0.590	0.501
2.39	0.419	0.502
3.13	0.319	0.508
3.77	0.265	0.513
4.32	0.231	0.519
4.72	0.211	0.526
5.36	0.1868	0.537
6.15	0.1627	0.550
6.68	0.1498	0.560
7.49	0.1335	0.572
9.08	0.1102	0.599
9.95	0.1005	0.610
10.97	0.0922	0.625
12.93	0.0773	0.650
13.47	0.0743	0.658
15.87	0.0631	0.684
14.35	0.0697	0.667

Run #81  
1010 psia  
o-H<sub>2</sub> → p-H<sub>2</sub>

Space Velocity (min <sup>-1</sup> )	$\tau$ (min)	x
0.947	1.056	0.508
1.475	0.678	0.508
1.848	0.541	0.508
2.45	0.407	0.504
3.09	0.323	0.501
3.68	0.271	0.498
4.26	0.233	0.492
4.83	0.207	0.487
5.81	0.172	0.477
7.04	0.142	0.463
8.38	0.1195	0.450
8.92	0.1122	0.442
10.57	0.0946	0.430
11.25	0.0889	0.423
12.59	0.0794	0.413
14.03	0.0713	0.403
15.38	0.0650	0.396
17.14	0.0583	0.386



